The Thesis Committee for Michael Chase Jones Certifies that this is the approved version of the following thesis:

Implications of Geothermal Energy Production Via Geopressured Gas Wells in Texas: Merging Conceptual Understanding of Hydrocarbon Production and Geothermal Systems

APPROVED BY

SUPERVISING COMMITTEE:

Supervisor: _____
William L. Fisher

_____
Suzanne A. Pierce

_____
Bruce L. Cutright

Implications of Geothermal Energy Production Via Geopressured Gas Wells in Texas: Merging Conceptual Understanding of Hydrocarbon Production and Geothermal Systems

By:

Michael Chase Jones, B.S. GEO. E.

Thesis

Presented to the Faculty of the Graduate School of

The University of Texas at Austin

in Partial Fulfillment

of the Requirements

for the Degree of

Master of Science in Energy and Earth Resources

The University of Texas at Austin

May 2016

Abstract

Implications of Geothermal Energy Production Via Geopressured Gas Wells in Texas: Merging Conceptual Understanding of Hydrocarbon Production and Geothermal Systems

Michael Chase Jones, M.S. EER
The University of Texas at Austin, 2016

Supervisor: William Fisher

This thesis evaluates the overall geothermal energy development potential of the state of Texas by combining resource assessment studies from both the hydrocarbon and conventional geothermal sectors. Cooperation between these industries is often shown to result in a symbiotic relationship that will benefit not only the respective industries, but also the public and regulatory environments. By outlining resource characteristics, technological specifications, thermodynamic foundations, and the specific geologic environments of the state that are related to geothermal and hydrocarbon production, this study attempts to update previous geothermal feasibility studies performed by academic and government institutions. This study suggests the undertaking of preliminary implementation surveys exploring a novel geothermal energy production method known as the *well bore heat exchanger*. Several numerical modeling studys assessing the optimized system parameters, ideal work rates, and electrical generation capabilities of this theoretical method of production are summarized in this study. As a power generation method, the well bore heat exchanger model is uniquely suited to areas of concentrated hydrocarbon production due to its potential application to abandoned wells.

Retrofitting wells with a well bore heat exchanger system avoids plugging and abandonment procedures, thus production companies are saved from a cost with no potential payback while saving the geothermal industry exploration and drilling costs, which commonly make up over half of an overall project development budget. This study presents production history analysis of specific geopressured gas plays to create a geospatial distribution model for identifying the ideal location for application of this innovative clean energy production method

Table of Contents

List of Tables

List of Figures

1.0 INTRODUCTION

In its 2015 *Annual U.S. and Global Geothermal Power Production Report*, the Geothermal Energy Association lists six different means by which geothermal power production projects are classified. Those listed as "conventional hydrothermal" make up the majority of electricity generation projects in the United States (Matek, 2015). These projects typically rely on three major components being present: heat, fluid, and permeability. Unfortunately, electricity generation from this clean and renewable resource has been stagnant at best over the last 25 years. According to the latest United States Energy Information Administration Monthly Energy Review published in March, 2016, the United States has yet to surpass its highest annual net geothermal electricity generation level (16,800 MWh) set in 1993. In that same timespan, solar PV generation has more than tripled while wind has increased nearly 40 times over. As more conventional hydrothermal resources in the US are developed, locating and producing geothermal reservoirs that contain heat, fluid, and permeability (referred to in this study as the "three imperatives") becomes more difficult.

1.1 Objective

This study aims to review novel ways of extracting geothermal energy that do not rely on the aforementioned 3 imperatives while attempting to merge conceptual understanding of hydrocarbon and geothermal exploration and production practices in order to help bolster the Texas geothermal sector. Specifically, this study will focus on the emerging potential of producing geothermal energy through existing oil and gas infrastructure. Texas makes

for an ideal focus area to consider new means of geothermal energy production. The state's vast geopressured sedimentary basin is largely untapped in terms geothermal utilization. Texas also has an immense network of oil and gas wells and associated records that could potentially be used to classify the subsurface resource.

1.2 Methods

This study will compare the various conventional forms of geothermal energy extraction to several novel approaches, with emphasis on the application of the hypothetical *well bore heat exchanger* (WBHX) model presented by many authors. These novel approaches will then be weighed by how well they apply to the conditions present in Texas. Before selecting which technologies are most feasible, underlying resource classifications, utilization methods, thermodynamic properties, and geologic conditions were examined in order to properly understand the overall viability of potential projects. Emphasis is placed on linking together existing oil and gas exploration studies, production studys, geologic surveys, and resource assessments with the limited studies specifically related to geothermal energy in Texas. A final analysis was performed in order to select optimum locations for implementation. This analysis will be performed by using geographic information systems (GIS) software and data from the National Geothermal Data System.

2.0 RESOURCE TYPES AND UTILIZATION METHODS

Background information regarding the conditions that allow for the generation of geothermal energy and the energy production methods themselves are presented in this section. Both resource and production types are split into conventional and unconventional categories. Considering the similarities in exploration/production methods and the common co-mingling of geothermal and hydrocarbon systems in Texas, this study seeks to combine the descriptive frameworks for each resource into a more unified nomenclature scheme.

2.1 Geothermal resource characterization

In order to describe potential areas of geothermal production and their specific characteristics, a few working definitions must be established within the context of this study. A *geothermal system* refers to a specified area's geological, hydrogeological, and thermodynamic characteristics. A *geothermal resource* is defined by an economically sufficient quantity of extractable heat within a drillable depth that has not necessarily been explicitly discovered (Rybach and Muffler, 1981). The term *reserve*, which is used synonymously in both the petroleum and geothermal sectors, implies a resource that has previously been identified and is commercially recoverable with existing technology (Glassly, 2010; Society of Petroleum Engineers, 2007). The term *play*, often used in classifying hydrocarbon accumulations, has recently been nominated for use in the geothermal field by Inga S. Moeck (2014). A play, as it applies to petroleum production, is defined by the identification of a stratigraphic or structural setting with defined

hydrocarbon source rock, reservoir unit, and stratigraphic trap (Doust, 2010). Moeck's (2014) proposed definition for this shared term includes areas that share a common heat source, fluid migration pathway, reservoir capacity, and mechanism of heat production to the surface. In 2014, the U.S. Department of Energy (DOE) Geothermal Technologies Office (GTO) established a similar framework. The GTO submitted the "Play Fairway Analysis Funding Opportunity Announcement," with an initial acceptance of 11 competitively selected projects (Weathers et al., 2015). Currently, six of these projects are continuing with Phase II of the play fairway analysis (US DOE GTO, n.d.). The resource characterization specific to this study utilizes a broader scope of this play concept, which is presented in *4.0 Nature of Geothermal Systems in Texas.* In the context of this study, *conventional* resources and production methods will refer to those that have successfully produced and maintained commercially viable geothermal operations. *Unconventional* will refer to geothermal conditions and related production methods that remain relatively unproven or have yet to be commercially developed on a large scale.

2.1.1 Conventional geothermal systems

Conventional hydrothermal-geothermal systems are the most commonly exploited geothermal resource worldwide. On the most basic level, all hydrothermal resources require three major components: a heat source, a permeable reservoir, and a supply of a mobile fluid. In addition to these "three imperatives," Ronald DiPippo (2012) lists two additional constraints, which include an overlying impervious cap-rock and a reliable fluid recharge mechanism. Most of these conventional resources are situated in areas of

large-scale geologic motion associated with the shifting of tectonic plates. When a tectonic plate undergoes stress in tension, compression, or shear, the unloading of this mechanical potential energy comes in many forms (Figure 1).

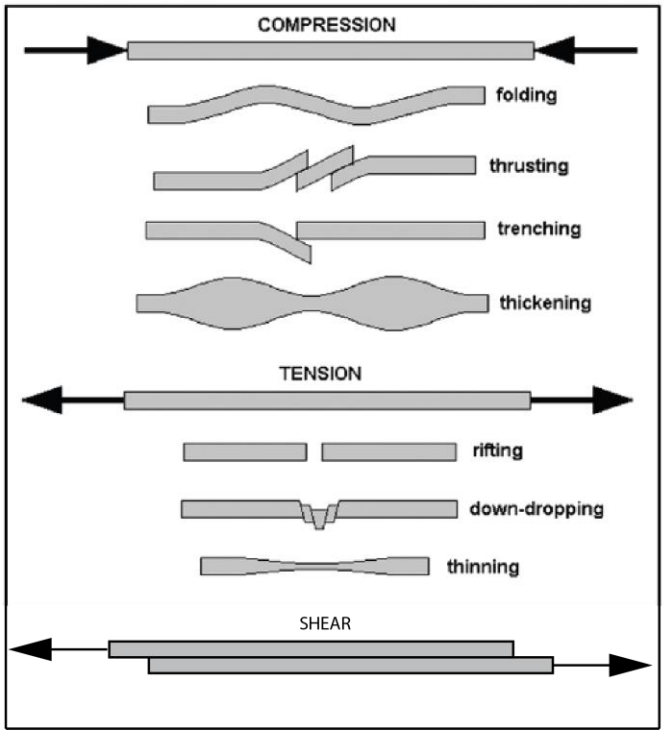

Figure 1. Tectonic stress regimes and associated unloading mechanisms (modified from DiPippo, 2012)

Compression stresses are relieved by folding, thrusting, trenching, and thickening. Tensile stresses result in rifting, down-dropping, and thinning. Shear stresses are observed in areas where tectonic plates slide past each other, represented by *transform faults* such as the San Andreas fault in California. The unloading of these stresses often gives way to abnormally high *geothermal gradients (*DiPippo, 2012). Geothermal gradient values describe how subsurface temperatures increase as a function of depth and

represent an important factor in determining the commercial viability of geothermal systems. This value is calculated by the following equation:

$$\nabla T = \frac{T_F - T_S}{z} \quad (1)$$

$$where:$$

$$\boldsymbol{\nabla T}\ is\ the\ geothermal\ gradient$$
$$\boldsymbol{T_F}\ is\ bottom\ hole\ formatin\ temperature$$
$$\boldsymbol{T_s}\ is\ ambient\ surface\ temperature$$
$$\mathbf{z}\ is\ depth$$

The average conductive geothermal gradient is 1.7 °F/100 feet, which is determined using theoretical depth and temperature values representative of the conditions experienced in the upper portions of the mantle (DiPippo, 2012). Areas represented by geothermal gradient values higher than 1.7°F/100 feet are considered favorable to geothermal energy production due to shallower drilling requirements. In few cases, conventional hydrothermal systems with higher than average geothermal gradients are found in areas that have not undergone tectonic deformation. Instead, highly radiogenic igneous intrusions generate the heat carried to the surface by a mobile fluid. Exploration for these systems often starts with locating surface thermal manifestations such as geysers, fumaroles, hot springs, mud pots, and steam-heated pools. If an underlying geothermal system does not display these surface features, it is described as being a *blind* target (Hanson et al, 2014).

2.1.2 Unconventional geothermal resources

Unconventional geothermal systems are those that typically lack one of the three imperatives and have thus not been continuously produced on a commercial scale. The most well-understood of these unproven resources include those classified as hot dry rock systems, magma energy systems, and geopressured-geothermal systems. These systems are most often considered blind targets, making them difficult to locate and less commercially viable than conventional systems.

Hot Dry Rock

Hot dry rock (HDR) systems contain high temperatures but lack subsurface fluid or adequate permeability to produce fluid to the surface. Potential HDR resources are made viable by the use of hydraulic fracturing. If sufficient reservoir volume and permeability are created through stimulation, other wells are drilled that target the conductive fractures. Water is introduced to the reservoir via an injection well and returned to the surface after passing through the hot, fractured rock. Ideally, the network of wells and fractured rock create a closed loop in which no fluid is lost to the formation (DiPippo, 2012). The term "enhanced/engineered geothermal systems" (EGS) was initially used to describe this production scheme associated with HDR systems. Over the years, however, the term has expanded in meaning and now describes many of the production practices outlined in section 2.2.2 *Unconventional geothermal energy production methods.* (Breede et al., 2013; MIT et al., 2006).

Magma Energy

Relatively shallow magma bodies are also thought to be potential sources of geothermal energy. If a well is able to contact accumulations of superheated molten rock, an injection pipe introduces cold water at high pressures. As the magma cools, solidifies, and cracks under the thermal stresses applied, pore space and permeability are created (DiPippo, 2012). Beyond the conceptual models, magma resources are poorly understood. For over a decade, the DOE sponsored the *Magma Energy Program*. The program's accomplishments were limited to initial site selection and early stage drilling, reaching depths of 9,831 feet before being abandoned due to shifts in DOE funding. More recently, an Icelandic industry-government consortium known as the Iceland Deep Drilling Project (IDDP), unexpectedly encountered shallow accumulations of rhyolite magma. The IDDP study describing this encounter referred to potential drilling of production and injection wells as a "high priority" (Elders et al., 2013).

Geopressured Geothermal

The final and most thoroughly analyzed unconventional geothermal system classification described in this study is the geopressured geothermal system. These systems are characterized by abnormally high *pore pressure gradients*. Similar to temperature values in geothermal gradients, pressure values within the fluid filled pores of geologic formations increase as a function of depth. The *hydrostatic pore pressure gradient* describes pressures exerted by a column of water from a datum, such as sea level, to a given depth, and is representative of normal subsurface pore pressure gradients. In

intervals dominated by a *lithostatic pore pressure gradient*, pore pressures exceed hydrostatic conditions and the fluids contained in pores must support the weight of the overlying formations and fluids. The term *overpressure* describes any pressure value exceeding the hydrostatic pressure gradient and is used synonymously with the term *geopressure* (DiPippo, 2012; Deming, 2002). The relationship between hydrostatic and lithostatic pore pressure gradients is displayed graphically in Figure 2.

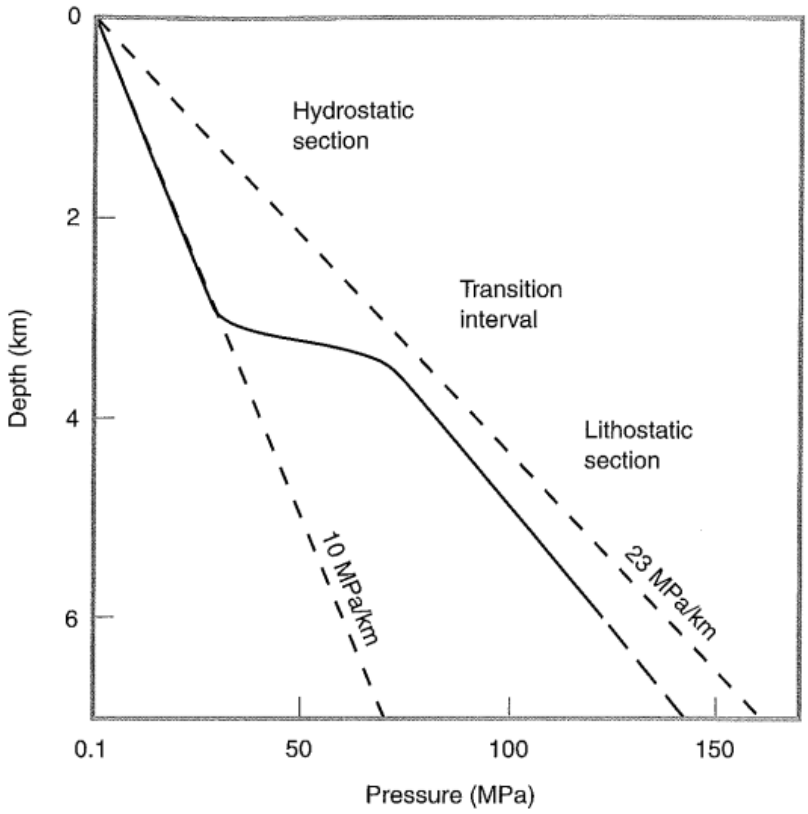

Figure 2. Plot of pressure as a function of depth showing pressure gradient classification boundaries (Deming, 2002)

Deviations from hydrostatic pressure conditions are a result of various structural, depositional, and engineered geologic conditions. For example, abnormally low pore

pressure gradients are typically associated with drained hydrocarbon reservoirs. In the case of geopressured geothermal systems, abnormally high pore pressure gradients are caused by the rapid burial and isolation of water-filled sediment. Deming (2002) describes a common mechanism that causes geopressure as *compaction disequilibrium.* Under normal conditions, sediments undergo compaction when subjected to overburden stress. As sediment compacts, water is expelled and pore pressure remains at normal hydrostatic levels. However, when a low-permeability sediment inhibits fluid flow, geopressure develops as the pore fluid is forced to support the overburden stress (Hart et al, 1995). Since pressure at a constant volume is directly proportional to temperature, heat is concentrated within these geopressured sediments. Geologic environments associated with geopressure development typically involve rapid deposition of alternating layers of sand and shale displaced by faults. A simplified conceptual model for such a system is shown in Figure 3.

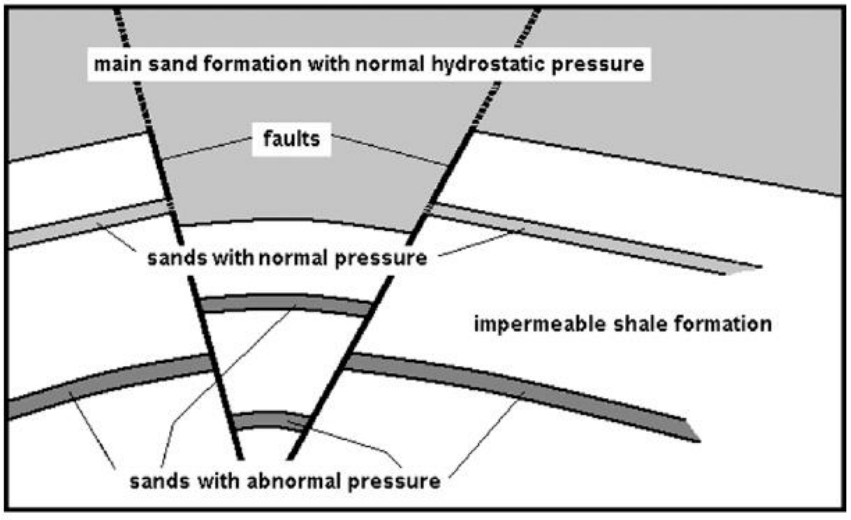

Figure 3. Conceptual model of geopressured sediments (DiPippo, 2012)

Compared to hydrothermal systems which contain only thermal energy, geopressured systems contain thermal energy in the form of the heated fluid, mechanical energy in the form of reservoir pressure, and chemical energy in the form of co-produced methane found within the same reservoirs. (DiPippo, 2012).

2.2 Geothermal energy production methods

The relationship between resource and production method is vital when trying to achieve the most efficient energy extraction possible. The same divide that separates conventional and unconventional resources exists between the various methods used to extract energy from subsurface heat. Conventional electricity generation using hydrothermal resources is primarily accomplished one of three ways: dry steam power plants, flash steam power plants, and binary cycle power plants. Direct use of the thermal energy stored in hydrothermal systems is an alternative to electricity production and is also considered a conventional method. Unconventional methods reflect the necessity for innovation within the geothermal sector. Some approaches presented here are purely theoretical while others have shown viability through various subsidized pilot programs. Unconventional methods presented here include hybrid power systems, oil and gas co-production, and well-bore heat exchanger systems. Elementary thermodynamic descriptions of production methods are outlined in *Chapter 3: Geothermal Thermodynamics.*

2.2.1 Conventional geothermal production

Dry Steam

The first commercial application of geothermal energy came in 1904 in the form of a small steam engine operating on dry steam produced from the volcanically active town of Larderello, Spain. Today, dry steam power plants account for roughly 27% of world-wide geothermal generation capacity while dry steam resources make up only 5% of all geothermal systems (DiPippo, 2012). The application of early mechanical energy extraction and the capacity vs. resource ratio demonstrate the simplicity of this utilization method. Figure 4 shows the process of extracting steam, processing it for use, generating electricity through a steam turbine and generator, and condensing the steam via cooling tower to facilitate reinjection.

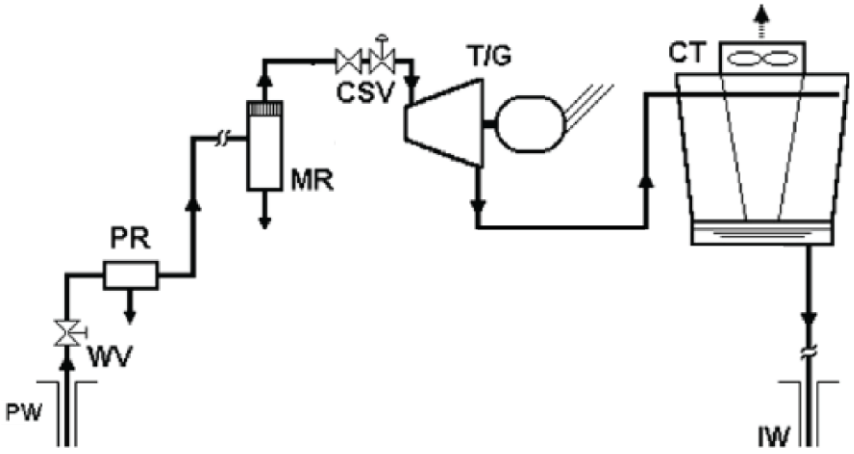

Figure 4. Simplified dry steam geothermal electricity generation schematic. PW-Production well, WV-Wellhead Valve, PR-Particulate remover, MR-Moisture Remover, CSV-Control and stop valves, T/G-Turbine/Generator, CT-Cooling tower, IW-Injection well (modified from DiPippo, 2012)

Flash Steam

Flash steam power plants utilize the thermodynamic principal of *flash evaporation* or "flashing," which is explained in Chapter 3, Section 3.1. This process allows generation systems to utilize liquid and mixed steam/liquid phase geothermal fluid. Flashing can occur across multiple steps in the production/generation process including: in the reservoir resulting from the drawdown in pressure experienced with production, in the production well resulting from pressure drops due to friction and gravity head, in inlets to surface facilities such as separators and control valves, and in specifically designed flash vessels commonly used in multi-flash cycles. Besides the additional step of flashing the geothermal fluid, this process of is identical to dry steam generation. In the simplified schematic shown in Figure 5, flashing occurs within the cyclone separator (CS).

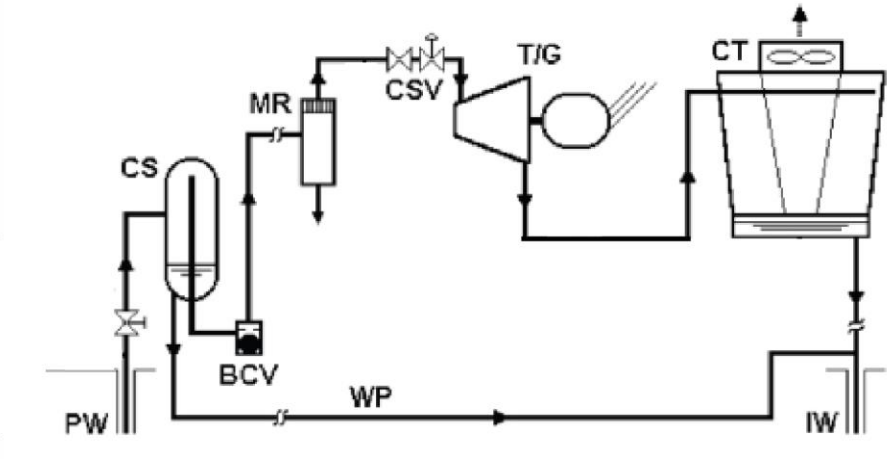

Figure 5. Simplified flash steam geothermal electricity generation schematic. WV-Wellhead Valve, CS-Cyclone Separator, WP-Water piping, BCV-Ball check valve, MR-Moisture Remover, CSV-Control and stop valves, T/G-Turbine/Generator, CT-Cooling tower, IW-Injection well (modified from DiPippo, 2012)

Binary/Organic Rankine Cycle

Binary system geothermal power plants utilize the Organic Rankine Cycle (ORC) to transfer heat from liquid geothermal brine to a secondary working fluid with a lower boiling point than water. The term binary refers to the separation of the working fluid and geothermal fluid into two closed systems. In the working fluid cycle, heated working fluid evaporates, passes through a turbine/generator, is cooled and condenses, and begins the cycle over again. On the geothermal fluid side, brine is extracted from the subsurface, passed over the working fluid, and reinjected into the subsurface. Figure 6 shows the basic schematic for the working fluid side of the binary cycle. In contrast to dry steam systems, binary systems make up 40% of all existing geothermal power plants but only account for 6.6% of the total generation capacity (DiPippo, 2012). This is due to the ability of binary cycle systems to utilize low temperature resources, such as the Democratic Republic of Congo Kiabukwa plant installed in 1952 that generated 200kW from 194 °F (90 °C) brine (Ormenda and Teklemariam, 2010).

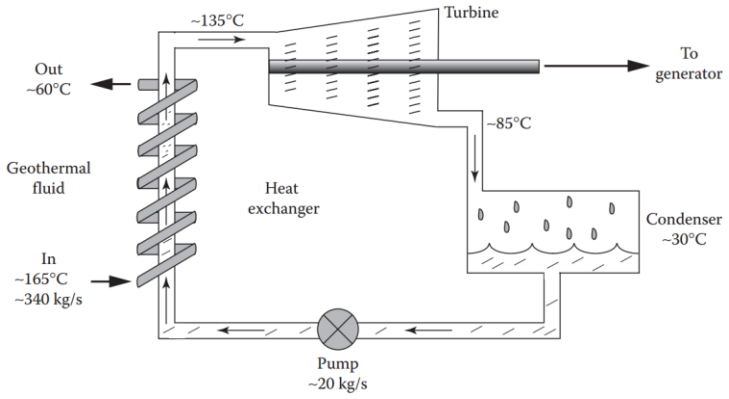

Figure 6. Schematic displaying the working fluid cycle of the binary geothermal system (Glassley, 2010)

Direct Use

Direct use geothermal applications avoid the inefficiencies that are associated with converting thermal energy to electrical energy. Instead, these applications use the geothermally heated brine to supply heat for various applications. Figure 7 lists various uses for differing geothermal resource temperatures.

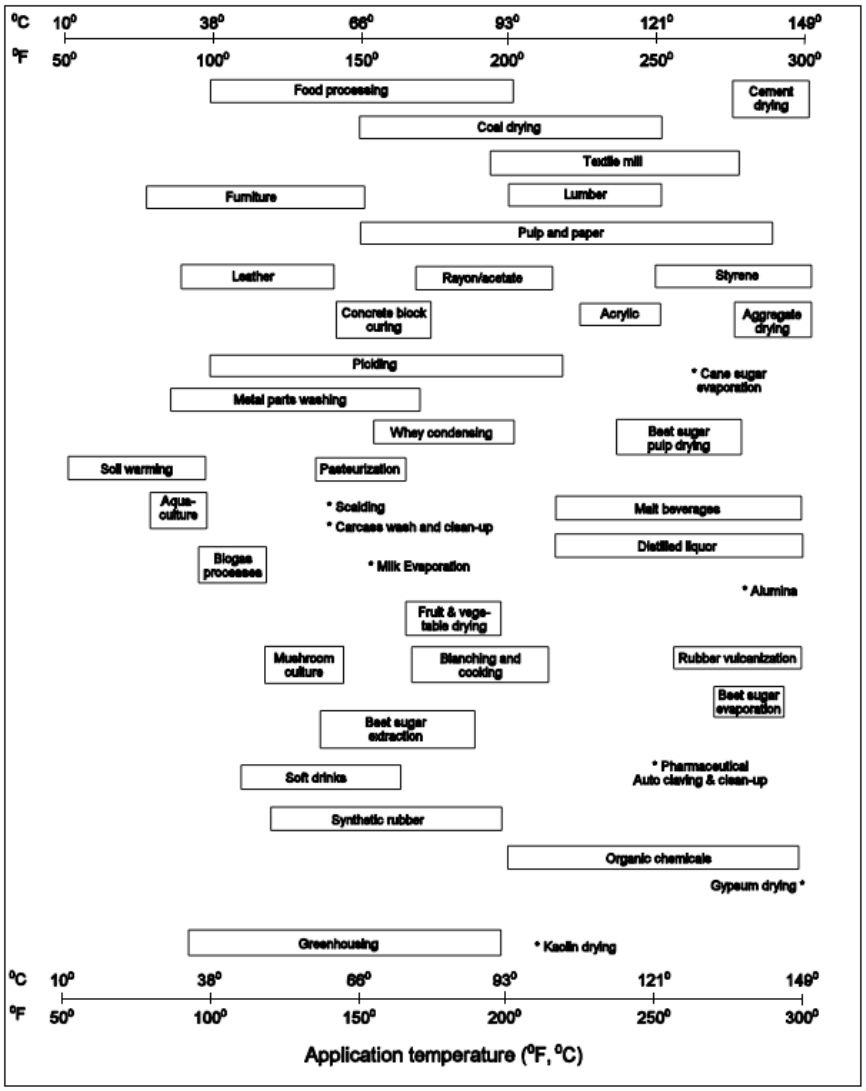

Figure 7. Geothermal direct use applications presented by required resource temperature (Lienau et al., 1994)

2.2.2 Unconventional geothermal production

Hybrid power systems

Hybrid power systems (HPS) combine two or more electrical power generation methods into one system. A multitude of different resource combinations and schematic configurations exist for HPS application, several of which involve geothermal energy. One unifying attribute allowing geothermal systems to work in unison with other generation methods is the utilization of heat extracted by ORC systems. In power plants fueled by natural gas, the same ORCs can be used to extract heat from exhaust gas produced as a byproduct of combustion. Increases in overall system efficiency are shown in processes that can successfully combine the heat extracted in both of these systems. A successful demonstration of this concept is discussed further in Chapter 4 Section 3.2 of this study entitled *DOE Pleasant Bayou Design Well and Hybrid Power System.*

Co-production

The oil field presents many opportunities for producing energy from a resource that otherwise would be considered a nuisance. In the most basic scenario, waterdrive reservoirs or reservoirs undergoing secondary waterflood recovery will encounter large volumes of produced water as a field matures. As the percentage of water produced from the well increases, the economic value of the well decreases due to lower oil recovery and the high cost of produced water disposal. In fields fortunate enough to contain adequately heated reservoirs, the point at which a well is considered *watered-out* can be

extended. Two major pilot programs have begun developing and demonstrating various oilfield applications that are powered by the thermal energy contained in produced water.

The Huabei Oilfield, located in the Chinese province of Huabei, is one of nine *giant oilfields* currently producing in China. The term giant oilfield refers to those initially containing 500 MMbbl of recoverable oil (Hallbouty, 2003; Höök, 2010). *Decline curve analysis* performed by Höök et al. (2010) and displayed in Figure 8 shows a declined but stabilized field-wide production rate of just under 100 Mbbl/day. Decline curve analysis is one of the most commonly implemented hydrocarbon production forecasting techniques and is particularly suitable when detailed data is not available. Utilization of co-produced geothermal energy has been recently applied to production practices in many of these mature waterdrive reservoirs in order to sustain economically viable production. As of 2009, six wells were producing 97.8% water at temperatures above 248°F from the LB reservoir located in the Huabei field. After increasing the flow rate of the existing waterflood injection well, two previously abandoned wells were re-entered to increase the daily fluid production rate to roughly 18,000 bbl/day. This allowed for operation of a 400 kW binary unit and subsequent transmission of 310 MWh of electricity to the grid, while increasing the watercut by only 1.1%. (Xin et al. 2012).

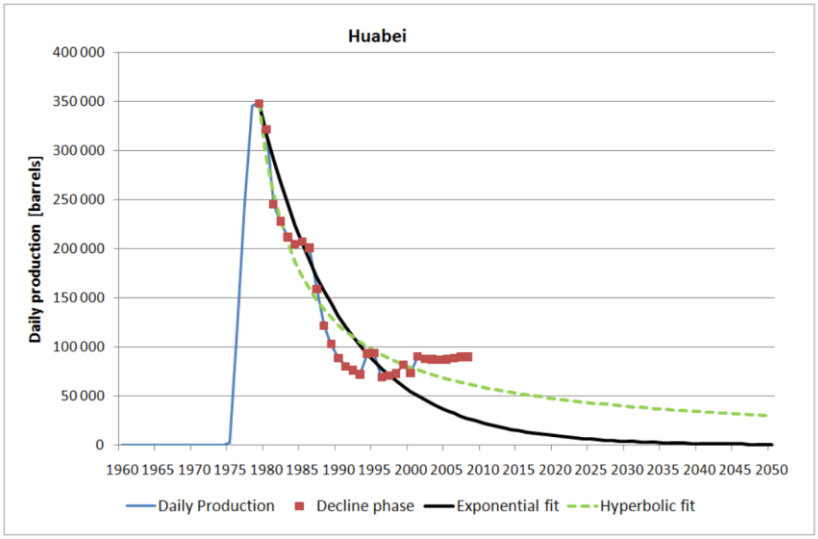

Figure 8. Huabei Field decline curve analysis (Höök, 2010)

A similar coproduction generation program was successfully demonstrated at what was formerly known as the Rocky Mountain Oilfield Testing Center (RMOTC), just north of Casper, Wyoming. Now property of the Stranded Oil Resources Corporation, the RMOTC was previously operated by the DOE as a testing ground for new oilfield technologies and processes. In 2008, an Ormat Energy Converter successfully generated electricity from coproduced fluids at capacities ranging from 150-250 kW. Since then, several coproduction projects have been funded through the American Recover and Reinvestment Act of 2009, including demonstration plants in North Dakota, Utah, and Texas (DOE GTP, 2010). Direct use geothermal applications also exist within the oilfield environment. Li et al. (2012) suggests using geothermal heat for *trace heating*, a process that lowers the viscosity of produced oil, making it easier to transport via pipeline. Utilization of geopressured geothermal fluid has also suggested for thermal enhanced oil recovery in the Gulf of Mexico coastal region (John et al., 1998). Most

recently, the "Energy Policy Modernization Act of 2016" (S.2012—114th Congress) has gained US Senate approval and seeks to amend several federal statues related to geothermal energy, including the Geothermal Steam Act of 1970 (30 U.S.C. 1003(b)). §3007 of this adds the following language to 30 U.S.C. 1003(b) in order to facilitate more coproduction of geothermal energy with oil and gas:

> *--Land under an oil and gas lease issued pursuant to the Mineral Leasing Act (30 U.S.C. 181 et seq.) or the Mineral Leasing Act for Acquired Lands (30 U.S.C. 351 et seq.) that is subject to an approved application for permit to drill and from which oil and gas production is occurring may be available for noncompetitive leasing…to provide for the coproduction of geothermal energy with oil and gas.*

Well-bore heat exchangers

When a hydrocarbon well reaches the end of its economically productive life, the production company is responsible for plugging and abandonment costs as well as restoration of the well site. Despite the benefits of field-wide pressure regulation, prevention of intra-field gas migration, prevention of cross-contamination from other productive zones, and protection of fresh water aquifers, this procedure is commonly seen as a cost that provides little benefit to the company abandoning the well (Operations and Environment Task Group, 2011). An alternative to this end of life cost could come from retrofitting the unproductive hydrocarbon well into a geothermal production system known as a well bore heat exchanger (WBHX). This transition is accomplished by

sealing the bottom and producing intervals of the well and altering the downhole components to allow for annular injection and concentric production flow. A diagram of this downhole flow scheme is shown in Figure 9.

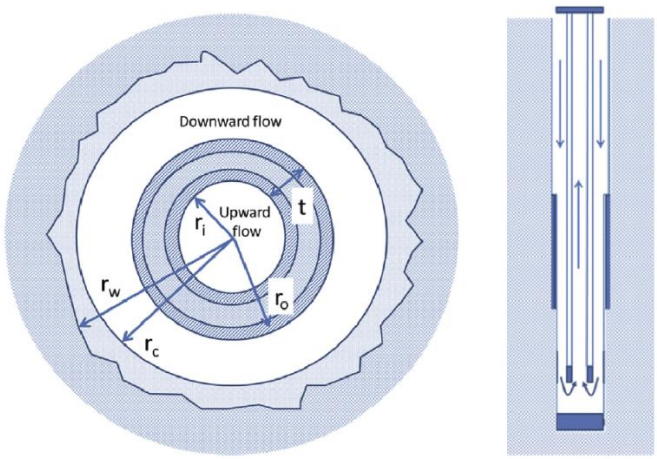

Figure 9. Simplified well bore heat exchanger diagram and flow pattern (modified from Alimonti and Soldo, 2016)

These hypothetical systems operate by extracting subsurface heat via conduction through the perimeter of a well bore. A circulating fluid is injected through the annular space of the well, reaches a maximum temperature at the well bottom, and is carried to the surface through an insulated production tubing. This method has previously been applied for direct use (Kohl et al, 2002; Lund, 2003), but no current power generation exists using this model. Several studies have analyzed the theoretical capability of such a system to generate electricity through ORC and flash steam processes. These studies considered varying resource characteristics (bottom hole temperature, depth, formation thermal conductivity), system characteristics (well bore dimensions, working fluid selection, flow

rates, thermal properties), and numerical modeling assumptions. Several of these studys are summarized below.

Nalla et al., (2004) HDR Application

Under commission of the DOE, the Idaho National Laboratory conducted an investigation into the design variables that govern the effectiveness of the WBHX model for environments representing HDR conditions. In this study, Nalla et al. (2004) present a numerical model created in the simulator TETRAD, a commercially available software package often used in geothermal reservoir simulations. Among other objectives, this model was used to generate an assumption of the ideal work rate within WBHX systems. The ideal work rate is defined as the amount of energy contained within the system that can be converted into usable work. Simulated runs of this model included a base case, several iterations of sensitivity analysis, and a best case scenario. The base case represented conventional geothermal drilling specifications which included a 12.25-inch wellbore (r_w = 6.125 inches in Figure 9), 3-inch production tubing (r_i=1.5 inches), a total depth of 18,350 feet, and a formation temperature of 662°F. The circulation rate of the simulation was set to 100 gpm (22.7 m^3/hour). Pseudosteady-state conditions (PSS) were observed after about 500 simulated days, and resulted in an ideal work rate of 129 kW. The sensitivity analysis compared variances in the following inputs: circulation rate, well diameter, well depth, casing length, tubing properties, working fluid properties, and formation thermal properties. Optimizing the offsetting relationship of the circulation

rate and effluent fluid temperature was determined to be of key importance in increasing the ideal work rate of the system, which is displayed in Figure 10.

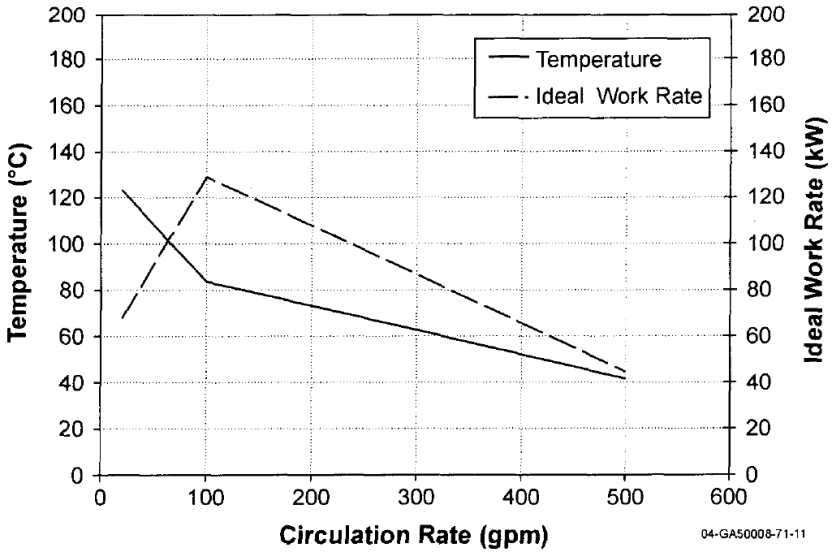

Figure 10. Parametric analysis results showing the relationship between circulation rate and effluent fluid temperature and ideal work rate (Nalla et al., 2004)

Another important result was observed upon modifying the thermal properties of the working fluid. It was found that the base properties of water resulted in the most ideal energy extraction. Finally, a "best case scenario" simulation was run with optimized inputs determined in the sensitivity analysis. This resulted in an ideal work extraction rate of 198kW. When this ideal work rate was applied to a commercially operating low temperature geothermal power generation system at the time of the study, the actual generation capacity was estimated to be less than 50kWe. This study does not state the specifications of this commercial generation system. The study concludes by stating that a WBHX system with such properties is not recommended for power generation but instead could be used in direct use applications.

Kujawa et al., (2006) Production Insulation, Circulation Rate, and Injection Temperature

The first WBHX model that proposed the use of abandoned oil and gas wells was developed by Kujawa et al. (2006). The dimensions of the wellbore considered in this model describe an abandoned well reaching a depth of 12,960 feet with a production casing radius (r_c) of 4.3 inches and a production tubing radius (r_i) of 1 inch. The assumed bottom-hole temperature was 222°F and the volumetric flow rates considered included: 2 m^3/hour (8.8 gpm), 10 m^3/hour (44 gpm), 20 m^3/hour (88 gpm), and 30 m^3/hour (132 gpm). Other parameters that were varied throughout simulation iterations include the injected water temperature and type of insulation protecting the production tubing. Calculated results of this model displayed in Table 1 only show ideal work rate and do not reflect potential conversion to electricity.

Table 1. Parametric analysis results showing the effect of varying circulation rates, injection fluid temperatures, and insulation materials on ideal work rate and effluent temperature. (Kujawa et al., 2006)

No.	$\dot{V}$, m^3/h	T_1, °C	Perfect insulation			Air gap			Polyurethane foam		
			T_2, °C	$\dot{Q}$, kW	Q, MWh/a	T_2, °C	$\dot{Q}$, kW	Q, MWh/a	T_2, °C	$\dot{Q}$, kW	Q, MWh/a
1	2	10	69.98	138.03	1163	64.42	124.68	1050	20.01	22.98	194
2	2	15	70.01	126.48	1065	64.53	113.35	955	20.57	12.77	108
3	2	20	70.03	114.92	968	64.65	102.17	861	21.08	2.48	21
4	2	25	70.04	103.39	871	64.76	90.91	766	21.64	–7.72	–65
5	10	10	44.68	400.97	3378	44.23	394.68	3325	17.39	84.96	716
6	10	15	45.63	353.73	2980	45.21	347.93	2931	19.98	57.28	483
7	10	20	46.56	306.54	2582	46.18	301.24	2538	22.63	30.20	254
8	10	25	47.53	259.51	2186	47.16	254.78	2146	25.24	2.70	23
9	20	10	31.67	502.53	4233	31.61	499.76	4210	16.72	154.76	1304
10	20	15	33.86	436.41	3676	33.79	434.03	3656	20.01	115.19	970
11	20	20	36.01	370.08	3118	35.94	367.97	3100	23.29	75.74	638
12	20	25	38.16	303.75	2559	38.10	301.95	2544	26.63	37.37	315
13	30	10	25.68	546.06	4600	25.68	545.04	4591	16.27	216.79	1826
14	30	15	28.55	471.05	3968	28.53	469.81	3958	19.87	168.19	1416
15	30	20	31.40	395.70	3333	31.39	394.57	3324	23.48	120.23	1013
16	30	25	34.25	320.37	2699	34.23	319.44	2691	27.11	72.93	614

This table shows that the ideal work rate is positively correlated to flow rate and negatively correlated to injected water temperature.

Davis and Michaelides (2009) Alternative Circulation Fluid

Davis and Michaelides (2009) sought to analyze the use of an alternative circulation fluid other than water to extract heat from the wellbore, while optimizing model inputs such as resource temperature, injection pressure, flow rate, and tubing radius. The selected circulation fluid was isobutane, which boils at a lower temperature and could potentially be produced from the WBHX in a supercritical state. This negates the need for a surface heat exchanger as the working fluid can be fed directly into a steam turbine. Well parameters chosen for this model come from data acquired from the Railroad Commission of Texas (RRC) and include a depth of 9,843 feet and a production casing radius (r_c) of 6 inches. The production tubing sizes considered include 3.5, 4, and 4.5-inch radii (r_i). Bottom hole temperatures varied between 287, 314, and 350°F. Injection pressures and fluid velocities involved in the parametric analysis are shown in Figure 11 along the x axis. When the model parameters are optimized to represent a BHT of 350°F, injection pressure of 30 bar, production tubing radius of 4 inches, and a fluid velocity of 3.5 m/s, predicted generation capacity reaches 3.4 MWe.

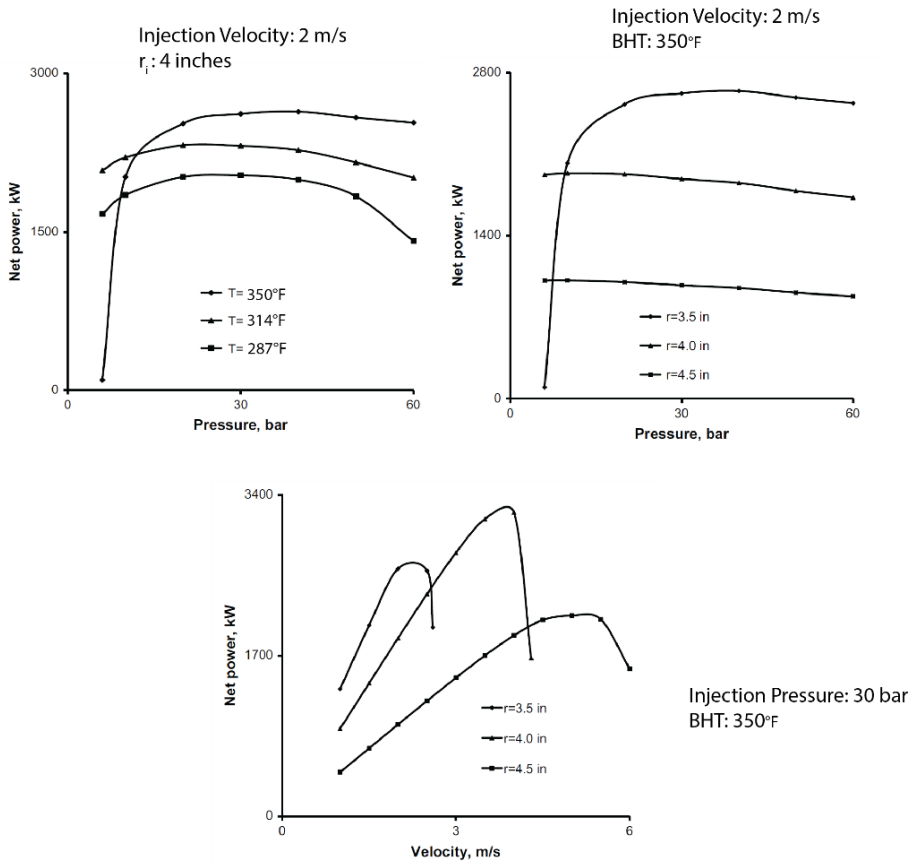

Figure 11. Parametric analysis of Davis and Michaelides (2009) WBHX model

Bu et al., (2012) Flash Steam WBHX

Bu et al. (2012) challenged the high capacity estimation posed by Davis and Michaelides (2009) by noting that their model did not account for any expected decrease in bottom hole temperature over time. Their model parameters included: a production tubing radius (r_i) of 2 inches, a production lining radius (r_c) of 6 inches, a depth of 13,123 feet, and a bottom hole temperature of 356 °F. This simulation found that circulated water would extract enough subsurface heat to vaporize and thus be able to generate power via the flash steam cycle. The fluid velocity was the only major parameter that was altered throughout the simulation. The relationship between effluent fluid temperature and fluid

velocity is shown alongside the associated mass flow rate in Figure 12a. It should be noted that when considering the flow of water, the mass flow rate unit of tonne/hour (t/h) is equivalent to the volumetric flow rate unit of m^3/hour. Both ideal work rate and net electrical power output were calculated with respect to fluid velocity in order to determine the optimum value for each. Figure 12b shows the ideal velocities for power production and thermal load demand to be 0.03 m/s and 0.05 m/s respectively. According to the plot shown in Figure 12a, these velocities correspond to mass flow rates of roughly 6.3 t/h and 10.6 t/h. Despite the initial challenge to the Davis and Michaelides (2009) model, Table 2 shows that the effluent temperature and associated energy production calculated from the optimized model conditions (fluid velocity = 0.03 m/s) did not decrease significantly over time.

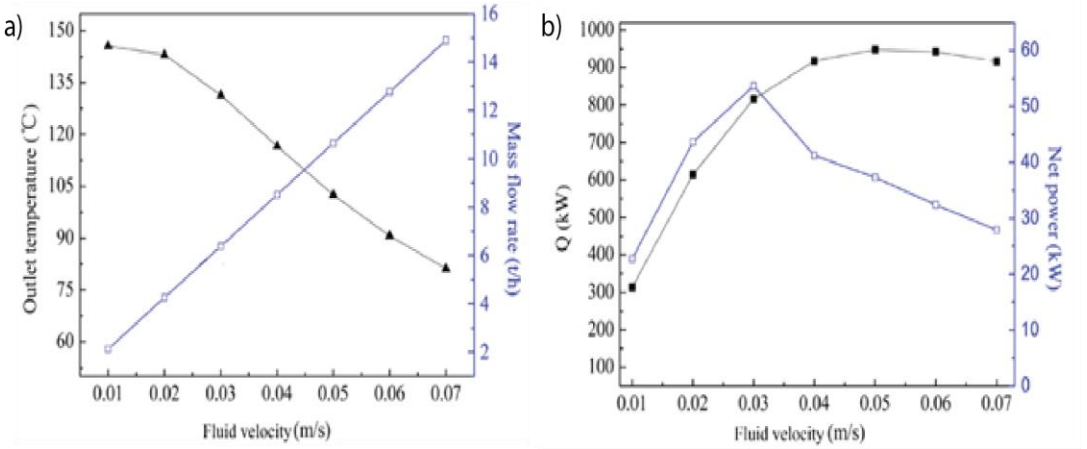

Figure 12. Circulation rate parameter optimization for effluent fluid temperature, electricity production, and ideal work rate (modified from Bu et al., 2012)

Table 2. Modeled results for fluid velocity =0.03m/s (modified from Bu et al., 2012)

Time (year)	T_{out} (°C)	P_{net} (kW)	e	Q (kW)
1	129.88	52.26		802.14
2	129.28	51.69		796.94
3	128.93	51.36		793.93
4	128.69	51.13		791.81
5	128.50	50.96		790.18
6	128.35	50.81		788.85
7	128.22	50.69		787.73
8	128.11	50.59		786.77
9	128.01	50.50		785.92
10	127.92	50.42		785.17

Cheng et al., (2013) Lower Generation Capacity from Alternative Circulation Fluid

Isobutene was again considered as a possible well bore circulating fluid in the model presented by Cheng et al. (2013). Wellbore dimensions assumed in this model include a production casing radius (r_c) of 4.9 inches and a production tubing radius (r_i) of roughly 2 inches. The bottom hole temperature at the assumed depth of 19,685 feet was 491°F. Similar to the Davis and Michaelides (2009) model, the circulating fluid velocity was varied to determine optimum conditions. Figure 13 shows a peak velocity of 0.18 m/s, roughly an order of magnitude less than the optimum velocity of Davis and Michaelides (2009). This chart, similar to Figure 12 from Bu et al. (2012), also attempts to display the optimum fluid velocity for the maximum ideal work rate within the system, although no peak was reached. The studyed maximum net electrical power capacity of this modeled system is 154 kWe. This study mentions that many of the previous models, including the one developed by Davis and Michaelides (2009), ignored the formation heat transfer and fluid momentum transport equations. Another cause of relatively low net power capacity

could be the extreme depth of the well and the pumping power required to facilitate circulation.

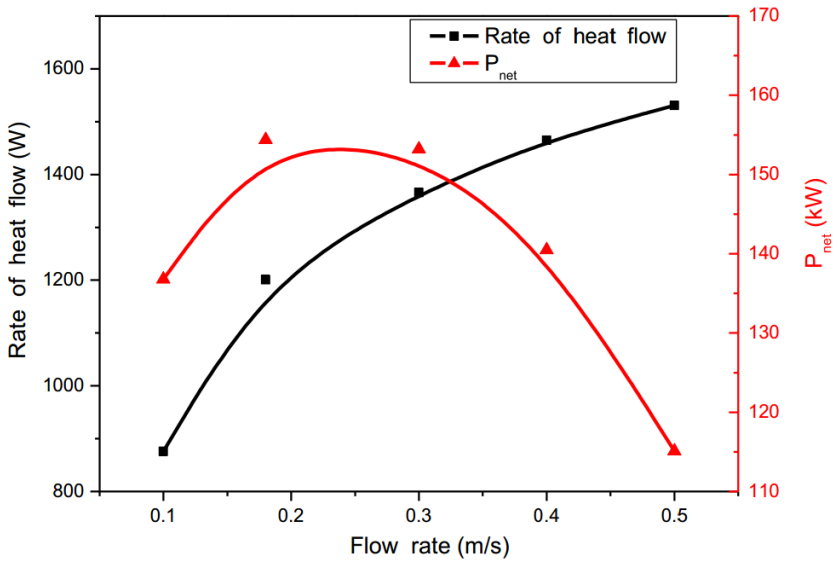

Figure 13. Relationship between flow rate and ideal/net work rate. (Cheng et al., 2013)

This study is concluded by noting that abandoned oil wells tapping hot geologic formations are often found clustered together. If these clusters could be connected, geothermal power output could potentially increase.

Templeton et al, (2014) Comparison of Previously Modeled Results

The final model assessed in this study comes from Templeton et al., (2014). Parameters from both Kujawa et al., (2006) and Bu et al., (2012) were imported into this model in order to compare simulated outcomes. Table 3 shows the comparisons against two iterations of the Kujawa et al., (2006) model for conditions reflecting different flow rates and fluid injection temperatures. Ideal work rates in the Kujawa et al. (2006) model

show overestimations of 25% and 135% for the lower flow rate simulation and the higher flow rate simulation respectively. This is studyedly due to an unrepresentatively low Nusselt number, which is used in determining convective heat transfer between the countercurrent injection and production flows.

Table 3. Comparison of the Templeton et al., (2014) model results to Kujawa et al., (2006) model results

Properties	Volumetric flow (2 m^3/h), T_{in} (10 °C)		Volumetric flow (30 m^3/h), T_{in} (25 °C)	
	Model results	Kujawa et al.	Model results	Kujawa et al.
T_{out} (°C)	52.73	64.42	28.88	34.23
Power (kW)	99.70	124.68	135.93	319.44
Nusselt#	72.8	9.1	145.7	52.4

The model comparison to Bu et al., (2012) is shown on Table 4. These results come from the parameters associated with optimum conditions as shown in Table 2. The suggested inaccuracies shown here are attributed to the use of the Dittus-Boelter relation, which describes convective heat transfer in smooth circular tubes. This relation loses accuracy when being applied to steep temperature gradients. Also, since the relation is applicable to circular tubes, the annular flow of the injected fluid is not accurately represented.

Table 4. Comparison of the Templeton et al., (2014) model results to Bu et al., (2012) model results

Properties	T_{out} (°C)		Power (kW)		Power overestimate
Year	Model results	Bu et al.	Model results	Bu et al.	
1	97.16	129.88	502.44	802.14	59.65%
2	94.46	129.28	482.22	796.94	65.26%
3	93.01	128.93	471.37	793.93	68.43%
4	91.99	128.69	463.78	791.81	70.73%
5	91.25	128.50	458.26	790.18	72.43%
6	90.62	128.35	453.49	788.85	73.95%
7	90.12	128.22	449.76	787.73	75.15%
8	89.72	128.11	446.76	786.77	76.10%
9	89.30	128.01	443.68	785.92	77.14%
10	88.97	127.92	441.19	785.17	77.96%

This study also discusses the implications of variations in injection fluid temperature. This study's modeled outcomes imply that a binary system would be limited to a re-injection temperature of 70°C (158°F), resulting in an ideal work rate of 40kW. This thermal power capacity would then be reduced further by the poor mechanical/electrical conversion efficiency.

3.0 GEOTHERMAL THERMODYNAMICS

It is important to have a general knowledge of basic thermodynamic principals in order to fully grasp the importance of each parameter controlling a geothermal energy production system. This section will briefly review certain elementary thermodynamic concepts and how they relate to the production of geothermal energy. Information presented in this section, including multiple equations and figures, is taken from William E. Glassley's text, *Geothermal Energy: Renewable Energy and the Environment* (2010).

3.1 First Law of Thermodynamics: Conservation of Energy

The first law of thermodynamics states that energy can neither be created nor destroyed and that all forms of energy are equivalent. When applying this concept to the inputs that control geothermal energy, such as heat contained in brine and mechanical energy generated in the turbine, energy is able to be transferred from one form to another throughout the system. This demonstrates that energy is conserved. This energy, when contained within a closed system described by certain *parameters of state* (temperature, pressure and volume), is called *internal energy*. Internal energy will only change in response to changes in the parameters of state within a given system. Pressure and temperature are changed by adding or removing heat from the system or by forcing work to be done to or by the system. This can be described by the following equation:

$$\Delta E = q + w \quad (2)$$

$$where:$$

$$\boldsymbol{\Delta E}\ is\ the\ change\ in\ internal\ energy$$

$$\boldsymbol{q}\ is\ heat\ added\ (positve\ value) or\ removed\ (negative)\ from\ the\ system$$

$$\boldsymbol{w}\ is\ work\ done\ to\ (positive\ value) or\ performed\ by (negative)\ the\ system$$

Work within a system is performed when a force related to the system is applied to and displaces a point or surface. In this sense, work can be defined as follows:

$$w = -P \times \Delta V \tag{3}$$

$$where:$$

$$\boldsymbol{w}\ is\ work$$
$$\boldsymbol{P}\ is\ pressure\ (constant)$$
$$\Delta\boldsymbol{V}\ is\ change\ in\ volume\ of\ a\ system$$

In a system in which a volume changes while retaining a constant system-wide pressure, the internal energy is a function work caused by a change in volume and the heat added to or removed from the system. This is demonstrated by substituting equation 2 for *w* in equation 1, as shown below:

$$\Delta E = q + -(P \times \Delta V) \tag{4}$$

The value of heat added to or removed from this system of constant pressure is called *enthalpy* (H). When applied to a geothermal system, enthalpy describes the useful energy that can be extracted from the geothermally heated fluid, which is measured in terms of joules of heat per kilogram of fluid (J/kg).

3.2 Second Law of Thermodynamics: Efficiency, Entropy, and the Carnot Cycle

In an ideal system, all of the energy contained in a specific amount of heat would be transferred to work. Mathematically, this system would be expressed by the following equation:

$$e = \frac{-w}{q} = 100\% \quad (5)$$

$$where:$$

$$e\ is\ the\ efficiency\ of\ the\ system$$
$$w\ is\ work\ done\ by\ the\ system\ (work\ done\ to\ the\ system\ would\ be\ positive)$$
$$q\ is\ heat\ added\ to\ the\ system$$

Ideal efficiencies of systems are typically studyed in terms of their *Carnot efficiency*, which illustrates the highest possible efficiency for a system operating between two temperatures. Carnot efficiency is based on the performance of the ideal Carnot cycle, displayed in Figure 14a. The Carnot cycle models a heat engine which converts thermal energy to mechanical energy *reversibly* and *adiabatically*. A process is considered reversible when each step of the process is carried out at equilibrium. The term adiabatic refers to a situation in which changes in initial state parameters, such as temperature and pressure, result directly from work performed on the system. While this is an ideal abstraction and such conditions are not realistically attainable, it allows for an important illustration comparing how heat, work, and efficiency are related. One such comparison that is useful in determining the efficiency of geothermal applications is commonly referred to as thermodynamic efficiency:

$$\eta = \frac{T_h - T_c}{T_h} \quad (6)$$

$$where:$$

$$\eta\ is\ the\ thermodynamic\ efficiency\ of\ the\ system$$
$$T_h\ is\ the\ temperature\ entering\ the\ system\ (hot)$$
$$T_c\ is\ the\ temperature\ exiting\ the\ system\ (cold)$$

This efficiency equation is derived from the adiabatic expansion and compression that takes place in the ideal Carnot cycle. The above equation demonstrates that the greater the temperature difference ($T_h - T_c$), the higher the efficiency.

Entropy is defined as the unattainable heat that is lost in the process of moving heat through a cycle. One way of illustrating this concept is through repetitive iterations of the Carnot cycle. As each run of the cycle takes place, the hot reservoir becomes cooler and the cold reservoir becomes warmer until they reach the same temperature. At this point, the system has reached maximum entropy. Entropy can also be described in terms of the amount of heat added to the system at a given temperature. As heat is added isothermally, the entropy rises. This can be seen in the following equation:

$$dS = \frac{dq}{T} \tag{7}$$

$$where:$$

$$dS\ is\ the\ change\ in\ entropy$$

$$dq\ is\ the\ amount\ of\ heat\ added\ or\ subtracted\ from\ the\ system$$

$$T\ is\ the\ temperature$$

Displayed alongside the physical model of the Carnot cycle are common diagrammatic depictions of the Carnot cycle including a pressure-volume (PV) diagram (Figure 14b) and a temperature-entropy (TS) diagram (Figure 14c).

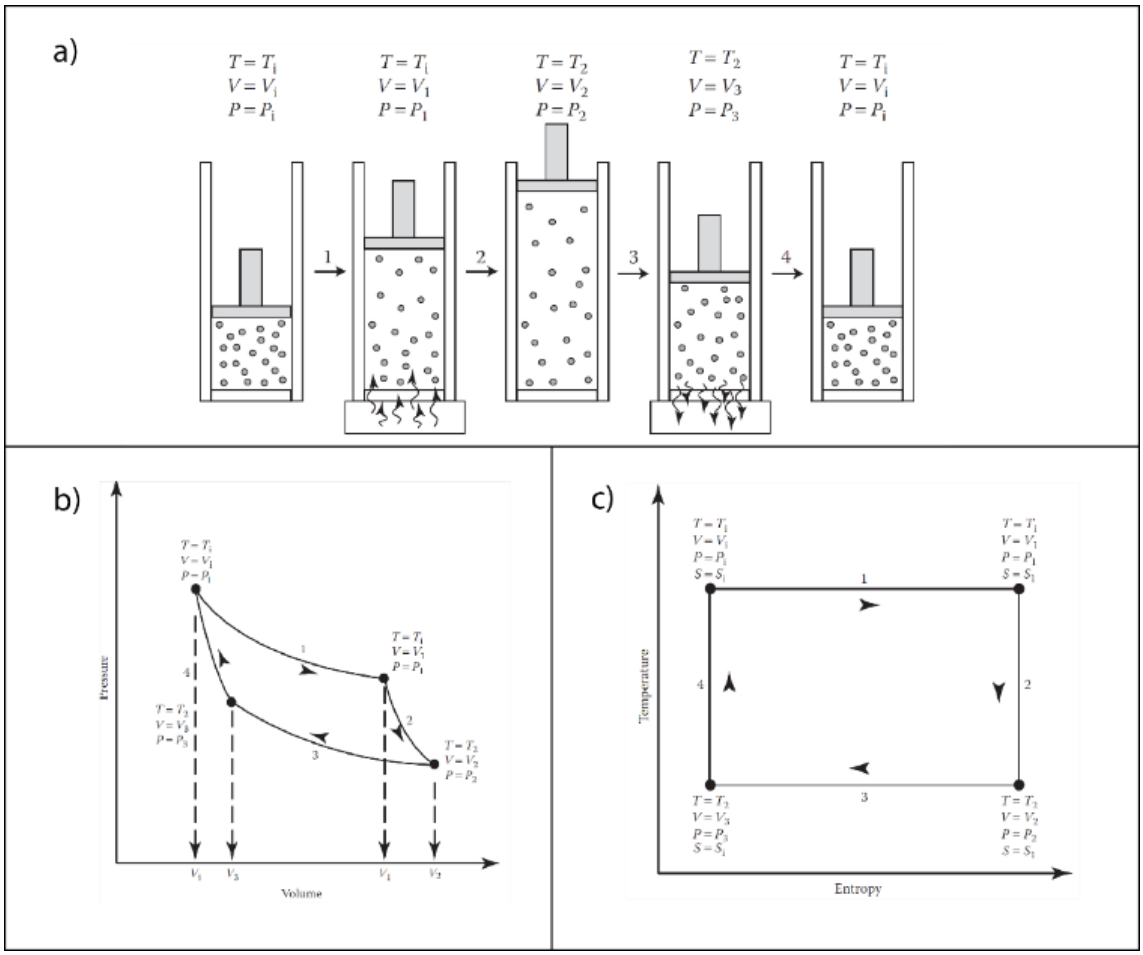

Figure 14. (a) Illustration of a Carnot power cycle, depicting the interaction of gas-filled cylinder with a frictionless piston. PV (b) and TS (c) diagrams describe various thermodynamic properties at each stage of the cycle. (Glassly, 2010)

3.3 Thermodynamics of Geothermal Resource Classification and Production

3.3.1 Conventional Geothermal Thermodynamics

The same diagrams that describe the ideal Carnot cycle are used to describe geothermal resources and power plant cycles that generate electricity from geothermal energy. Figure 15 displays a fluid phase curve with generalized pressure and volume values

plotted for different resource types. The phase of a particular resource affects the utilization of the heat contained in it. This diagram is a useful representation of how various resources differ in terms of the produced phase and the steam *quality* contained in that phase. Quality in this sense refers to the vapor to liquid ratio of a fluid. This is important to note when considering what type of energy production method to utilize.

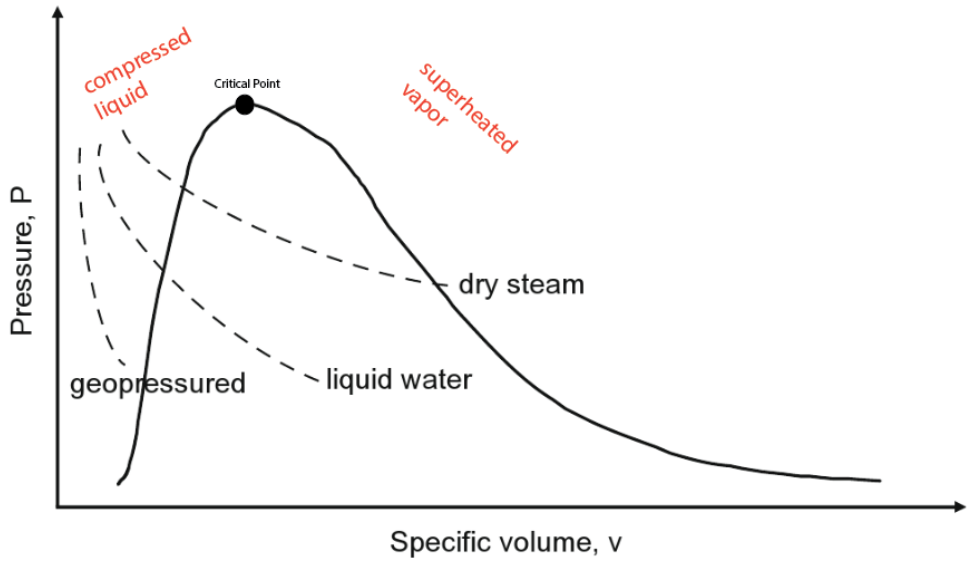

Figure 15. PV diagram for various geothermal resources (modified from Michaelides, 2012)

The solid line in the above diagram represents the phase boundaries of the working fluids in each system. Under this curve, liquid and steam coexist in equilibrium. Outside of the curve and to the left of the critical point, the working fluid is a liquid phase. Outside of the curve and to the right of the critical point, the working fluid is a steam phase. As the pressure decreases throughout production, the dry steam curve in the diagram approaches a quality of 100%, meaning it could be fed directly into a dry steam generation system. The liquid water curve never reaches the vapor boundary and would be produced as a

mixed phase fluid, containing both liquid and steam. This fluid would require flashing and separation before being used for generation. Flashing occurs when a liquid phase fluid containing some amount of heat is subjected to a rapid pressure drop. As the pressure drops, the fluid vaporizes and loses some amount of its heat. This process is shown in the upper T-S diagrams displayed in Figure 16. The geopressured trend never reaches the mixed phase boundary and stays a liquid throughout the entire production process. This demonstrates that geopressured resources are reliant on the binary system method of production.

The same diagrams that describe the ideal Carnot cycle are used to describe steam and binary cycle power plants that generate electricity from geothermal energy. These power plants utilize different cycles to generate electricity from geothermal heat. Different utilization methods take different paths through the T-S diagram, as shown below in Figure 16. In the flash and dry steam T-S diagrams, the curve shows the phase curve shape of water. The binary cycle displayed in the bottom right diagram shows a phase curve of a selected working fluid other than water, such as isobutene as mentioned in the earlier section.

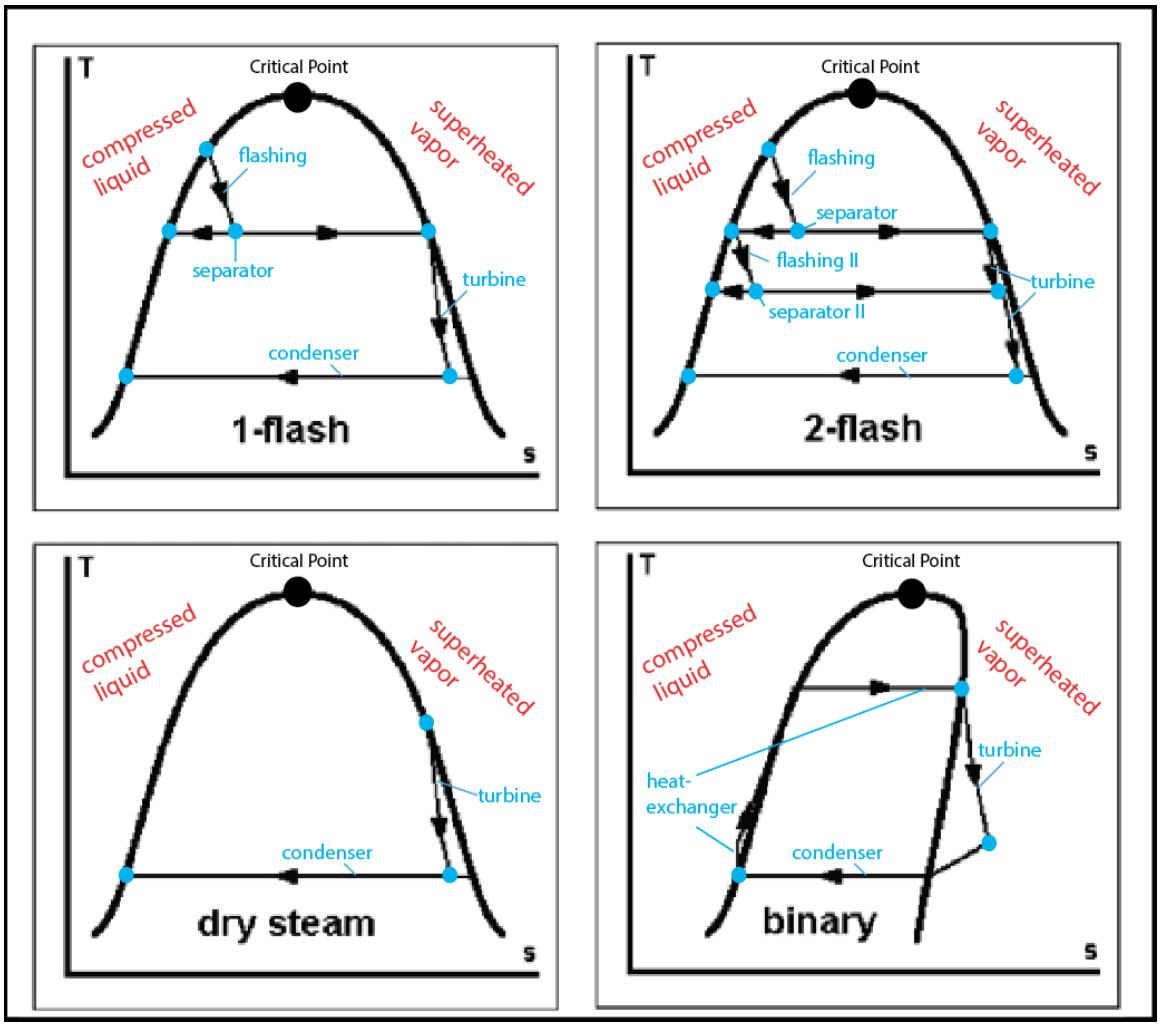

Figure 16. Simplified temperature-entropy diagrams for conventional geothermal generation (modified from DiPippo, 2012)

3.3.2 Unconventional geothermal thermodynamics

While most of the unconventional methods mentioned in Chapter 2 utilize the simple binary Rankine Cycle system, the two proposed WBHX models that simulated the use of isobutene as a circulating fluid utilize the *supercritical* Rankine Cycle. This power cycle allows for the extraction of thermal energy from *sensible heat* sources, which describes the heat variations related to resource temperature variability, instead of those related to

phase change. The ability to extract thermal energy at a variable temperature scale allows for more efficient operation due to increases in effective temperature differences (Gu and Sato, 2002). This process is shown in T-S diagram coordinates in Figure 17.

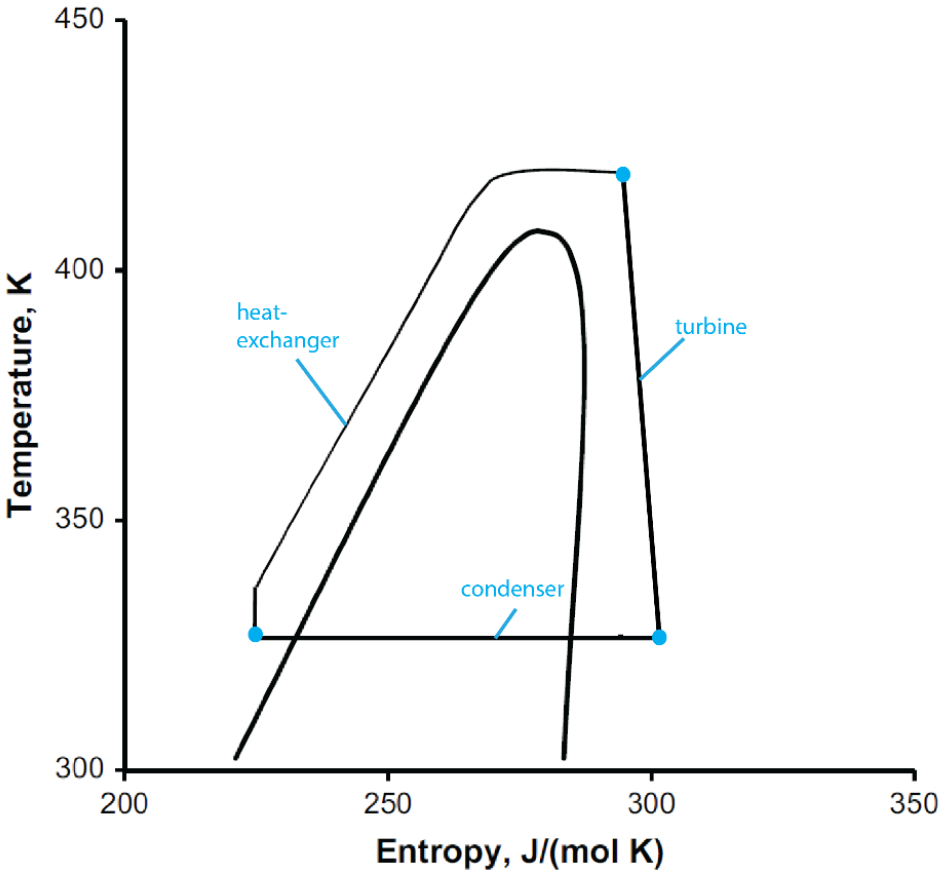

Figure 17. Temperature-entropy diagram for a supercritical power cycle (Modified from Davis and Michaelides, 2009)

4.0 NATURE OF GEOTHERMAL SYSTEMS IN TEXAS

Two plays were chosen for analysis: the growth faulted depositional wedges of the Tertiary System, and the tight sands present in the Jurassic Cotton Valley Group. Both of these plays contain geopressured gas reservoirs, most often created by the continued buildup overburden sediment on sand units that were hydraulically isolated during or shortly after deposition. Oil resources are not associated with these geopressured reservoirs, and therefore are not accounted for in this assessment. Each group/formation is given a general description in terms of its depositional environment, current geopressured gas production trends, geopressured gas reservoir properties, and previously studied geothermal fairways. Well data from the National Geothermal Data System (NGDS) was used to display spatial group/formation trends and associated bottom hole temperatures in the areas of interest. A total of 2,866 wells of the 42,601 well data set contained useful information regarding the stratigraphic bottom hole location of wells in the area assessed. The combined geologic, hydrocarbon reservoir conditions, and geothermal systems background presented in the following sections seeks to combine recent assessments from the oil and gas industry with previously supported investigations into geopressured-geothermal resources. Emphasis is placed on the maturity of natural gas field production within each group or formation by assessing existing accumulations and potential for growth. This was performed in order to determine groups and formations with significant numbers of operators potentially considering well abandonment in the near future. Wells tapping mature units, defined as those that have begun to experience significant production decline (Babadagli, 2007) would be

considered ideal candidates for unconventional geothermal resource development as described in the previous chapter. This strategy of utilizing oil and gas industry information for geothermal exploration was pioneered by the DOE Geopressured Geothermal Program in 1977 and has continued to be pursued by Southern Methodist University by way of the *Power Plays: Geothermal Energy in Oil and Gas Fields* conferences and access to the NGDS made possible by extensive oil and gas well survey. It is this same sentiment that drives the context and scope of this study.

4.1 Tertiary Depositional Wedge Geothermal Play

Tertiary system sediments were deposited as gulf-thickening wedges in the current Coastal Plains region of Texas. In their most downdip extent, these wedges thicken sharply due to the development of growth faults. These growth faults are often a result of denser sands being deposited on unconsolidated shelf-slope shales (Coleman and Galloway, 1990). The faults developed contemporaneously to sediment deposition (Bebout et al., 1978), which often results in significant expansion of the downthrown sediment strata (Ewing, 1986). Winker (1982) describes these expansive strata as mainly deltaic sequences which, upon faulting, are isolated from shallow water-equivalent sandstones, thereby forming a structural seal, commonly forming geopressured gas reservoirs. Figure 18 shows a general model for three of the four formations to be examined in the sections below.

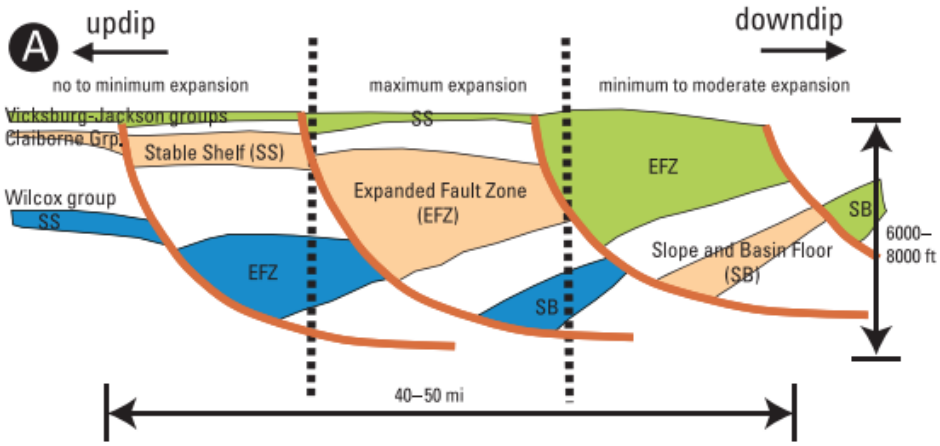

Figure 18. Conceptual model of growth faulted strata in the Texas Gulf Coastal Plains (Warwick et al 2007; altered by Hackley and Ewing 2010)

For regional geospatial reference, the Texas Coastal Plain is separated into south, central and east coastal plain regions as defined by Baker, 1995 (Figure 19).

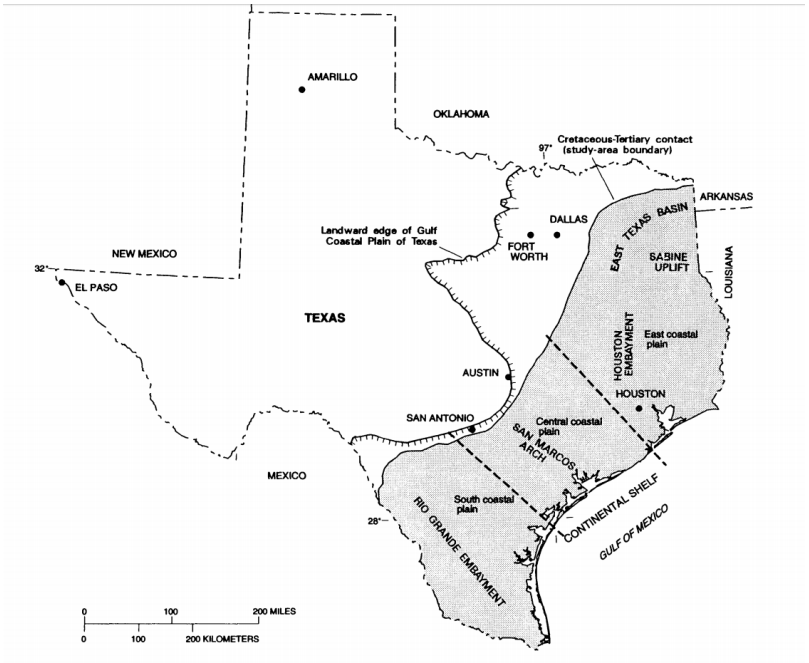

Figure 19. Index map of Texas Gulf Coastal Plains (Baker, 1995)

Three major growth fault trends, shown on Figure 20, exist within the Tertiary depositional wedge play: the late Oligocene Frio trend, the early Oligocene Vicksburg trend, and the Paleocene-Eocene Wilcox trend (Ewing, 1986). The specific groups and formations surveyed within this play include the Frio Formation, Vicksburg Formation, Claiborne Group, and the Wilcox Group.

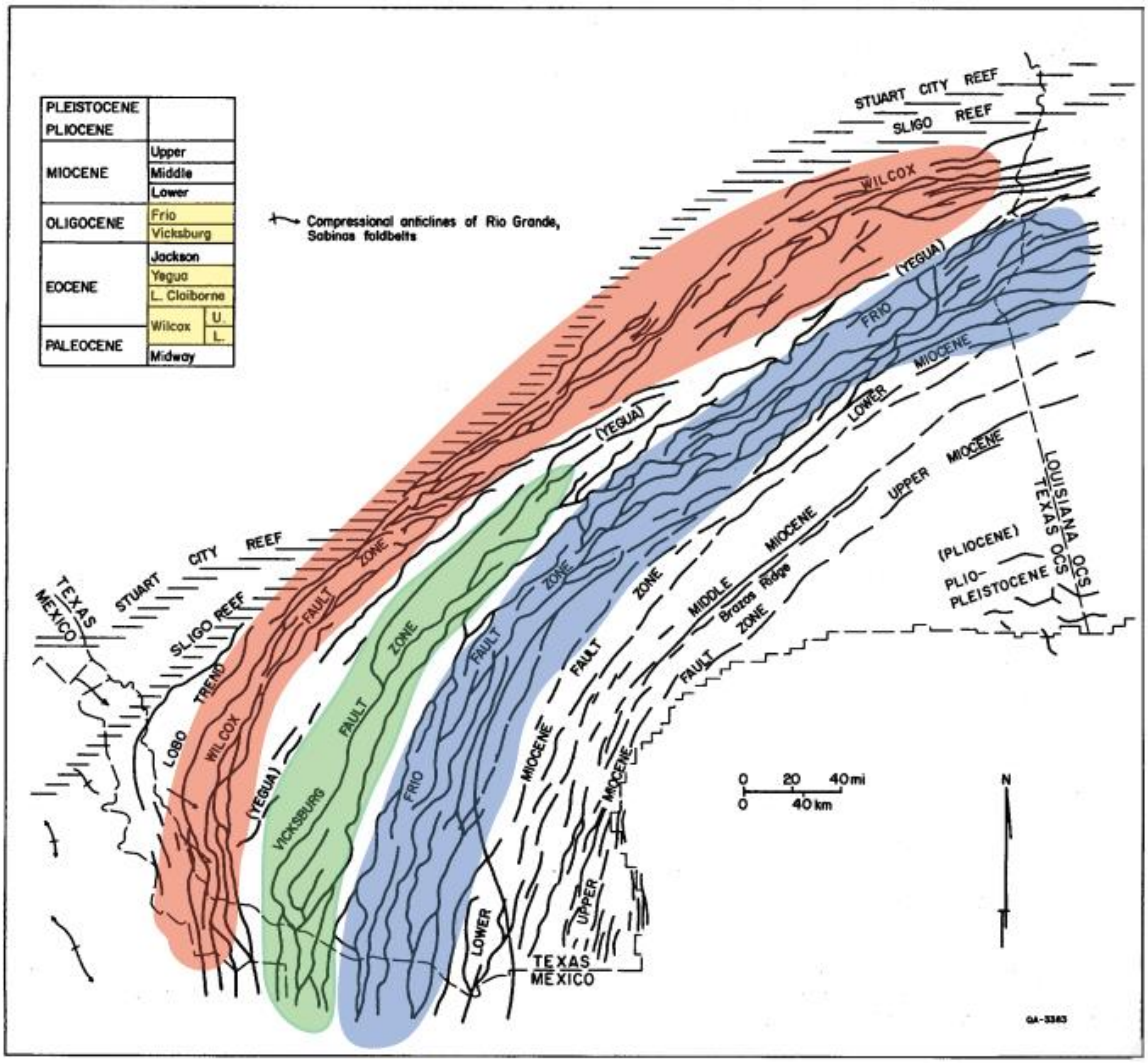

Figure 20. Growth fault trends and formations considered in the Tertiary depositional wedge play of the Texas Gulf Plains

4.1.1 Frio Formation

The Frio Formation is the youngest formation analyzed in the growth fault play. It is overlain by the Anahuac transgressive marine shale and lies on top of the Vicksburg Formation. Frio thickness ranges from less than 1,000 feet in its updip extent to more than 10,000 feet further down dip toward the present Gulf Coast. The Frio Formation trend observed from the NGDS is displayed in Figure 21. Candidate wells that tap reservoirs in the Frio Formation, as well as all formations present in the Tertiary depositional wedge play, trend parallel to the existing coastline. Being the youngest formation of a progradational wedge, Frio wells occur the furthest gulfward. Wells and predetermined geothermal fairways extend across south, central and east coastal plains.

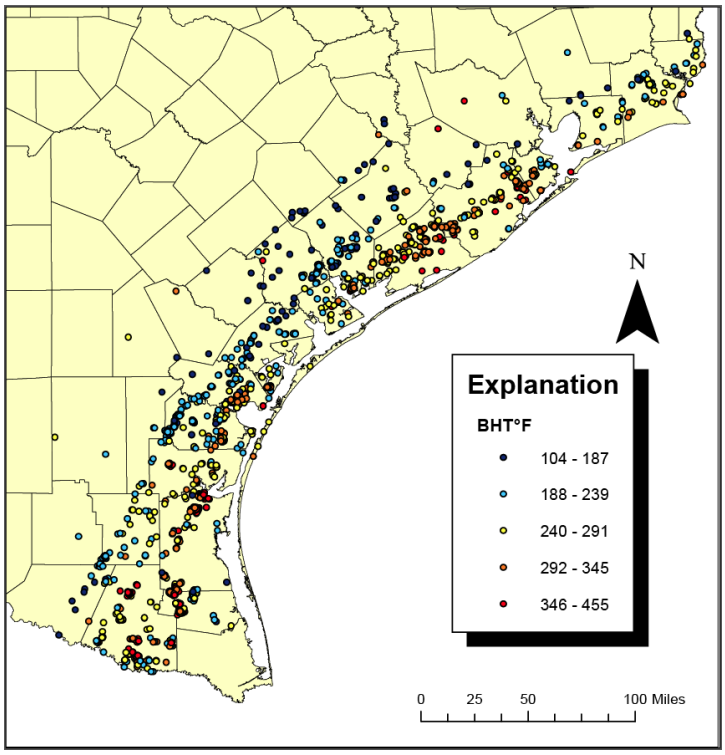

Figure 21. Frio Formation trend observed from NGDS wells.

Frio Depositional Environment

This gulfward thickening progradational wedge contains uplifted and eroded sediment from Mexico and the southwestern United States. The gulf-wide overall depositional environment of Frio/Vicksburg time as defined by Galloway et al (2000) is displayed in Figure 22.

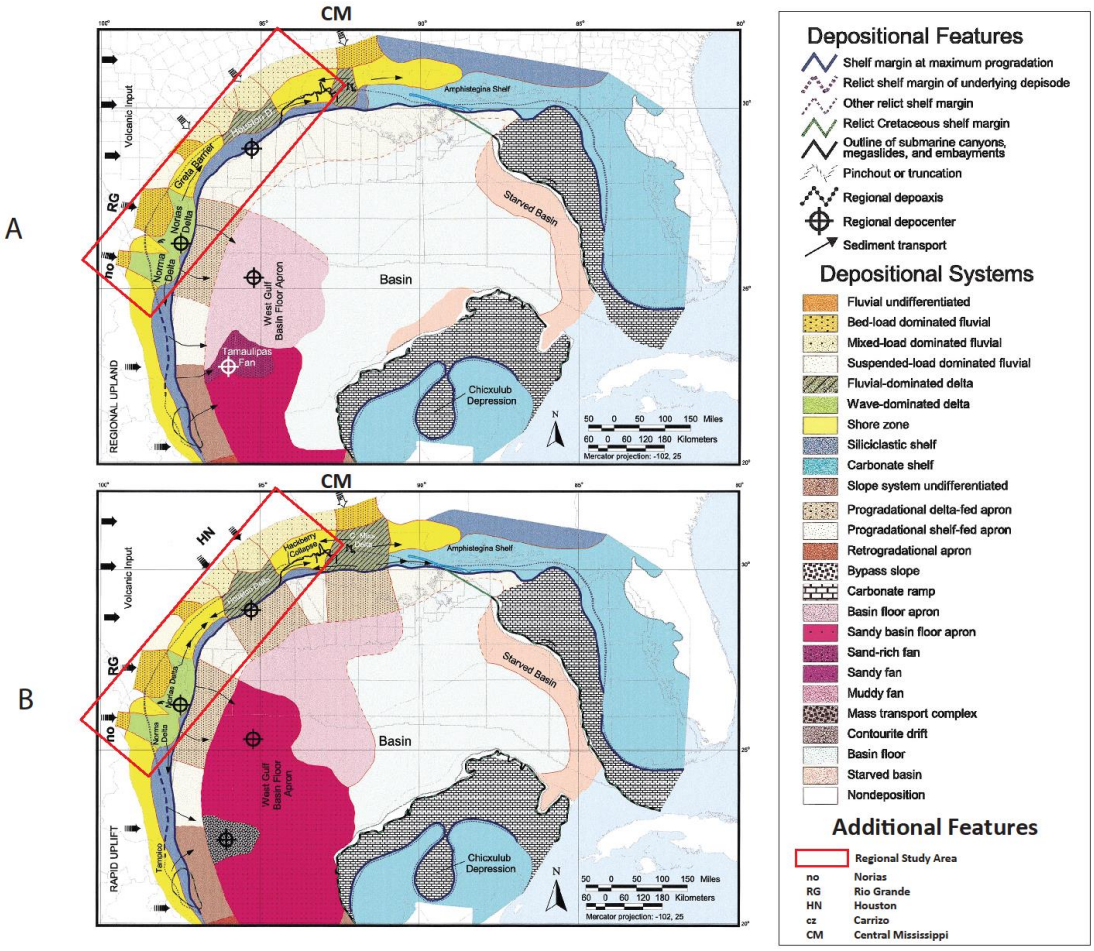

Figure 22. Depositional environments of late (a) and early (b) Frio/Vicksburg depisode (Galloway et al, 2000)

The late Frio/Vicksburg depositional map (Figure 22a) is more representative of Frio time given that the Frio is the younger of the two. In their 2000 AAPG bulletin,

Cenozoic depositional history of the Gulf of Mexico basin, Galloway et al (2000) introduced several sediment dispersal systems, referred to as dispersal axes, in order to describe the history of sediment influx into the Gulf. Principal areas of sediment dispersal of this time included the Norias and Norma deltas which lie on the major Rio Grande axis and secondary Norma axis respectively. Both Norias and Norma deltas represented sand rich, wave-dominated delta systems. Galloway et al. (2000), interprets the late Oligocene Gulf of Mexico to contain characteristics of long-term systems tract retreat. This is supported by the retrogradation of the Houston delta due to the slowing of sediment influx along its dispersal axis. Bebout et al., (1978) describe the principal sandstone distribution in the formation as elongated trends that lie parallel to the Gulf Coast, resembling barrier-bar and strandplain deposition. These specific facies architectures support the gradual transgression of the mid to late Oligocene described by Galloway et al. (2000)

Frio Geopressured Gas Production

Swanson et al. (2013) developed a total petroleum system (TPS) model for the Frio Formation. This model describes the necessary conditions needed for the development, migration, and accumulation of significant hydrocarbon deposits. Assessment Units (AU) were developed based on regional-scale structural and depositional features in Paleogene formations. AUs are defined as mapable volumes of rock that contain both discovered and undiscovered hydrocarbon fields that share similar geology and economics. The geographic distribution of Frio AUs and selected NGDS wells is shown

on Figure 23. This map shows that most high temperature wells lie in the Expanded Fault Zone, although several are also present in the Stable Shelf.

The Expanded Fault Zone is considered a mature exploration area with high well densities (IHS Energy Group, 2005; NRG Associates, Inc., 2006). 388 gas accumulations exceeding the minimum accumulation size (0.5 million barrels of oil equivalent (MMBOE)) have been discovered as of 2006 (NRG Associates, Inc., 2006). Cumulative oil and gas production curves can be seen in Figure 24 and 25. These curves display shapes that confirm the mature nature of the AU. A maximum of 130 undiscovered gas accumulations yielding a mean cumulative production of 1,321 bcf were estimated to be present in this AU. The majority of undiscovered gas accumulations are expected to be discovered in deeper extents of the AU (Swanson et al., 2013).

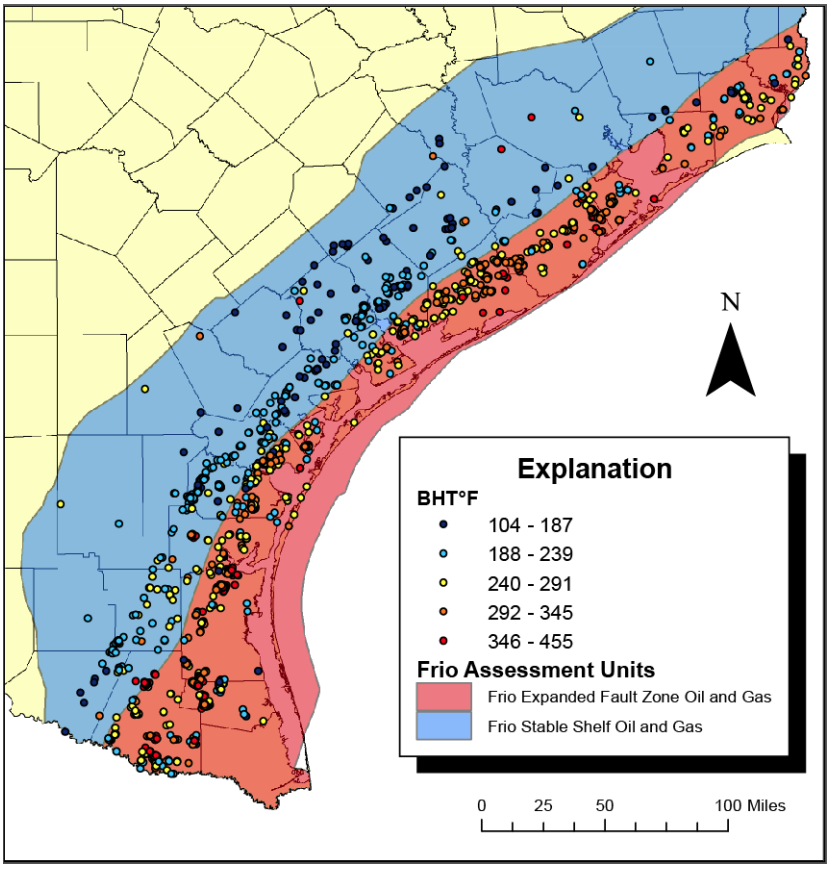

Figure 23. Frio oil and gas Assessment Units with NGDS wells (Swanson et al., 2013

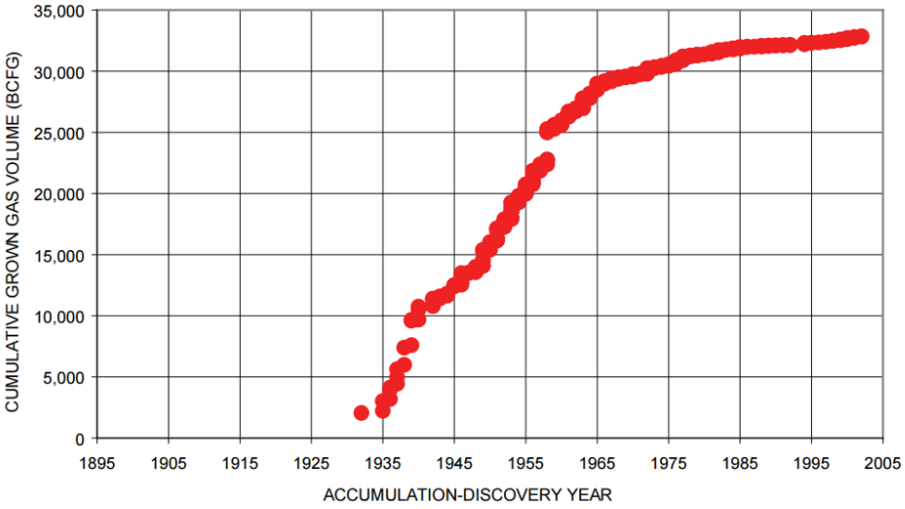

Figure 24. Peaking cumulative gas production trend in the Frio Expanded Fault Zone AU (NRG Associates, Inc., 2006; Swanson et al., 2013)

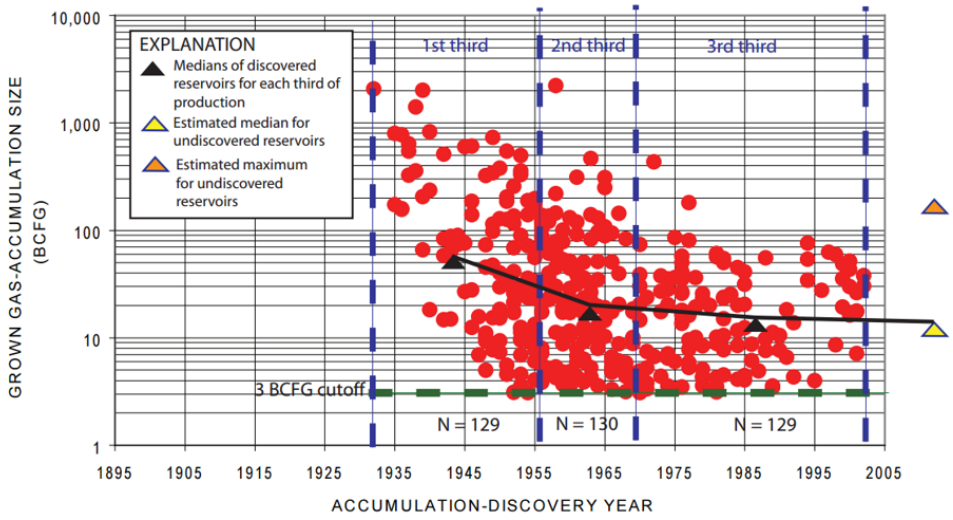

Figure 25. Downward trend in discovered Frio Expanded Fault Zone Oil and Gas accumulation size over time (NRG Associates, Inc., 2006; Swanson et al., 2013

Another forecasting study by Fisher and Kim (2000) was also assessed to determine maturity levels of fields that encounter Frio geopressured reservoirs, as well as geopressured reservoirs in the Vicksburg Formation, Claiborne Group, and Wilcox Group. The main directive of this study was to perform an ultimate recovery growth (URG) analysis of the Texas Gulf Coast Basin and East Texas. Six Frio Plays were selected based on studyed average completion depth and geographic location. Four of the six plays, including the Proximal Frio Sandstone, Rio Grande Embayment (FR-3); Downdip Frio Barrier/Strandplain Sandstone, San Marcos Arch (FR-6); Frio Sandstone, Houston Embayment (FR-9); and Frio Sandstone, Hackberry Embayment (FR-10) were considered "very mature," with average field discovery years between 1948-1961. The Distal Frio Deltaic Sandstone, Rio Grande Embayment (FR-1) and Frio Delta-Flank Shoreline Sandstone, Rio Grande Embayment (FR-2) are both described as "mature"

plays. Reserves in the Frio plays estimated as of 1996 range from 32-906 bcf. Figure 2 shows the locations of these specific plays and well data from the NGDS.

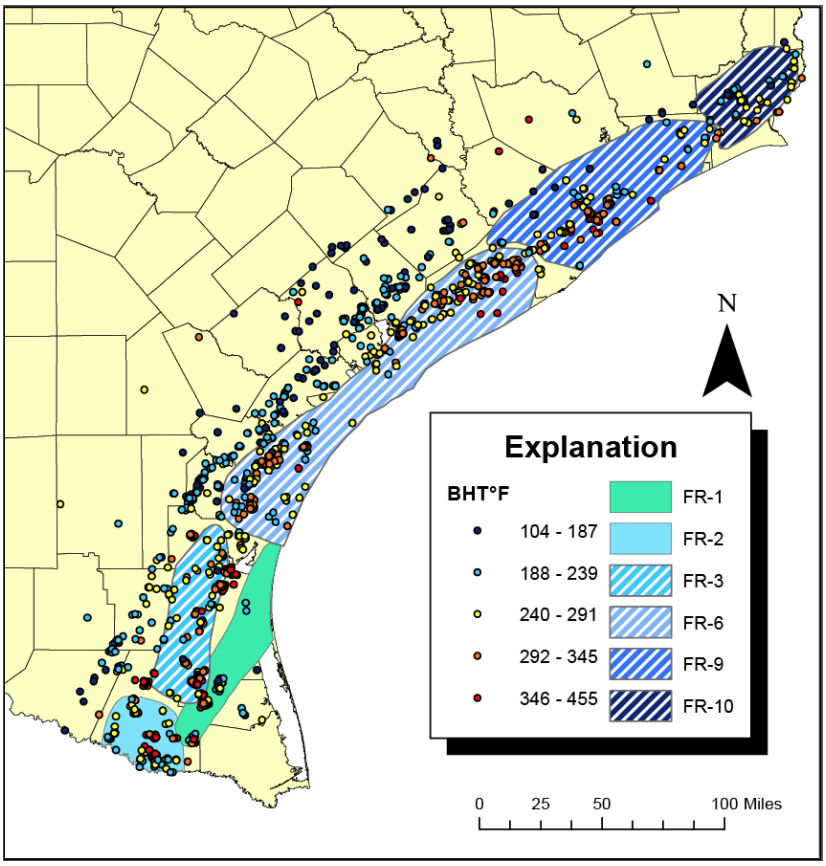

Figure 26. Fisher and Kim (2000) Frio play locations with NGDS wells.

Frio Geopressured Gas Reservoir Properties

Reservoirs within the Expanded Fault Zone of the Frio Formation and other fault zone AUs described below show extensive vertical thickening due to growth faulting. The average depth to these reservoirs is 9,050 feet. Permeability values vary from less than a few millidarcies in the south coastal plain to greater than 1,000 mD at 15,000 feet of depth in the central and east coastal plain (Loucks et al, 1984), with more conservative

but still high averages of 636 mD in the Expanded Fault Zone AU (NRG Associates, Inc., 2006). It should be noted that these values and many other values presented in this study are derived from core analysis, which are performed at atmospheric conditions. These measurements can be orders of magnitude higher than true in-situ permeability values (Loucks et al, 1984). In reservoirs deeper than 10,000 feet, development of secondary porosity controls the overall reservoir quality. At depth, quartz cement drastically reduces the primary porosity (Loucks, 2005). According to NRG Associates, Inc., average porosity is 27%, average reservoir pressure is 5,116 psi, and average reservoir temperature is 226 °F in the Expanded Fault Zone AU.

Frio Geothermal Fairways

Figure 27 shows Frio Formation study areas examined by three studys performed by the University of Texas' Bureau of Economic Geology (BEG).

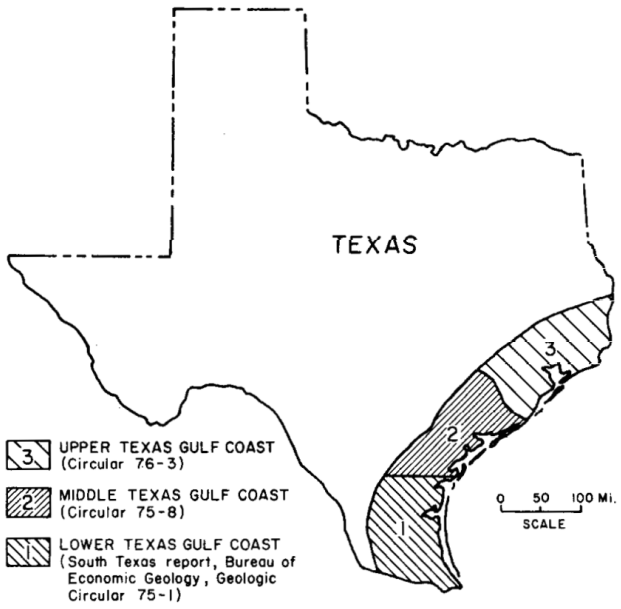

Figure 27. Study areas of Frio Formation geothermal surveys by the Bureau of Economic Geology (Bebout et al., 1978)

In each of the BEG studys, the formation was subdivided by six transgressive shales, referred to as "T markers". These subdivisions allowed for reservoir facies characterization, marker bound sand percentage maps, and the delineation of regional tops of geopressure structural contours that led to the development of the discrete fairway limits presented in Bebout et al., (1978). These areas include the Hidalgo, Armstrong, Corpus Christi, Matagorda, and Brazoria fairways. These fairways are displayed with selected NGDS wells on Figure 28. Three potential reservoir models were posited by Bebout et al., (1978) to represent the five fairways present.

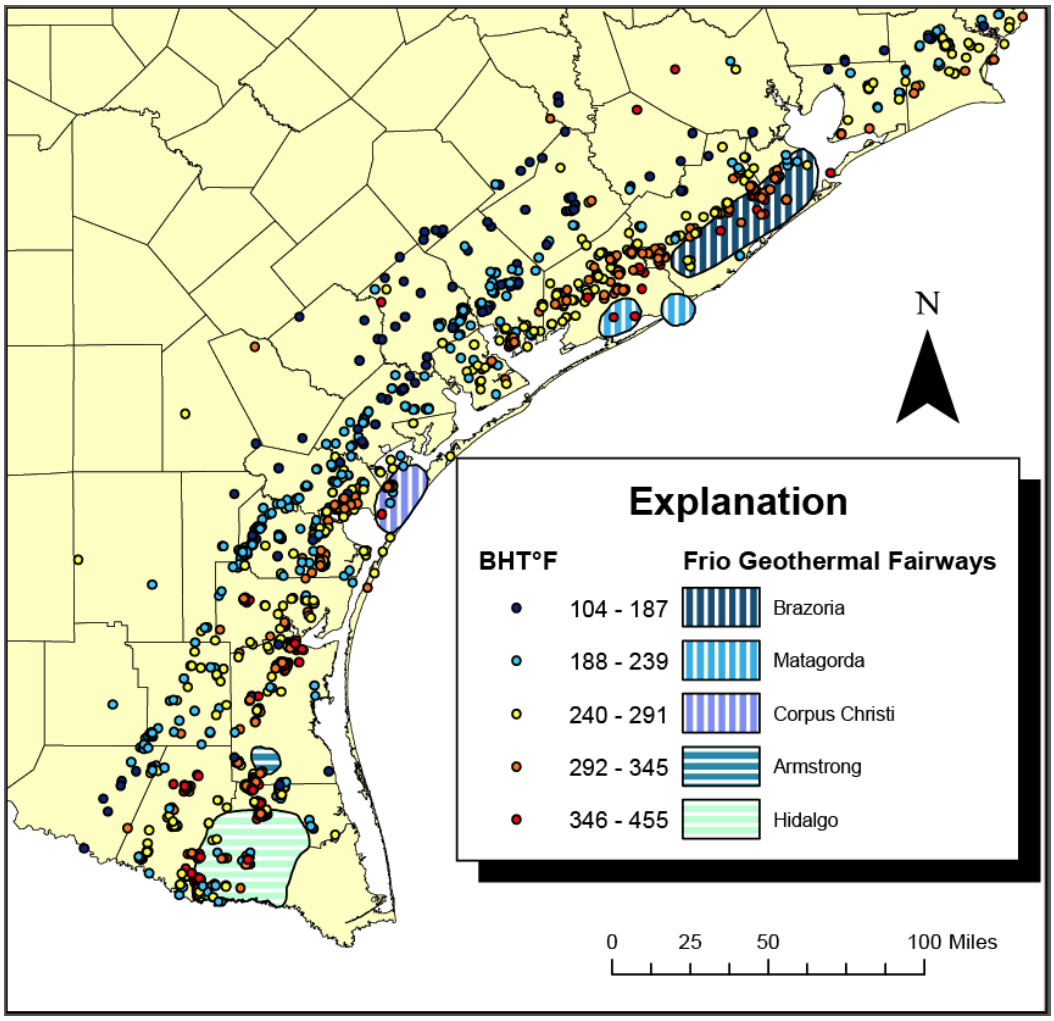

Figure 28. Frio geothermal fairways with NGDS wells (Bebout et al., 1978)

Model I encompasses reservoirs that anticipated to present in the Corpus Christi and Matagorda Fairways. Geopressured conditions are present below massive sandstones found at depths of 6000-9000 feet, resulting in temperatures of approximately 200 °F. Sands observed below the zone of geopressure are described as thin tongues that were separated from the main depocenter by post-Frio time growth faults. Distal ends of these sand tongues become thinner, finer grained, and reach temperatures of 300 °F. Bebout, Loucks, and Gregory (1978) considered neither fairways feasible due to the limited

vertical and lateral extent of the sand bodies and a regional lack of adequate permeability. Potential Corpus Christi reservoir sands interpreted between the T4-T5 markers lie updip or directly on the 200°F isotherm. Hotter sandstones exist in the T5-T6 interval downhole of the T4-T5 sands, however these sands range between 1-10 feet thick and are separated by equally thick shale sections. Porosity and permeability values averaging 9-22% and 5.3 mD respectively were determined from limited core data in this fairway (Seni and Walter, 1994). Three vertically extensive sandstone units of adequate temperature are believed to be present in the Matagorda fairway. The limiting factors here include low porosity and permeability values obtained from core samples in two of the three units. Cores in both of these fairways displayed favorable results in the upper extents of sands units, but showed very low porosities and permeability values in the deeper extents of sand.

Model II describes Frio sands present in the Hidalgo and Armstrong fairways. These potential reservoirs were deposited as high-constructive deltas and sandy strandplains which experienced syndepositional growth faulting resulting in significant thickening on the gulf side of the fault (Bebout et al., 1978; Bebout et al., 1975). Both fairways contain thick geopressured sand units that are laterally extensive. Factors limiting geothermal energy development in these fairways include permeability values of 1mD or less and low temperatures in the Armstrong fairway (Swanson et al, 1976; Bebout et al., 1978).

Model III describes the Brazoria fairway. This is the only Tertiary wedge geopressured-geothermal fairway that has been actively exploited for the generation of electricity. This

model interprets Frio sands in this area as deltaic in origin. High sediment levels during early Frio time resulted in rapid progradation and deposition of delta sands in large salt-withdrawal basins. Growth faulting that created geopressured conditions were caused by salt movement. Fault blocks down dip of growth fault zones are well correlated with the updip beds. Potential reservoirs in this fairway lie below the T5 marker (13,500 deep) in massive sandstones that locally exceed 1,000 feet in thickness. Deposition of these reservoir sands was interpreted to occur in a highly constructive deltaic environment (Fisher, 1969). Temperatures in excess of 300° and permeability values ranging up to hundreds of mDs make this fairway a primary candidate in terms of further conventional geopressured-geothermal production. Past development in the area, including the Pleasant Bayou #2 well, is discussed in section 3.3.2 *DOE Pleasant Bayou Design Well.*

4.1.2 Vicksburg Formation

Underlying the Frio Formation is the Vicksburg Formation. Within the study area, the formation is encountered at depths ranging between 3,000 and 5,000 feet and overlies the Jackson Formation. The Vicksburg Formation trend is displayed in Figure 29. Wells of interest and one predetermined geothermal fairway are located exclusively in the south coastal plain region that encompasses the Rio Grande embayment. Existing wells that tap the Vicksburg Formation are found along a similar trend to that of Frio wells.

Vicksburg Depositional Environment

The overall depositional environment of the early Oligocene Vicksburg Formation resembles that of the late Oligocene Frio Formation, although Galloway et al. (2000)

describe larger amounts of sediment influx during this pre-Frio time. Unlike the Frio Formation, Vicksburg sediment was dispersed via four axes: Norias, Rio Grande, Houston, and Central Mississippi, with the latter contributing less sediment and lying outside of the study area.

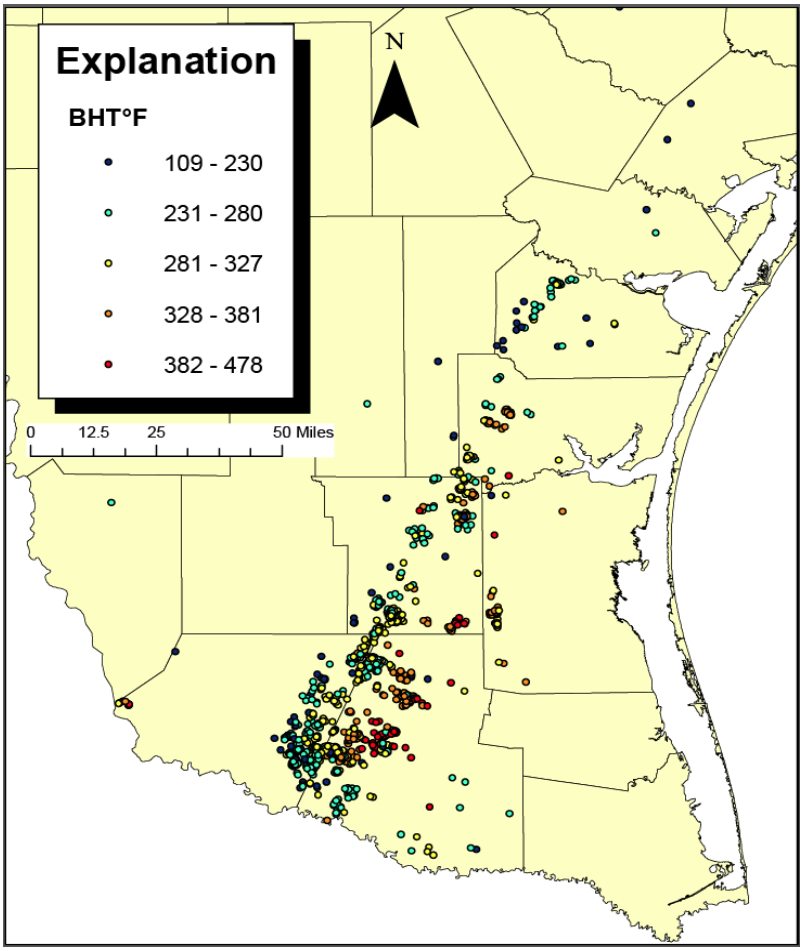

Figure 29. Vicksburg Formation trend observed from NGDS wells.

The overall depositional environment of this formation is displayed on Figure 22b. While the Norma and Norias deltas were also wave-dominated prior to Frio time, fluvial-dominated delta characteristics existed in the Houston axis area (Galloway et al, 2000).

The Vicksburg Formation is made up of these three major deltas rapidly prograding to the underlying Jackson shelf slope (Combes, 1993; Coleman and Galloway, 1990).

Vicksburg Geopressured Gas Production

In south Texas, several giant geopressured gas fields tap the Vicksburg Formation. These fields are largely associated with highly constructive shelf margin delta sands (Han, 1981; Loucks, 1978), although turbidite sands have also been interpreted in deeper strata of the formation (Dramis, 1981). Coleman and Galloway (1990) separate fields of this area into two plays, (wave-dominated deltas and barriers/stacked deltaic depocenters) while Langford et al (1994) classifies all fields of the Vicksburg Formation in the south coastal plain as the "VK-1" play. Of these fields, the McAllen Ranch is the most widely studied and will serve as a reference for hydrocarbon reservoir properties and production trends for this play. The A. A. McAllen No. 1 discovery well was completed in 1960. More than 770 Bcf of gas has been produced from 33 different reservoirs within the Vicksburg Formation in this field. Of these reservoirs, the designated "S" unit accounts for approximately 40% of the gas produced field-wide. Figure 30 shows the declining then revived production trend of the various reservoirs within this field. Individual wells in this field are estimated to produce 1-10 bcf of gas over a projected 20-year lifespan (Langford et al, 1994). USGS resource estimates for the larger scale Vicksburg Expanded Fault Zone Gas and Oil AU predicted a mean undiscovered gas volume of 9,511 bcf (USGS, 2007). Fisher and Kim (2000), also studyed on the Vicksburg Sandstone, Rio Grande Embayment (VK-1) play. As of 1996, reserves were estimated to be around

1,714 bcf leading to the qualitative classification of “mature”. The VK-1 play and NGDS well data are shown on Figure 31. The ultimate recovery growth of the VK-1 play was rated among the top of all plays assessed by Fisher and Kim (2000).

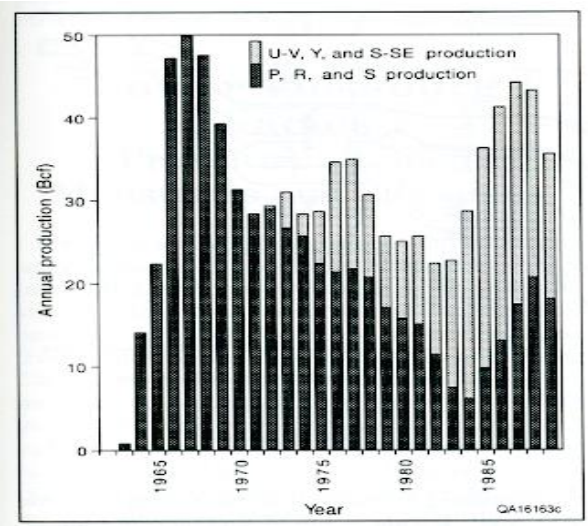

Figure 30. Production history from various reservoirs in the McAllen Ranch field (Langford et al., 1994)

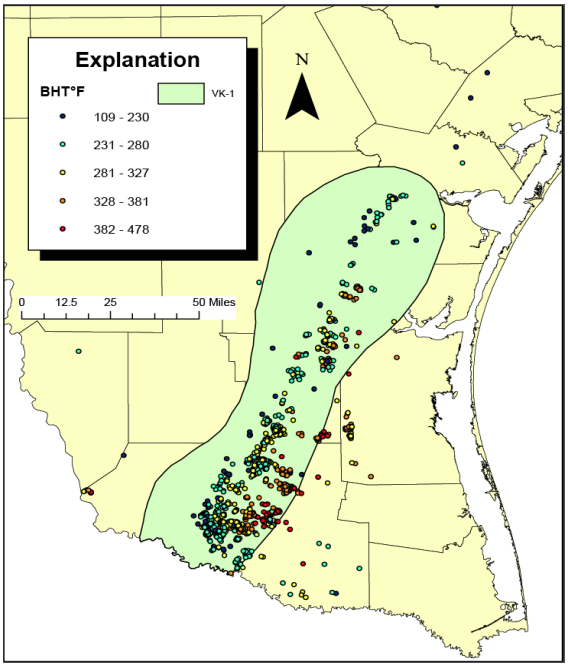

Figure 31. Fisher and Kim (2000) Vicksburg play location with NGDS wells.

Vicksburg Geopressured Gas Reservoir Properties

Sand units in the McAllen Ranch field reach geopressured conditions (measured as high as 0.94 psi per foot) at depths between 7,000 and 8,400 feet (Marshall, 1978; Berg and Habeck, 1982). The initial bottom-hole pressures observed in production of the S reservoir ranged between 10,800 and 12,500 psi. 535 air permeability tests and porosity measurements were performed by Richt and Kozik (1971) on reservoir core samples from throughout this field. Porosity values for these same samples ranged between 16-25%. Much of this porosity is considered secondary, resulting from the leaching of feldspar grains. Primary porosity has largely been eliminated by the precipitation of quartz, carbonate, and iron cement (Loucks, 1978). Roughly 60% of the air permeability tests showed values of less than 1mD and roughly 6% of tests resulted in permeability values of greater than 10 mD. Permeability varies greatly not only across fields within the VK-1 play, but also within the individual reservoir units that make up each field. Faulting, depositional characteristics, and diagenetic processes result in a high degree of reservoir heterogeneity as interpreted by Langford et al (1994).

Vicksburg Geothermal Fairway

Swanson et al., (1976) identified 47 gas fields from six south Texas counties that produce from geopressured Vicksburg fields in order to analyze their production trends, well logs and completion data, geologic setting, bottom-hole temperatures, reservoir quality, and well tests. While plans for potential demonstration power plants were not recommended for any areas studied, four Vicksburg and one Wilcox prospect areas were cautiously

recommended for further assessment. Loucks, (1978) limited the extents of an interpreted geothermal fairway tapping Vicksburg geopressured sands to 385 square miles in an area previously defined by Swanson et al, (1976). The Loucks "Vicksburg Fairway" is displayed on top of the Fisher and Kim VK-1 play boundary in Figure 32. The Loucks fairway contains 1,300 feet of geopressured sand with temperatures exceeding 300°F. However, low permeability values recorded from core and reservoir heterogeneity limit the applicability of conventional geothermal energy production. Constraints on fluid flow are caused by unfavorable primary porosity values due to cementation and lack of secondary porosity development (Langford et al, 1994).

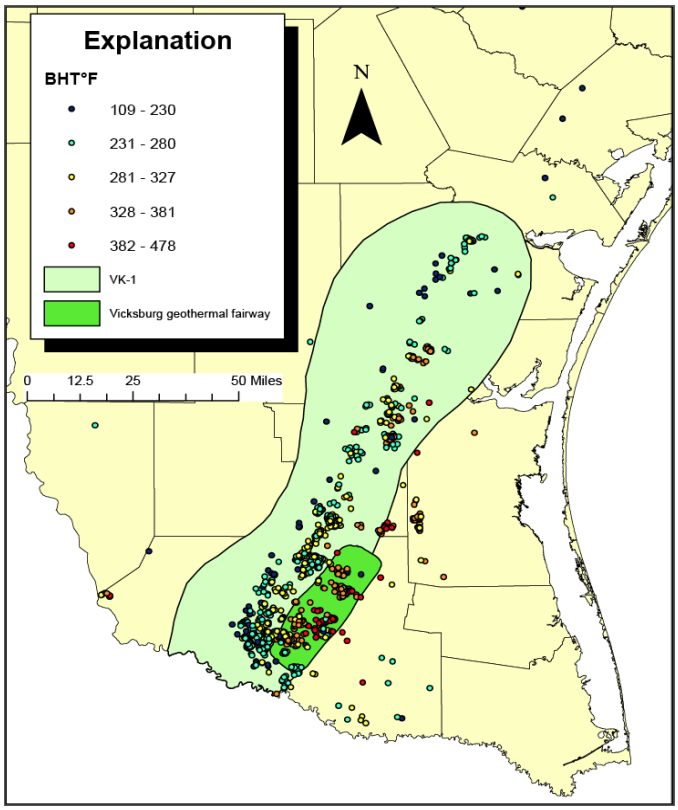

Figure 32. Fisher and Kim (2000) Vicksburg play and Loucks (1978) geothermal fairway location with NGDS wells

4.1.3 Claiborne Group

The middle Eocene Claiborne Group is made up of several alternating formations of predominantly sand and shale. The formations are listed as follows from youngest to oldest: Yegua sand, Cook Mountain Formation, Sparta sand, Weches Formation, Queen City sand, Reklaw Formation, and basal Carrizo sand. The Claiborne Group stretches across the entire Texas gulf coast as shown from the NGDS wells displayed in Figure 33.

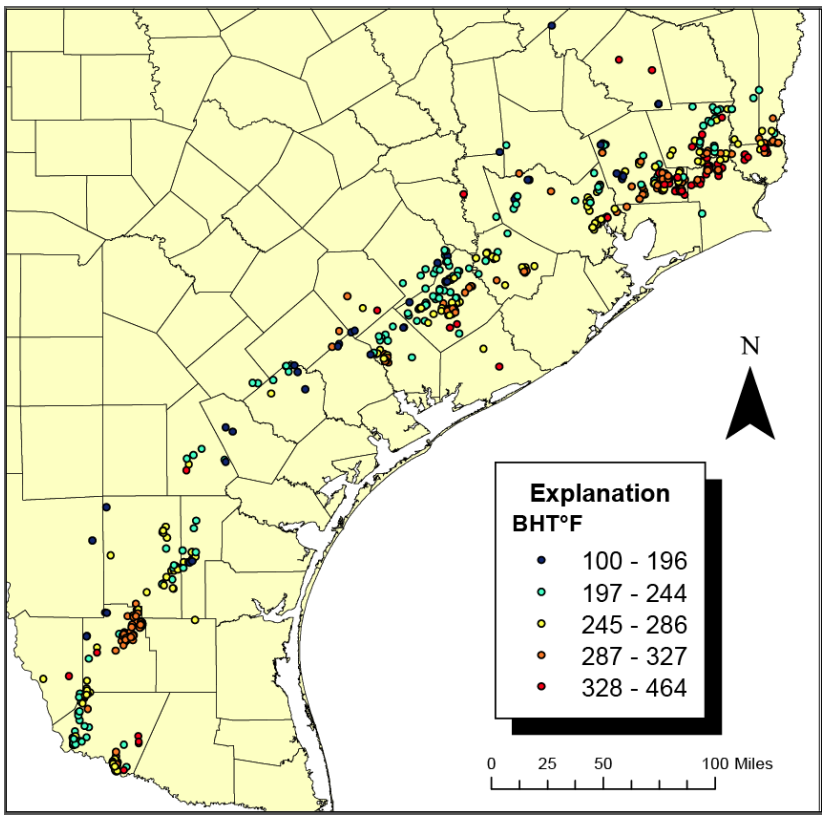

Figure 33. Claiborne Group formation trend observed from NGDS wells.

Claiborne Group Depositional Environment

The gulf-wide depositional setting of Claiborne Group time as defined by Galloway et al. (2000) is displayed in Figure 34.

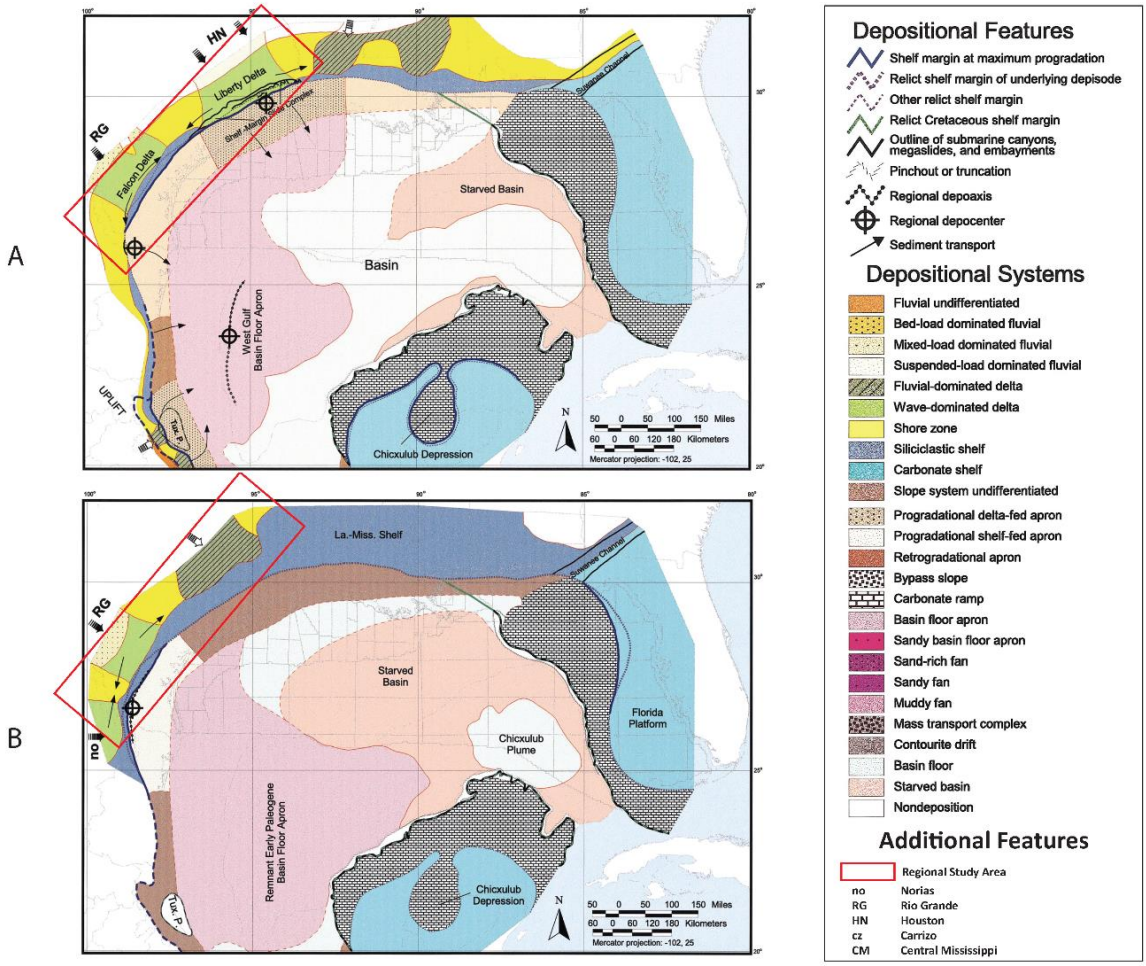

Figure 34. Depositional environments of the upper (a) and lower (b) Claiborne Group depisode (Modified from Galloway et al, 2000)

The Yegua Formation, overlain by the Moodys Branch Formation of the Jackson Group, is the uppermost formation of the Claiborne Group. Major sand depocenters in Yegua time included the Falcon and Liberty deltas, located on the Rio Grande and Houston dispersal axes respectively. The Falcon delta was transformed by decreasing sediment load into a barrier bar/strandplain dominated shore zone, while continued progradation of the Liberty delta resulted in a mass wasting sequence that formed a 15-mile shelf margin basinward expansion. The Sparta sand represented a time of reduced sediment influx into

the study area. A small wave-dominated platform delta was reworked into barrier bar/strandplain systems that are present from northern Mexico to the Houston Embayment. Shelf margins stayed relatively in place during Sparta sand deposition (Galloway et al, 2000). The Queen City sand was initially believed to show little progradation, despite high sediment influx (Galloway and Williams, 1991). This initial finding was later revised by Galloway et al. (2000) when deeper wells confirmed the presence of shelf edge sands. Sediment dispersal mainly occurred across the Rio Grande and Norma axes (Guevara and Garcia, 1972). Delta systems present on both axes are connected by narrow barrier bar/strandplain facies while a sand-rich shore zone developed from the smaller, fluvial dominated delta system developing in the Houston embayment (Galloway et al, 2000). Carrizo sand deposition is unique in that its principal dispersal axis lies between the Rio Grande and Houston dispersal axes. The resulting Rosita delta system was the product of large bed-load dominated and smaller mixed load fluvial systems reaching the paleo-shelf. This delta showed minimal progradation due to the high rate of expansion caused by growth faulting of the underlying Wilcox shelf margin (Galloway et al, 2000). This high rate of growth faulting creates confusion when trying to separate the basal Claiborne Group Carrizo sand from the Wilcox Formation (Hackley, 2012). These reservoir containing sand formations are bound by the transgressive marine facies of the Cook Mountain, Weches and Reklaw Formations. A cross-section of the stratigraphy of this group seen in Figure 35 was developed by Hackley (2012) based on correlation of spontaneous potential and resistivity well logs.

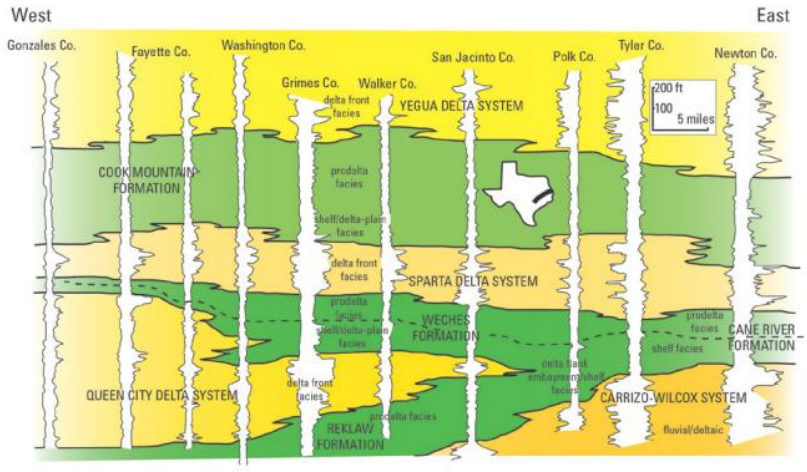

Figure 35. Generalized cross section of the Claiborne Group (Hackley, 2012)

Claiborne Group Geopressured Gas Production

The first production of oil and gas from the Claiborne Group occurred in 1866 within the Nacogdoches field, which is credited as being the first Texas oil field. Hackley (2012) developed a TPS model for the Claiborne Group similar to the aforementioned Frio TPS model. This model uses a similar classification system as the Frio TPS model developed by Swanson et al., (2013). Before defining specific AUs, Hackley divided this group into upper and lower sections. The upper section includes the Sparta sand, Yegua sand, and Cook Mountain Formation. The lower section, which is mainly observed to be productive in south Texas, represents the Carrizo sand, Reklaw Formation, and Queen City sand. Geopressured reservoirs of the Claiborne Group are expected to occur within 4 AUs: Upper Claiborne Expanded Fault Zone Gas, Upper Claiborne Slope and Basin Floor Gas, Lower Claiborne Expanded Fault Zone Gas, and Lower Claiborne Slope and Basin Floor Gas. However, several NGDS data points showing high BHTs lie in the Stable Shelf AUs as well (Figures 36 and 37).

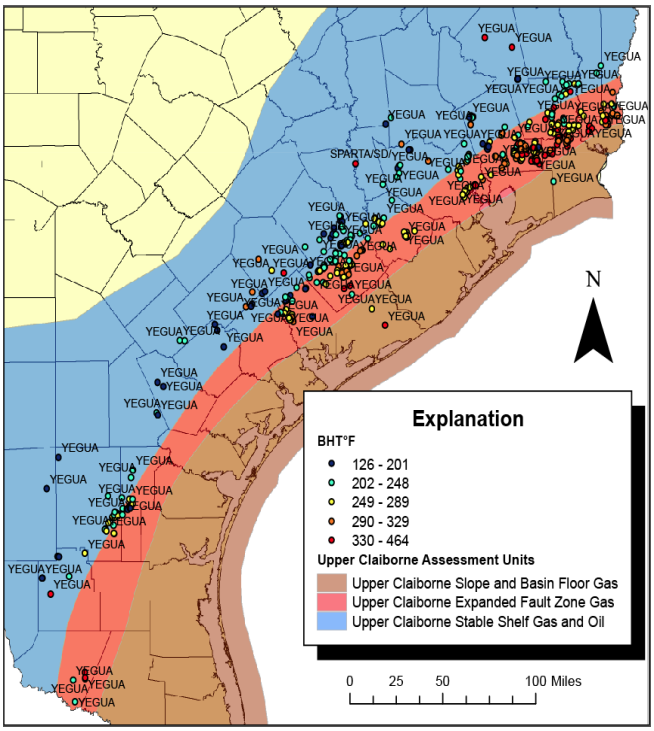

Figure 36. Upper Claiborne Group oil and gas Assessment Units (Hackley, 2012) with NGDS wells

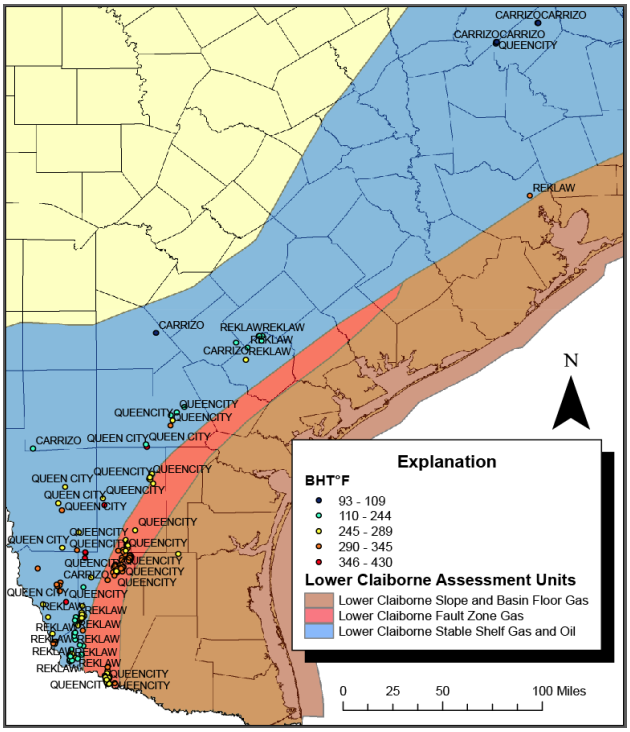

Figure 37. Lower Claiborne Group oil and gas Assessment Units (Hackley, 2012) with NGDS wells.

The Upper Claiborne Expanded Fault Zone is a well-established production unit containing more proven reserves and estimated undiscovered gas accumulations than its lower Claiborne equivalent. An upside of 360 undiscovered accumulations totaling 4,740 bcf is predicted for this AU. Figure 38 shows a relatively flat production trajectory, implying the AU is sub-mature.

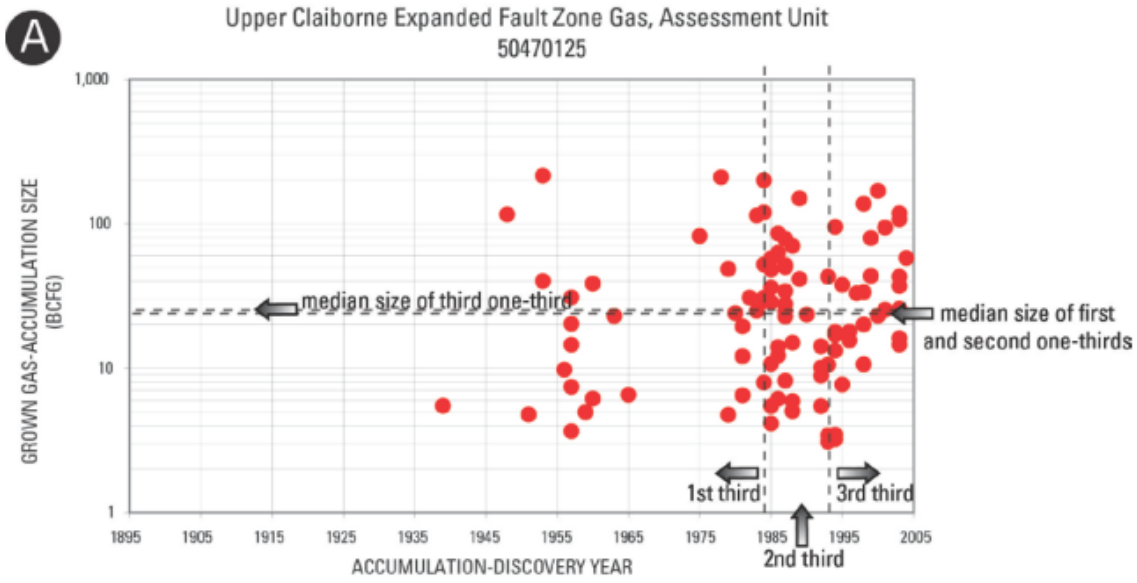

Figure 38. Level trend in discovered Upper Claiborne Expanded Fault Zone accumulation size over time (NRG Associates, Inc., 2006; Hackley, 2012)

The Upper Basin Floor AU is only considered in a hypothetical nature, as there are currently no reservoirs producing above the minimum production value. A mean undiscovered volume estimate of 9,107 bcf from a maximum of 500 undiscovered accumulations were estimated to be present in this frontier AU. The Lower Claiborne Expanded Fault Zone is a fairly under-explored unit, consisting of only 10 discovered gas

accumulations and a maximum upside of an additional 50 undiscovered accumulations. (NRG Associates, Inc., 2006; Hackley, 2012). The mean estimated undiscovered volume of gas is 987 bcf. The immature nature of this AU is shown by the upward trajectory in Figure 39.

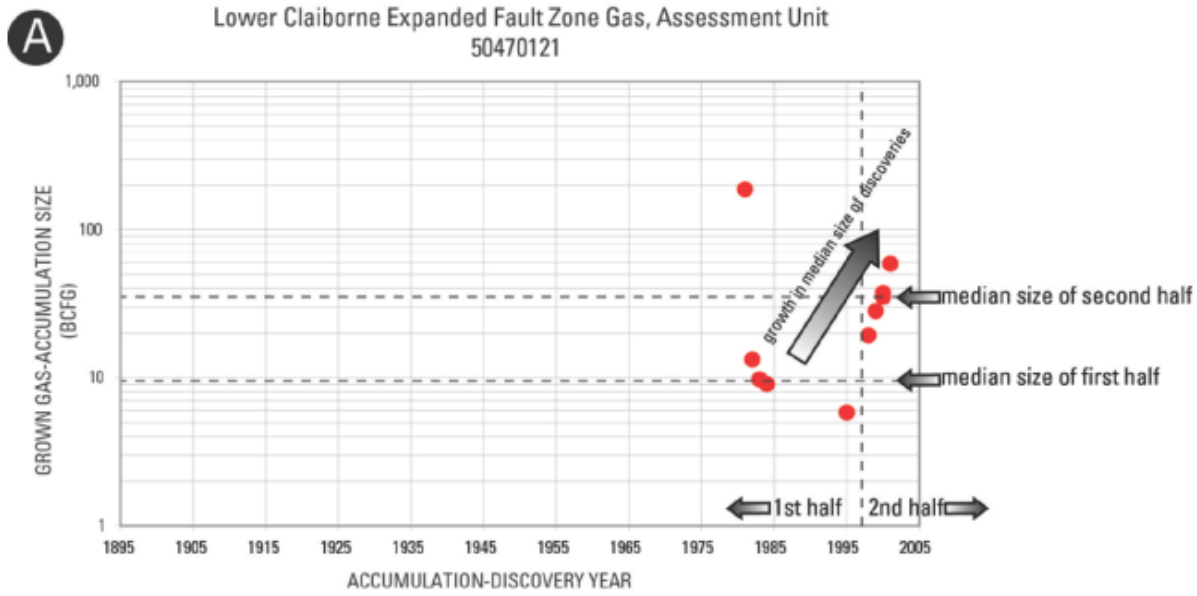

Figure 39. Upward trend in discovered Lower Claiborne Expanded Fault Zone accumulation size over time (NRG Associates, Inc., 2006; Hackley, 2012)

The Lower Claiborne Slope and Basin Floor AU also lacks existing proven reserves, although a maximum 200 undiscovered accumulations estimated to make up a mean volume of 3,620 bcf are predicted. Altogether, the average estimate of undiscovered resources in considered AUs of the Claiborne total roughly 18,000 bcf. The two plays observed in the Fisher and Kim (2000) study include the upper Claiborne Yegua Sandstone, Houston Embayment (EO-3) and Yegua/Jackson Sandstone, Rio Grande Embayment (EO-4). The locations of these plays, along with a projection of the upper

Claiborne AUs (Hackley, 2012) and NGDS wells are shown on Figure 40. This map shows that the EO-3 only partially falls within the extents of the Expanded Fault zone AU but still contains several wells encountering relatively high bottom hole temperatures. This play is considered to be very mature, with 624 bcf reserves as of 1996.

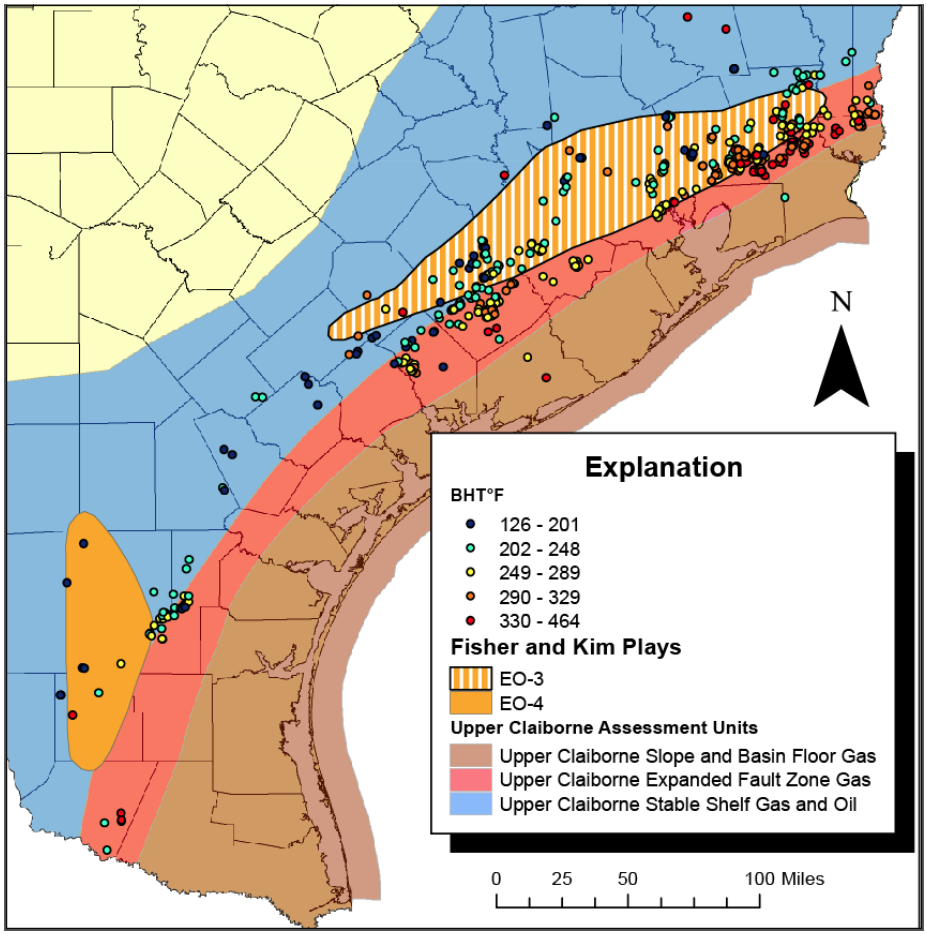

Figure 40. Upper Claiborne group oil and gas Assessment Units (Hackley, 2012), Yegua play units (Fisher and Kim, 2000), and NGDS wells.

Claiborne Group Geopressured Gas Reservoir Properties

Reservoirs of the lower Claiborne Group are found at depths between 8,000-14,000 feet and are thickest in south Texas. Permeability and porosity values of sands observed in

the Mestena Grande field of Jim Hogg County fell between 19-25mD and 15-25% respectively (Burnett, 1990). Reservoir temperatures were not assessed in the TPS model and quantitative pressure assessments were limited in the AUs where no current production exists. Figure 41 shows pressure gradients present in the updip stable shelf and fault zone AUs for both the upper and lower Claiborne extents. This figure shows that geopressured conditions are common in the expanded fault AUs and also occur within selective stable shelf wells.

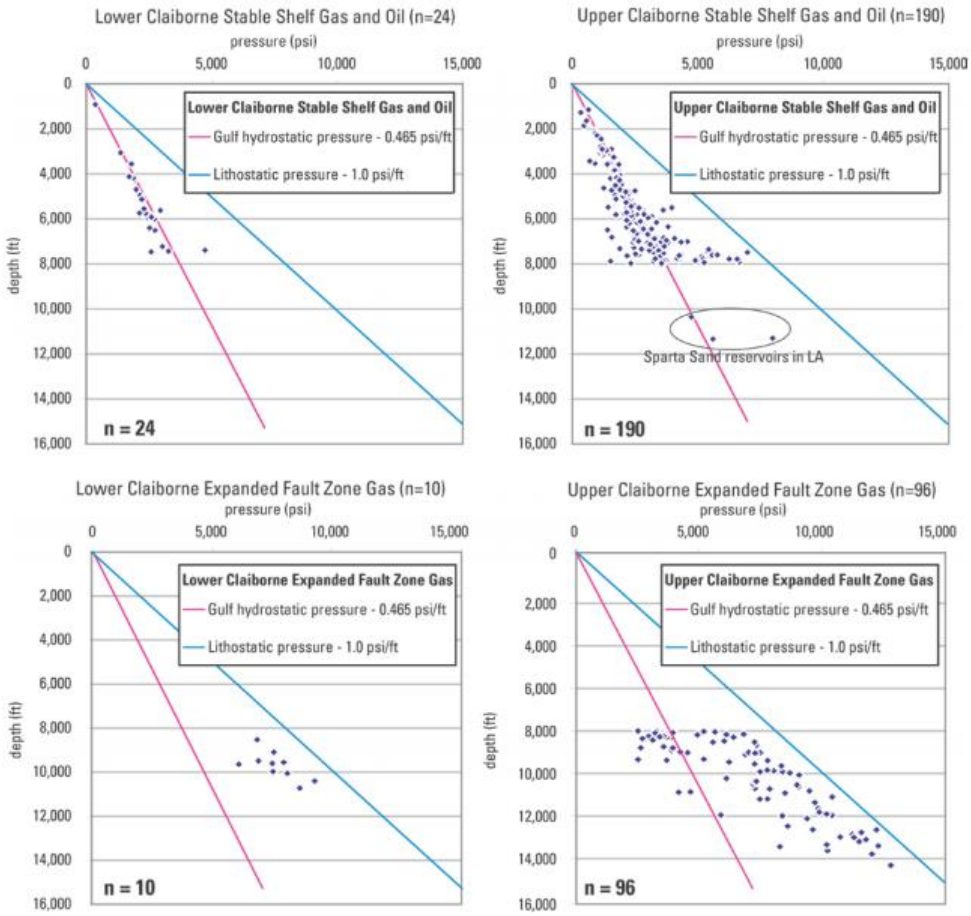

Figure 41. Depth vs pressure of selected Claiborne AUs (Hackley, 2012)

Upper Claiborne reservoirs including potential undiscovered gas reservoirs can be found at a wide range of depths (5,000-16,000). Permeability values as high as 175mD are observed in the downdip extents of the Yegua Formation and are associated with porosity percentages of 27% (NRG, 2006). These values seem more encouraging than those studyed by Miller (1993), who cited 1-20mD and 16% values in deeper downdip Yegua sands.

Claiborne Group Potential Geothermal Areas

No prior assessment of geothermal resources has been performed on the formations within the Claiborne formations. The Lear Koelemay No. 1 Well producing gas from the Leger sand of the Yegua formation was assessed as a part of the Department of Energy (DOE) Wells of Opportunity program. This well and the other wells observed in Texas through this program are described later in the chapter in section *3.1 DOE Wells of Opportunity.*

4.1.4 Wilcox Group

The Wilcox Group is the oldest strata analyzed in the growth faulted Tertiary depositional wedge play. It is also the most landward accumulation, which indicates that Tertiary deposition was cumulatively progradational. NGDS wells displaying the Wilcox Group trend are shown in Figure 42. Being the oldest formation considered in a progradational wedge, Wilcox wells occur the furthest landward. Wells and predetermined geothermal fairways extend across south, central and east coastal plains.

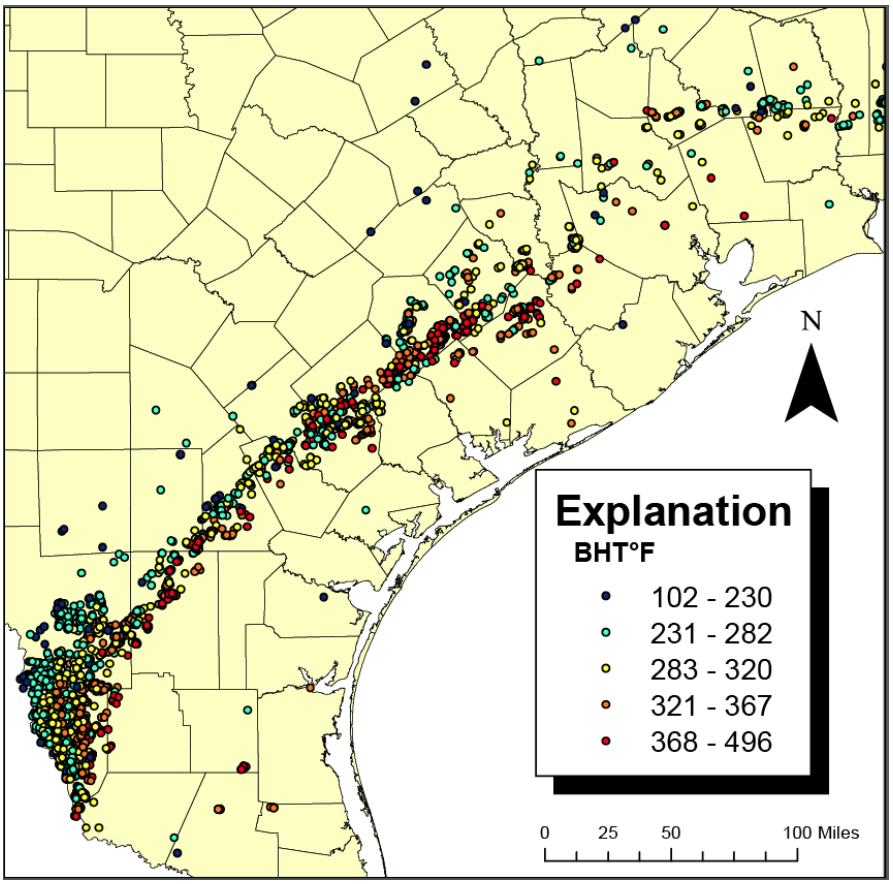

Figure 42. Wilcox Group trend observed from NGDS wells

Wilcox Group Depositional Environment

The gulf-wide depositional environment of Wilcox Group time as defined by Galloway et al., (2000) is displayed in Figure 43. The uppermost extent of the Wilcox Group within the study area is believed to have been deposited originally in the Rio Grande axis as a wave dominated delta termed the Lasalle delta (Xue and Galloway, 1995). Continued deposition and reworking of this and other deltas outside of the study area added as much as 20 miles of progradation to the existing lower Wilcox shelf margin. Upper/middle Wilcox time is also characterized by the development of four submarine incised canyon

systems, including the Yoakum, Lavaca, Smothers, and Hardin channels. Both the Yoakum and Lavaca systems have been studied extensively. According to McCulloh and Eversul (1986) and Dingus (1987), the Yoakum canyon was incised during a major transgressive event associated with middle Wilcox time. Thick occurrences of shale and discontinuous sands dominate these canyon environments. The lower Wilcox time Lavaca canyon was formed during progradational conditions and cut through delta predominantly delta facies. Sand distribution in the Lavaca canyon is much more favorable than that of the Yoakum canyon (Galloway et al, 1991). This lower section of Wilcox strata represents the first major Cenozoic influx of sediment into the Gulf Basin. Sediment source and sink were both created in response to the Laramide orogeny: uplands from the southern Rocky Mountains to Mexico were uplifted and eroded while tectonic tilting a seismicity caused the Lobo megaslide located in the western margin of the Gulf. Dispersal was primarily focused on the Houston axis where bed load fluvial and fluvial dominated delta lithofacies formed the Houston delta. Smaller, fluvial dominated deltas were also deposited in the south Texas area. Sandy shore zone and shelf lithofacies received sand from these smaller deltas and filled much of the Lobo megaslide embayment.

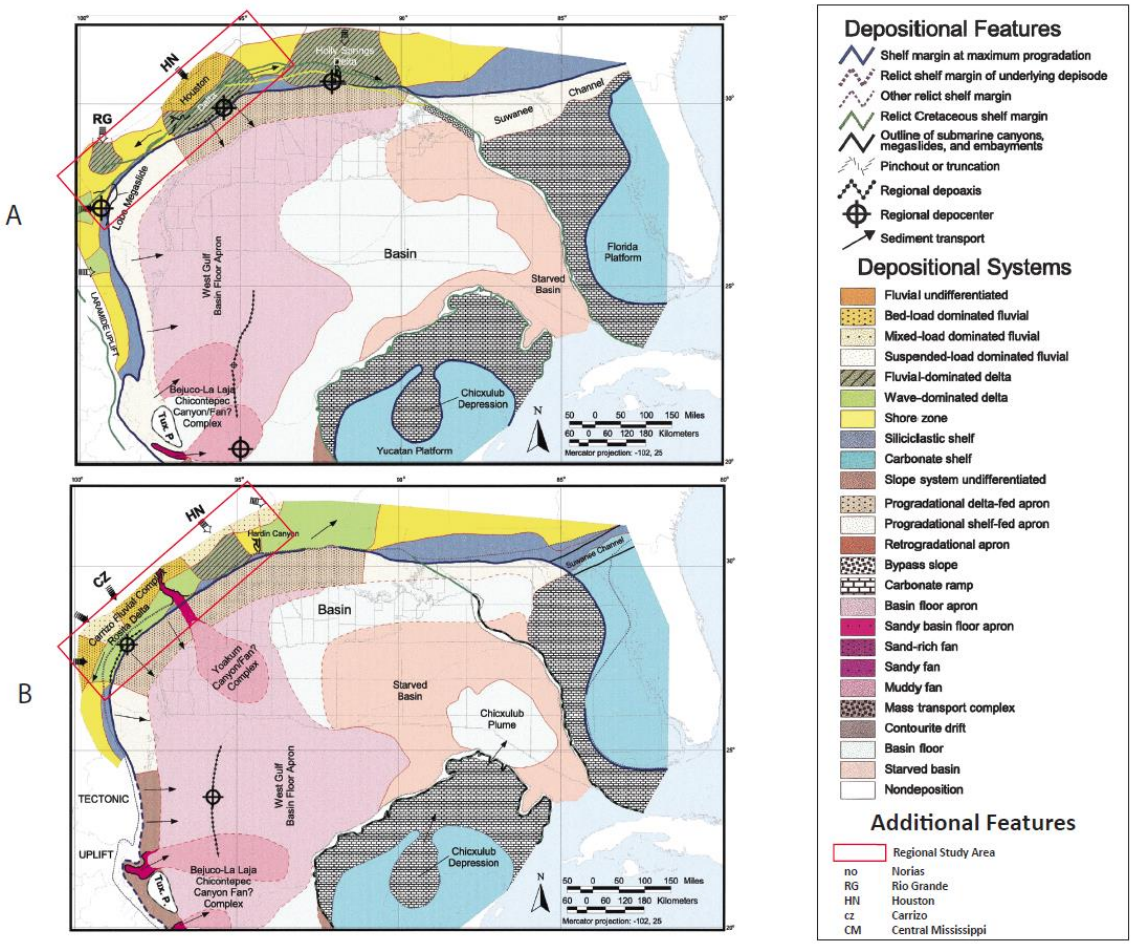

Figure 43. Depositional environments of the upper (a) and lower (b) Wilcox Group depisode (Modified from Galloway et al, 2000)

Wilcox Group Geopressured Gas Production

Although there is no full study, Four Wilcox assessment units are included in the total undiscovered resources assessment of the Upper Jurassic-Cretaceous-Tertiary Composite gulf coast total petroleum system. Three of these assessment units were inferred to contain geopressured reservoirs based on similarities to assessment units of previous formations. The Wilcox Expanded Fault Zone Gas and Oil AU, Wilcox Slope and Basin Floor Gas AU, and the Wilcox-Lobo Slide Block Gas AU combined average estimate

undiscovered gas volume was over 36,000 bcf (Warwick, 2008). Figure 44 and 45 show a relatively flat grown accumulation over time trajectory, indicating a sub mature-to mature production stage.

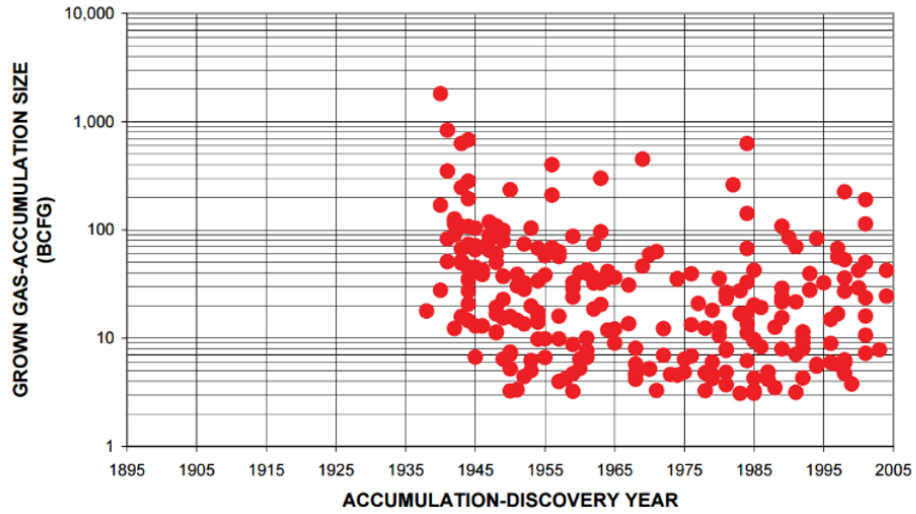

Figure 44. Level trend in discovered Wilcox Expanded Fault Zone accumulation size over time (NRG Associates, Inc., 2006; Warwick, 2008)

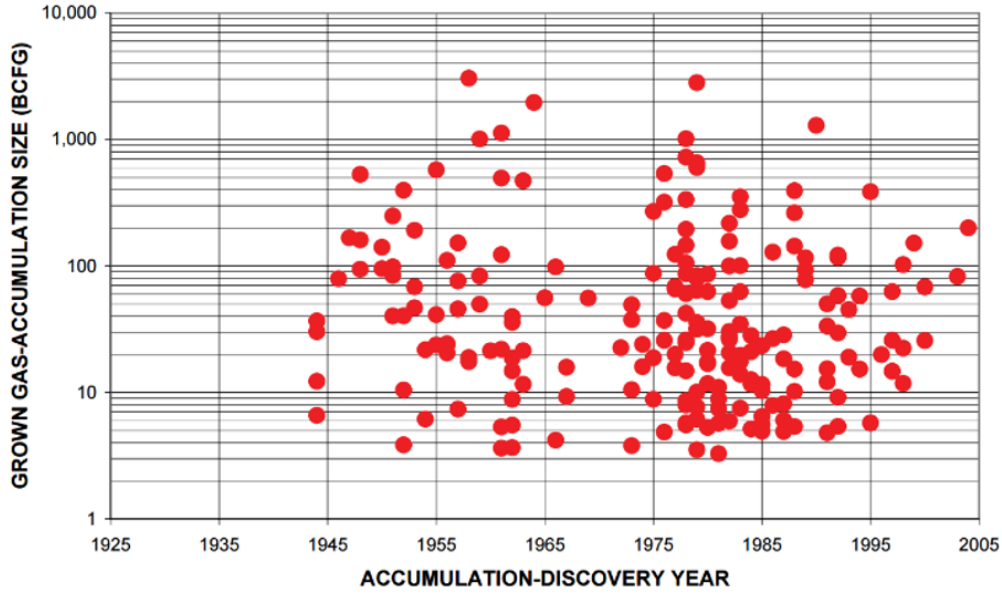

Figure 45. Level trend in discovered Wilcox-Lobo Block accumulation size over time (NRG Associates, Inc., 2006; Warwick, 2008)

The Fisher and Kim (2000) assessment listed three Wilcox plays all of which were determined to contain potentially geopressured reservoirs. Locations of these plays are shown alongside NGDS wells on Figure 46. Maturities of exploration in these plays range from "relatively immature" to "very mature". Reserve levels as of 1996 include 961 bcf in the Wilcox Sandstone Houston Embayment (WX-1), 2.1 tcf in the Wilcox Lobo Trend (WX-2), and 2.3 tcf in the Wilcox Sandstone Rio Grande Embayment (WX-4). All Wilcox plays were determined to be of top URG potential.

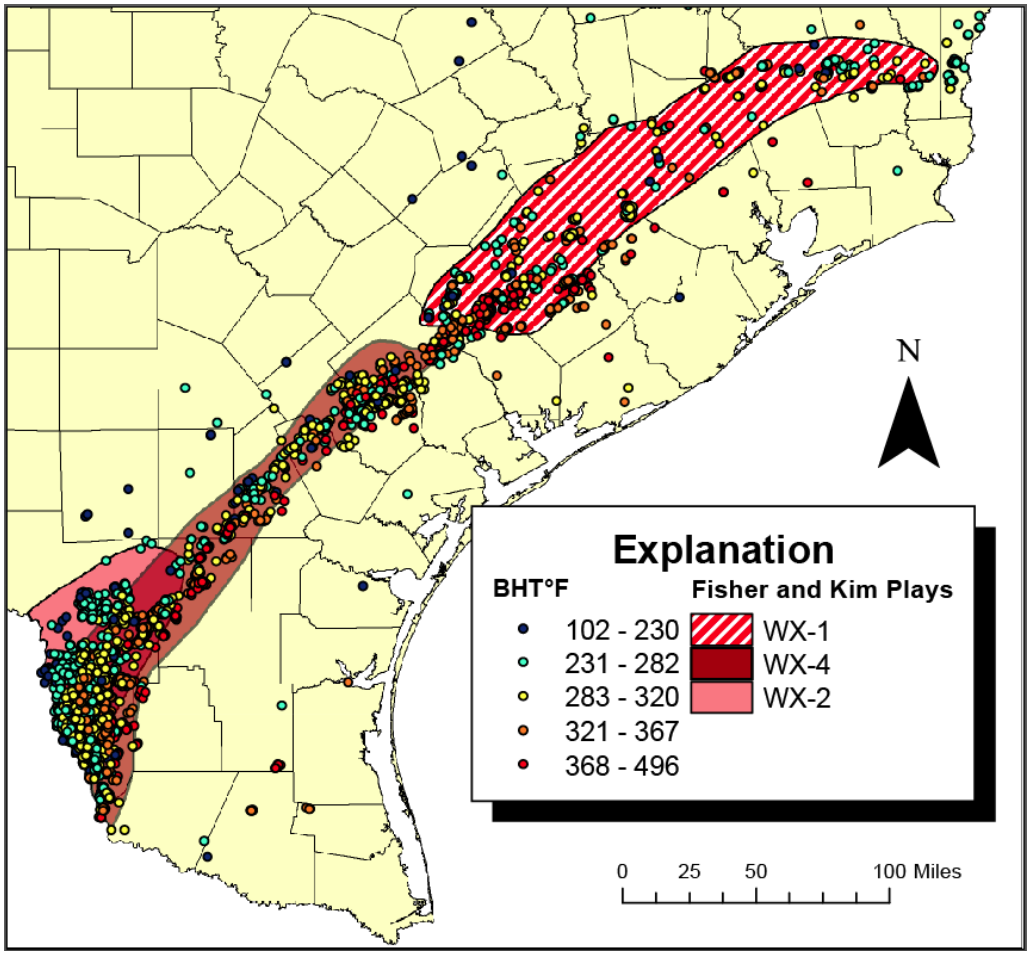

Figure 46. Fisher and Kim (2000) Wilcox play locations with selected NGDS wells

Wilcox Group Geopressured Gas Reservoir Properties

Fields in the WX-1 play are primarily seated in the Wilcox fault zone. This fault section expands from its updip thickness of 2,000 feet to over 8,000 feet (Seni et al., 1992). The average depth to reservoirs in this play is 10,657 feet (Fisher and Kim, 2000). The Sheridan Field in Colorado County is a major field producing from Wilcox strata and will serve to provide reservoir characteristics for this play. Producing reservoirs are thin, tight, and lenticular. Porosity values averaged between 17.8 and 12.1% and average permeability values ranged between 21.6 and 11.3 mD. These values were calculated from core data. Reservoir temperatures were observed between 234-273° F at depths ranging between 8,141-10,600. Over this same interval, pressure values between 3,590-4,287 psi. This indicates that geopressured environments (pressure gradient exceeding 0.5psi/ft), were not reached in this field at the time of study (Hill and Vogel, 1949). Average completion depth for the WX-2 play is 9,611 (Fisher and Kim, 2000). In 1980, the Federal Energy Regulatory Commission (FERC) classified the Wilcox-Lobo trend as a "tight" gas play. This implies that the play is un-economical to produce without the use of hydraulic fracturing or horizontal drilling. Supporting this are in-situ gas permeability values in the range of 0.0003 to 0.5 mD and porosity values between 12-25% (Robinson et al., 1986). Bottom hole temperatures of wells reaching depths of 11,000 are shown to exceed well above 300° F and geopressured conditions are encountered at depths as shallow as 6,000 feet. The WX-4 average completion depth is 9,867 feet. Fisher and Kim (2000) list the Seven Sisters field of Duval County as a major field in this play, with many reservoir units, including the Howell, Reagan, and House sands are producing from

depths ranging from 11,000-15,000 feet (Spetseris, 1984). The Howell sand is the deepest of these reservoirs. Cores recovered at depths ranging between 15,000-15,300 feet showed favorable properties in an isolated area of the reservoir aptly named the "sweet spot". Permeability values in this promising portion of the reservoir typically range from 0.1-30mD with a maximum recorded value of 100mD. These values are associated with the connectivity of preserved primary porosity and secondary macro-micro porosity developed by the dissolution of feldspars and other unstable minerals. A bottom-hole temperature 394° F was recorded. (D'Agostino, 1985)

Wilcox Group Geothermal Fairways

In BEG studys similar to those performed on the Frio Formation, geothermal fairways were delineated in the down dip growth faulted sections of the Wilcox Group (Figure 47). Although numerous stratigraphic markers were used locally throughout the growth fault trend, the tops of two major progradational cycles observed along the entire gulf coast were used to separate this formation into upper and lower units. These units are separated by shale-rich transgressive unit. Upper Wilcox sand distribution is concentrated in the south coastal plain and forms the reservoirs present in the Zapata, Duval, and Live Oak fairways. Lower Wilcox sand depocenters that make up the De Witt, Colorado, and Harris fairways are found in the central and eastern coastal plains. Two reservoir models based on the upper and lower Wilcox depositional/structural characteristics describe these 8 fairways. Both models are composed of highly constructive, vertically continuous, lobate delta-front sandstones.

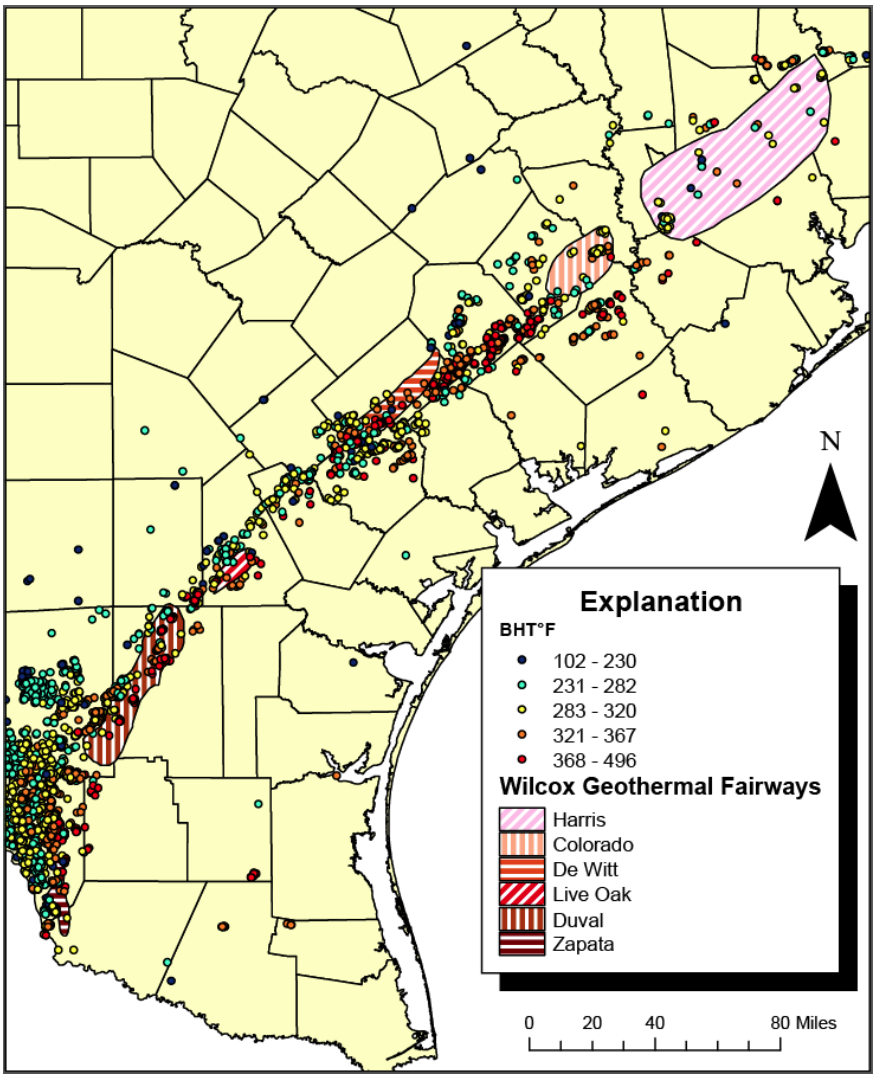

Figure 47. Wilcox geothermal fairways with NGDS wells (Bebout et al., 1982)

Similar to Frio sandstones, the tops of reservoir sand accumulation in each model show the highest permeability values with reservoir quality decreasing with depth. The Zapata, Duval, and Live Oak fairways are associated with three different delta lobe complexes (Seni et al, 1992). The upper Wilcox, bound by the regional progradational markers, is further subdivided locally by 3-4 markers that are correlated across the three model I fairways. This correlation is shown on Figure 48.

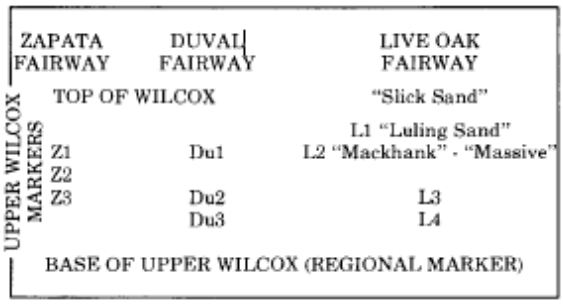

Figure 48. Correlation of stratigraphic markers across model I Wilcox fairways (Bebout et al, 1982)

The reservoir quality of sands described by Model I, while based on a limited sample size, vary widely with depth. Bebout et al. (1982) recorded porosity values between 7-24% and permeability values between 0.1-40 mD. More discouraging values were studyed by Seni et al, (1992), citing average permeabilities of 0.01-0.5 mD occurring at suitable depths, pressures, and temperatures.

Model II lower Wilcox reservoirs of the De Witt, Colorado, and Harris fairways are found in the central and eastern Texas Coastal Plain. The depth to top of geopressure ranged between 10,000 and 12,000 feet. Reservoir temperatures exceeding 300° were encountered at depths ranging between 11,000 and 13,000 feet. Local stratigraphic markers were also observed in these fairways, although only one of these markers was found to correlate across the Colorado and Harris fairways. Despite the generally negatively correlated depth/permeability trend, lower Wilcox k values are studyed to range between 0.01-545 mD. The Cuero fault block in the De Witt fairway contains a cumulative 550 feet of geopressured reservoir quality sand. Tops of eight upward coarsening, prograding parasequences with fluid temperatures of 300° F and permeability

values over 100 mD have the highest potential for conventional geothermal energy production. (Bebout et al, 1982).

4.2 Jurassic Cotton Valley Play

The Cotton Valley Group is composed of the Cotton Valley sand and Bossier Formations. This Jurassic sediment package represents the first influx of clastic deposition into the Gulf of Mexico since Late Triassic continental rifting. (Salvador, 1987; Worrall and Snelson, 1989). The Cotton Valley sand is separated into "massive" sands, found in the east Texas study area, and "blanket" sands found in northwest Louisiana. These strata form a separate depositional wedge from the aforementioned tertiary wedge play. The Cotton Valley trend of the east coastal plain is shown in Figure 49.

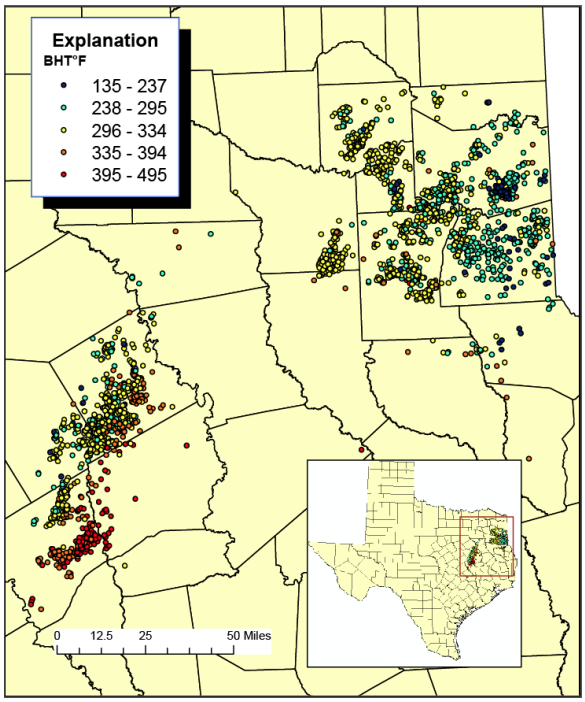

Figure 49. Cotton Valley geothermal play trend observed from NGDS wells.

Cotton Valley Depositional Environment

This group was deposited in the East Texas Basin. The area of deposition is structurally confined by the Sabine Uplift to the east, Mexia-Talco Fault System to the northwest, and Angelina-Caldwell Flexure to the south. Elshayeb (2004) describes depositional systems in the Cotton Valley sand, however, the basal Bossier shale was not included in the dissertation. These settings consist of four facies associations (FA) and 23 individual facies. FAs are defined by Galloway (1989) as genetically related geologic units deposited and altered by sedimentary and biotic processes inherent to an area of deposition. The FAs presented by Elshayeb include: Offshore/shoreface transition, Shorface-foreshore, Tidal inlet, and Back barrier-coastal plain. The Back barrier-coastal plain FA is observed in the upper most sections of the Cotton Valley Group. Tidal flats, washover deposits, brackish bay sand fill, and other shallow environment depositional features characterize this FA. The Tidal inlet FA typically lies directly underneath the Back barrier-coastal plain FA and is composed of channelized, pebbly, highly bioturbated barrier inlet sediment. The seemingly contradictory presence conglomerate forming pebbles and heavy bioturbation reflect changes in depositional energy, possibly resulting from channel switching and channel abandonment. The Shorface/foreshore FA is found stratigraphically all throughout the Cotton Valley Group. Depositional characteristics within this FA vary widely. This is due in part to the dynamic conditions experienced in nearshore conditions. The Off-shore/shoreface transition FA is representative of the lowermost and middle sections of the Cotton Valley sand. Sediment included in this FA includes basal silty shale coarsening upwards into fine-grained sand and eventually

grading into Shoreface/foreshore FA strata. The FAs listed above do not contain mention of the basal Bossier shale. Williams and Mitchum (1997), describe the Bossier as the down dip marine equivalent of the shallowing-up, regressive unit that is interpreted in this group. Isolated reservoir quality sands are present in this formation and are interpreted as turbidites occurring in prograding complexes (Williams and Mitchum, 1997; Newsham and Rushing, 2002). Bossier sands appear to have been transported from further northwest of the Cotton Valley Group trend and are located in isolated lows created by faulting, subsidence, and salt movement in the basin. Marine sediment caps the isolated sand units, which indicates a possible marine transgression in which very little sand above the wave base was preserved (Newsham and Rushing, 2002). The regressive, prograding trend of the entire Cotton Valley Group supports the large-scale depositional wedge model.

Cotton Valley Geopressured Gas Production

The USGS undiscovered resource assessment classified the Cotton Valley Group into four assessment units: Cotton Valley Blanket Sandstone Gas Assessment Unit, Cotton Valley Massive Sandstone Assessment Unit, Cotton Valley Updip Oil and Gas Assessment Unit, and Cotton Valley Hypothetical Updip Oil Assessment Unit. Of these AUs, only the Cotton Valley Massive Sandstone Assessment Unit contains wells observed in NGDS data (Dyman and Condon, 2006). Similar to the Wilcox-Lobo trend, the low permeability sands of the Cotton Valley massive trend were designated as tight plays by FERC. After this official designation and ensuing price incentives, production

from low permeability sands soared, increasing from 2.2 bcf in 1976 to over 70 bcf in 1980 (Meehan and Pennington, 1982). 547 bcf of gas are estimated to make up the total undiscovered resource of the massive sand AU. Dyman and Condon (2006) did not include the Bossier Formation in their assessment of undiscovered resources. Production from these tight turbidite reservoirs is most common in the western extents of the East Texas Basin (Newsham and Rushing, 2002). This formation is mentioned in the Fisher and Kim (2000) assessment but again, qualitative field maturity for production from this formation was not made available. As discussed below, some assessments have theorized that Bossier sands represent a continuous, basin-centered gas accumulation system.

Cotton Valley Group Oil and Gas Reservoir Properties

The Dyman and Condon (2006) study did not describe overpressure conditions in Texas Cotton Valley reservoirs. Core data and bottom-hole measurements from Mimms Creek and Dew fields in Freestone County were analyzed by Newsham and Rushing (2002). Pressures of Cotton Valley sands reached 6,000 psi, indicating only marginally geopressured conditions. The Moore, Shelley, Bonner and York sands reservoir units are more highly pressurized, with pressure gradients ranging from 0.6-0.9 psi/foot. These units, ranging in depth from rough 12,000-13,500 feet, exhibit bottom-hole temperatures ranging between 280-325°F. These Bossier intervals show relatively low reservoir qualities, with porosity values between 1-17% and permeability values not exceeding 1mD. Unlike previously described geopressured systems, the abnormally high pressures in the Cotton Valley Group are not believed to be caused by hydraulically isolated sand

units undergoing compaction. Instead, Newsham and Rushing (2002) believe the primary cause of geopressure is native hydrocarbon generation. The specific reservoir environment is described within the context of a total petroleum system to include a continuous, basin centered gas system generating and maintaining reservoir conditions. The shales that represent the majority of this formation are referred to as source rocks in TPS models of the entire Travis Peak-Cotton Valley system (Popov et al., 2001). This is supported by the lack of mobile liquid water existing in the turbidite sand reservoirs (Newsham and Rushing, 2002).

Cotton Valley Group geothermal fairways

There are no assessments of the Cotton Valley Group in terms of its geothermal potential.

4.3 Previous Geothermal Exploration and Pilot Programs

Citing the need to reduce dependency on fossil fuel by increasing the development of alternative energy resources, The DOE established a geopressured-geothermal energy program. The goals of the program included the following: assess extent of geopressured reservoirs, determine technical feasibility, establish economic incentives or constraints, identify potential environmental effects, and resolve legal and institutional barriers associated with commercial use of geothermal resources in the gulf coast (Division of Geothermal Energy, 1980). The program was able to combine the efforts of industry contractors, private consultants, universities, and national labs. Two separate testing programs were established to accomplish the aforementioned goals. The Wells of Opportunity program utilized wells drilled by the oil and gas industry that penetrated

through geopressured reservoirs. The Design Well program performed exploration drilling operations in areas potentially favorable to geopressured-geothermal production. The Locations of Wells of Opportunity and Design Wells are shown on Figure 50. This figure, along with the rest of the information presented in this section comes from the *Gulf Coast Geopressured-Geothermal Program Summary Study Compilation* compiled by John et al., (1998).

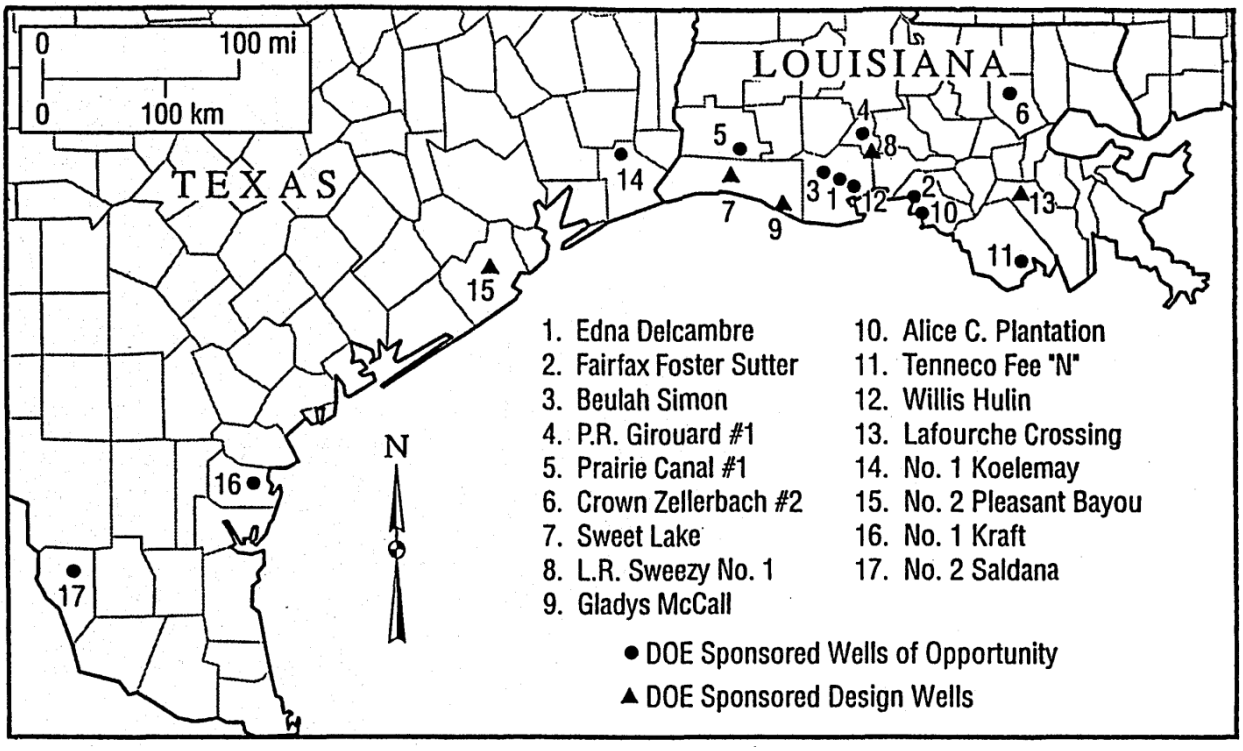

Figure 50. Locations of Wells of Opportunity and Design Wells commissioned by the geopressured-geothermal energy program (John et al., 1998)

4.3.1 DOE Wells of Opportunity

In 1977, the Wells of Opportunity program began gathering data from existing unproductive oil and gas wells. Wells were screened for further study by published oil

and gas industry activity and direct contact with operators. Upon satisfying general location, depth, and drilling criteria and before production tests were performed on selected wells to determine reservoir and fluid characteristics, electric logs and core samples of prospective wells provided the basis for initial evaluation of temperature, bottom-hole pressure, gross and net sand thickness, porosity and permeability, brine salinity, and reservoir extent. Production tests consisted of alternating drawdown flow and buildup sequences. Brine and gas samples were taken during flow periods to assess salinity and gas composition. Each tested site required a new well or the utilization of a nearby abandoned well to use as a disposal well for the produced brine. Issues associated with re-injection of brine included sanding up of injection horizons and plugging problems associated with the injection of produced solids.

Three Texas wells were selected for testing: Lear Petroleum Exploration Inc. #1 Koelemay, Riddle Oil Company #2 Saldana, and Coastal States Gas Producing Company #1 Pauline Kraft.

Koelemay No. 1

In the 13 days the Koelemay well was flowed for testing, 2200-3200 bbls/day of water was produced to the surface at temperatures of 206° F from a reservoir bottom-hole temperature of 260° F. Producing from the Doyle Field in Jefferson County, the target production horizon contained net sand accumulation of 79 feet. This well tapped a Claiborne Group Yegua Formation sand, locally referred to as the “Leger Sand,” at a depth of 11,700 feet with core derived permeability and porosity values of 85 mD and

26% respectively. These encouraging values could not be confirmed due to two-phase saturation near the well bore caused by an unexpected accumulation of oil and gas. After producing a significant amount of hydrocarbons, testing was postponed and control of the well was returned to the operator. Although this well and all wells tested in this program drastically underperformed their initial maximum flow capacity estimate, permeability-thickness, bottom-hole temperature and pressure, and salinity measurements of the Koelemay Well of Opportunity exceeded expectations.

Saldana No. 2

1,200-1,950 bbls/day flowed from the Wilcox 1st Hinnant sand over 9 days of testing performed on the Martinez Field based Saldana well in Zapata County. This reservoir was encountered at a depth of 9,745 with a net sand interval of 75 feet. 20 mD permeability and 20% porosity values were initially determined from core tests, with a 12.5 mD permeability value recorded via production test. The 300° F reservoir produced brine to the surface at a maximum temperature of 220° F. Permeability-thickness determined in the production test underperformed initial estimates while salinity, bottom-hole temperature, bottom-hole pressure, and brine salinity were all underestimated.

Pauline Kraft No. 1

The Kraft Well of Opportunity in Nueces County attempted to test the Frio Anderson reservoir sand. The operator at the time of testing was interested in converting the dry hole into a source of energy for an ethanol production facility. Unfortunately, before the testing could be completed, the 5-inch production casing failed. High repair costs,

unresponsiveness to acid frac treatment, and overall poor initial results led to the early abandonment testing.

It should be noted that these wells were initially intended to produce oil and gas, resulting in bottom-hole targets that are not aligned with the best possible geothermal brine drainage position. It was assumed that reservoirs encountered in this assessment would be small and would not necessarily lead to the discovery of commercially viable geothermal reservoirs. Still, novel practices were carried out and the ability to predict reservoir properties through economical means was effectively tested. This program was the first to use an annular flow technique to test reservoir properties. This gave operators the ability to perform flow tests while avoiding problems associated with movement of down hole wireline tools. Major discrepancies between predicted and observed reservoir quality indicate that advances in geopressured-geothermal reservoir modeling are necessary. By providing estimates and performance data, the DOE Wells of Opportunity Program provides a base upon which more representative models can be created.

4.3.2 DOE Pleasant Bayou Design Well and Hybrid Power System

The Design Well program objectives included gathering data on reservoir production and environmental impacts in areas that contain favorable geologic conditions. In total, four design wells were successfully completed. A fifth well, displayed on Figure 50 as “13. Lafourche Crossing”, was proposed but no drilling activity was recorded.

In 1979, DOE completed the Pleasant Bayou No. 2 Design Well in Brazoria County. This well was the first completed in the Design Well program and the only well located

in Texas. The Pleasant Bayou No. 1 well was initially spudded in 1978. This well was successfully drilled to a depth of 15,765 feet before unstable hole conditions resulted in a stuck pipe during core cutting. The hole was plugged back at a depth of 8,400 feet and was later repurposed as a disposal well.

The selection of the location and target horizon for the Pleasant Bayou program came as a result of extensive geologic review by the University of Texas Bureau of Economic Geology and Center for Energy Studies. The Austin Bayou prospect area in the Brazoira Fairway was selected as the area most likely to contain suitable permeability, temperature, reservoir volume, and pressure. Secondary porosity developed as a result of grain leeching and is largely responsible for the favorable reservoir porosity values of around 20%. An interval of more than 600 feet of sandstone occurs in the target zone below the T5 marker. 30% of the entire 660 foot was estimated to contain sand with permeability values over 20mD. The reservoir selected for production contained 60 feet of continuous, bed load channel sand at a depth of roughly 14,650 feet displaying permeability values ranging between 100-400mD.

Production testing began in November of 1979. Multiple phases of testing continued until 1983, when the well was temporarily abandoned following a tubing “parting” failure and scale buildup. The well was inactive until 1986 after cleanup procedures were completed and a new production tubing was installed at a depth of 13,968 feet. Surface facility rehabilitation occurred in 1987 and 1988 after which long term production continued until August 1990.

A combination of geothermally heated brine and associated dissolved methane were used to operate a hybrid power system (HPS). By combining exhaust heat from the 650kW gas engine with the geothermal fluid operating the 541 kW binary loop, overall gains in efficiency ranged between 15.3-30.8%. Figure 51 shows a schematic of the HPS.

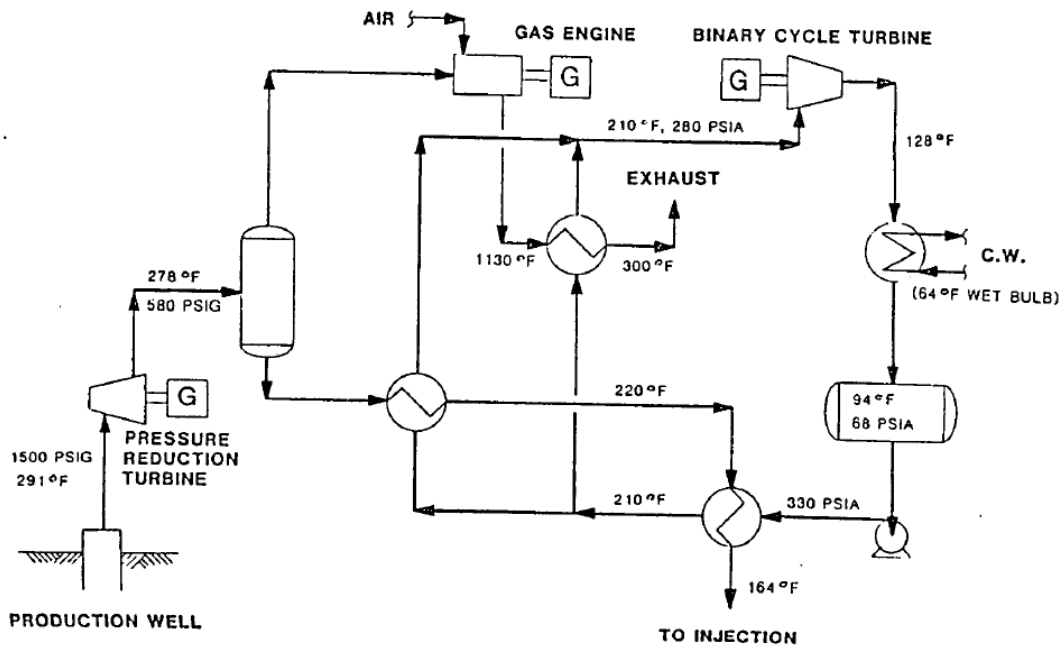

Figure 51. Hybrid power system flow diagram showing key operating conditions (John et al., 1998; adapted from Hughes, 1983).

The above flow diagram shows the working fluid loop splitting after the geothermal preheater, but before entering the main binary heat exchanger. Roughly 86% of the working fluid was vaporized in the binary heat exchanger while the remaining 14% was sent through the exhaust heat exchanger. After parasitic loads totaling 209 kW, net capacity amounted to 982 kW. The minimum brine flow rate during HPS operation was 15,600 bbl/d (455 gpm or 103 m^3/hour) at a well head temperature of 291°F and was coproduced with natural gas at a ratio of roughly 23 scf/bbl .

5.0 RECCOMMENDED IMPLEMENTATION

Upon considering the nature of the total geothermal energy system within the state of Texas and the means by which such systems could be potentially harnessed, the remainder of this study will focus on the overall applicability of the WBHX production model. The factors that led to this selection as described in Chapter 4 *Nature of geothermal systems in Texas* include: low to moderate reservoir temperatures, low reservoir permeability values, inconsistent or unknown presence of a mobile working fluid, extensive drilling depths required to reach candidate reservoirs, and presence of a potentially reusable infrastructure. This chapter will outline the process of creating a geospatial distribution model that could be used to determine the optimum location(s) of WBHX geothermal facilities in abandoned oil and gas wells. This chapter will conclude with a brief discussion of the results and the implications of applying this suggested utilization to the areas determined to be most suitable.

5.1 Geospatial distribution model

Bottom hole temperature data from 42,601 wells were obtained from the NGDS and are displayed in Figure 52. Using ArcMap Analysis and Spatial Statistics tools, areas containing high concentrations of oil and gas wells with exceptionally high BHT were delineated. Identifying statistically significant clusters of hot wells could lead to increases in economic viability and system efficiency if this resource is to be utilized at scale. These benefits would be a result of the ability to select clusters near existing power

distribution infrastructure and an overall increase in power output resulting from the ability to connect multiple clustered WBHX systems in series (Cheng et al., 2013).

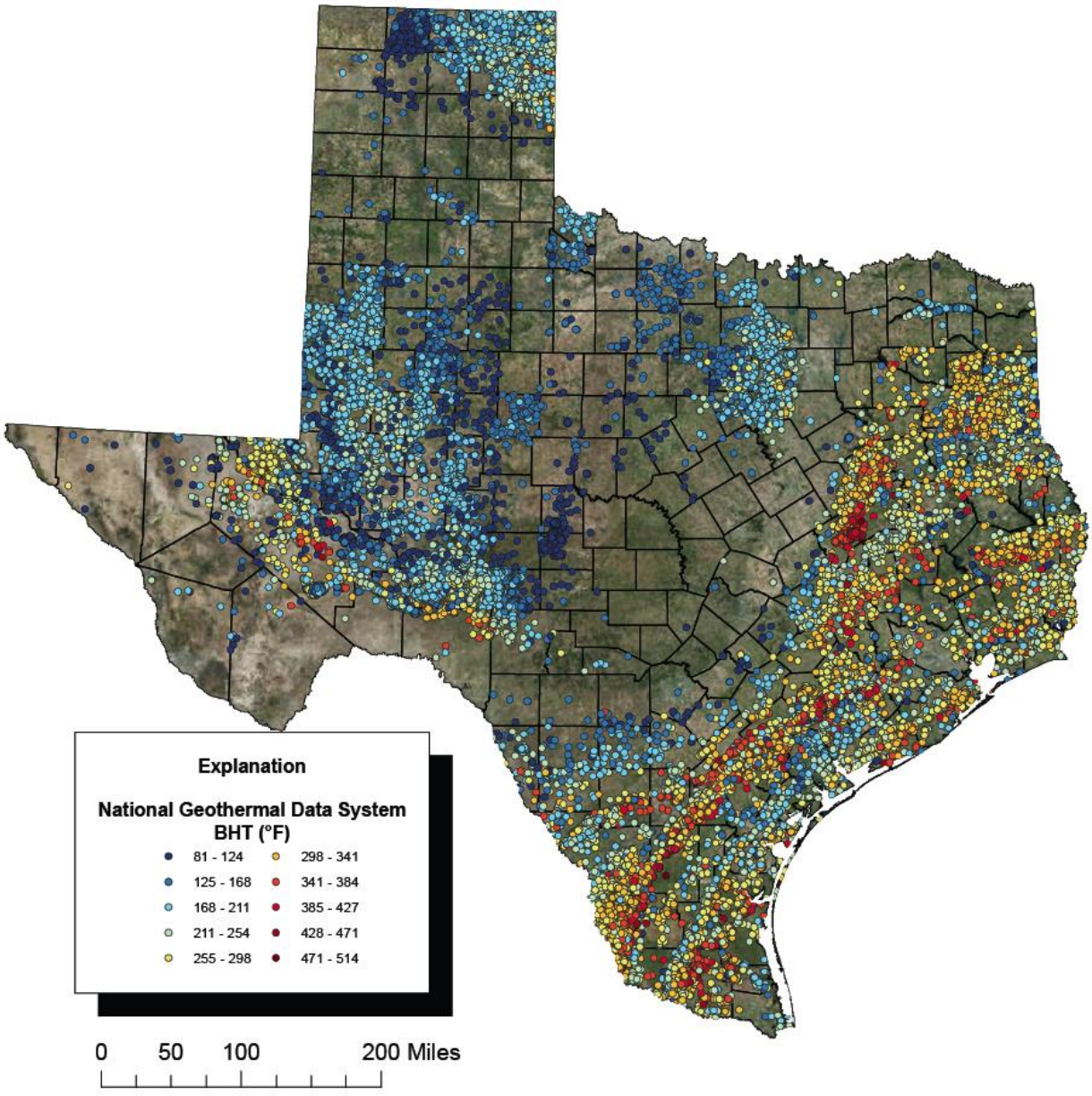

Figure 52. National Geothermal Data System features in the state of Texas

The Cluster and Outlier Analysis tool, which solves for the Anselin Local Moran's *I* statistic of spatial association, was the main analysis tool used to identify concentrations of wells with high bottom hole temperatures.

$$I_i = \frac{x_i - \bar{X}}{S_i^2} \sum_{j=1, j \neq i}^{n} w_{i,j}(x_i - \bar{X}) \tag{8}$$

$$where:$$

$$\boldsymbol{I_i}\ is\ the\ statistic\ of\ spatial\ association$$
$$\boldsymbol{x_i}\ is\ the\ selected\ attribute\ of\ feature\ i\ (bottom\ hole\ temperature)$$
$$\boldsymbol{\bar{X}}\ is\ the\ mean\ value\ of\ the\ selected\ attribute\ (mean\ bottom\ hole\ temperature)$$
$$\mathbf{w}\ is\ the\ spatial\ weight\ between\ feature\ i\ and\ j$$
$$\boldsymbol{n}\ is\ the\ total\ number\ of\ features$$

$$\boldsymbol{S_i^2} = \frac{\sum_{j=1, j \neq i}^{n} w_{i,j}}{n-1} - \bar{X}^2$$

When a given feature (i.e. well) is surrounded by other features with similar attribute values (i.e. bottom hole temperatures) the value of *I* is positive. Such grouped features with similar attribute values are considered clusters.

Different conceptualizations of spatial relationships determine the spatial weight input displayed equation 8. These conceptualizations determine how many neighboring features should be considered or at what distance from the feature another feature be considered a neighbor. Due to the irregular spacing of features in this dataset, the Delaunay Triangulation spatial relation was selected for use in this application. This allows the distribution pattern of the data itself to determine how many neighbors are considered for each feature.

This statistical test seeks to prove or disprove a *null hypothesis* of *complete spatial randomness.* A null hypothesis typically refers to a test of association between two phenomena (Cambridge Dictionary of Statistics, 2010). If a feature is believed to be associated with some underlying spatial process, then the null hypothesis of a random distribution of attributes is to be rejected. In order to quantify this association between an attribute and spatial process, the Cluster and Outlier Analysis tool generates a z-score and a p-value. The p-value represents the probability that a given spatial pattern is a product of randomness. The z-score represents standard deviations in a normal distribution pattern. Very small p-values and z-scores with large absolute values indicate that an attribute and spatial distribution are closely correlated and are not a product of randomness.

Given the large size of this dataset and use of the Delaunay Triangulation spatial relation, initial runs of this analysis resulted in clusters that contained many neighboring features and failed to provide insight into ideal WBHX cluster locations. Thus, it became necessary to institute a lower bound or "floor" on the bottom hole temperature attribute in order to produce a more insightful spatial pattern. This temperature floor was raised incrementally over several iterations. The resulting outputs, when stacked in order of higher floor bounds overlying lower floor bounds, created a "composite cluster overlay," displaying a heat-map-like pattern showing discretized clusters of increasing temperature attribute values. Temperature values of each increasing floor increment were based on an equal interval classification scheme containing 10 classes as displayed on the histogram in Figure 53.

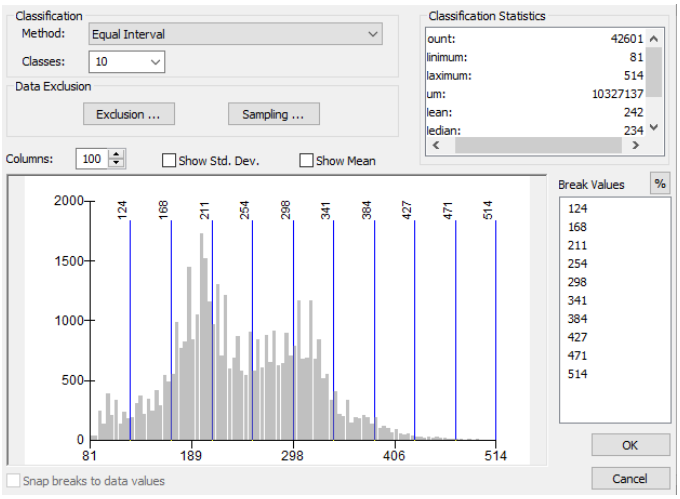

Figure 53. Histogram of interval classification floor selection scheme

Altering the method of classification and number of classes allows for varying outputs based on a desired composite cluster resolution or an altered emphasis from the attribute values to the features themselves. For example, using the *quantile* method of classification would ensure an equal number of features per class. This allows consideration of an escalating floor that removes an equal number of wells in each iteration. Results from an intermediate cluster analysis iteration from the composite cluster overlay are displayed on Table 5 and display *I* values, z-scores, and p-values for the lowest temperature wells within this cluster. These results show z-scores and p-values that would indicate a rejection of the null hypothesis of complete spatial randomness. Final results of this composite cluster analysis are displayed geographically by a 1-mile buffer around the clustered features. This arbitrary buffer distance was chosen to allow for interpretation of clustering from both a state wide and regional basis. Figures 54 through 58 show the scale of interpretation available at these levels and mark four areas containing high attribute value clusters.

Table 5. Cluster analysis results attribute table

ID	BHT°F	*I statistic of spatial association*	Z-Score	P-Value	Cluster Type
4166	363	1.530043317	3.422801472	0.000619793	HH
4173	360	1.910823789	3.823120345	0.000131773	HH
4202	358	1.575321856	4.170145781	3.04405E-05	HH
5064	354	1.265403967	2.830823144	0.004642839	HH
6032	358	1.104396812	2.923600975	0.00346008	HH
6092	358	1.545333704	4.373418567	1.22316E-05	HH
6109	363	0.728824801	2.18800357	0.028669342	HH
6858	363	0.815488353	1.99861905	0.045649588	HH
6893	363	1.444498004	2.890155105	0.003850518	HH
6896	349	0.707187352	2.123054175	0.033749312	HH
7104	358	0.746019893	1.974972537	0.048271265	HH
7105	358	1.152970213	2.579317289	0.009899581	HH
7131	364	1.174106419	2.877428108	0.004009313	HH
9495	358	0.759512504	2.280119224	0.022600618	HH
9592	356	1.202373606	2.689828965	0.007148865	HH
9595	354	1.362651834	3.607205426	0.000309513	HH
15822	360	0.92910058	2.629535047	0.008550172	HH
15998	363	0.695277619	2.087304586	0.03686061	HH
16274	360	1.054076396	2.790402168	0.005264261	HH
16422	361	1.057465458	2.365680332	0.017996976	HH
18450	363	0.966450669	2.735232391	0.006233625	HH
19444	360	1.314476166	2.630023972	0.008537885	HH
19546	363	0.916129897	2.2452455	0.024752377	HH
19598	358	0.927676513	2.273540982	0.022993599	HH
20484	361	1.145676348	3.032868451	0.002422412	HH
20959	356	0.70368841	2.226929042	0.025952016	HH
21417	363	0.901033665	2.015754173	0.043825688	HH
22393	361	0.81655617	2.001235781	0.045366987	HH
22648	360	1.273219413	3.12030878	0.001806616	HH
22661	358	0.99540284	2.226850922	0.025957239	HH
24794	361	0.808202866	2.139571688	0.032389397	HH
25456	363	0.966450669	2.368558725	0.017857545	HH
26036	354	0.862291913	2.440472614	0.014668058	HH
27833	356	0.842106735	2.063848544	0.039032079	HH
27856	361	1.171293147	2.870534064	0.00409779	HH
28440	360	1.153199765	2.826195451	0.004710451	HH

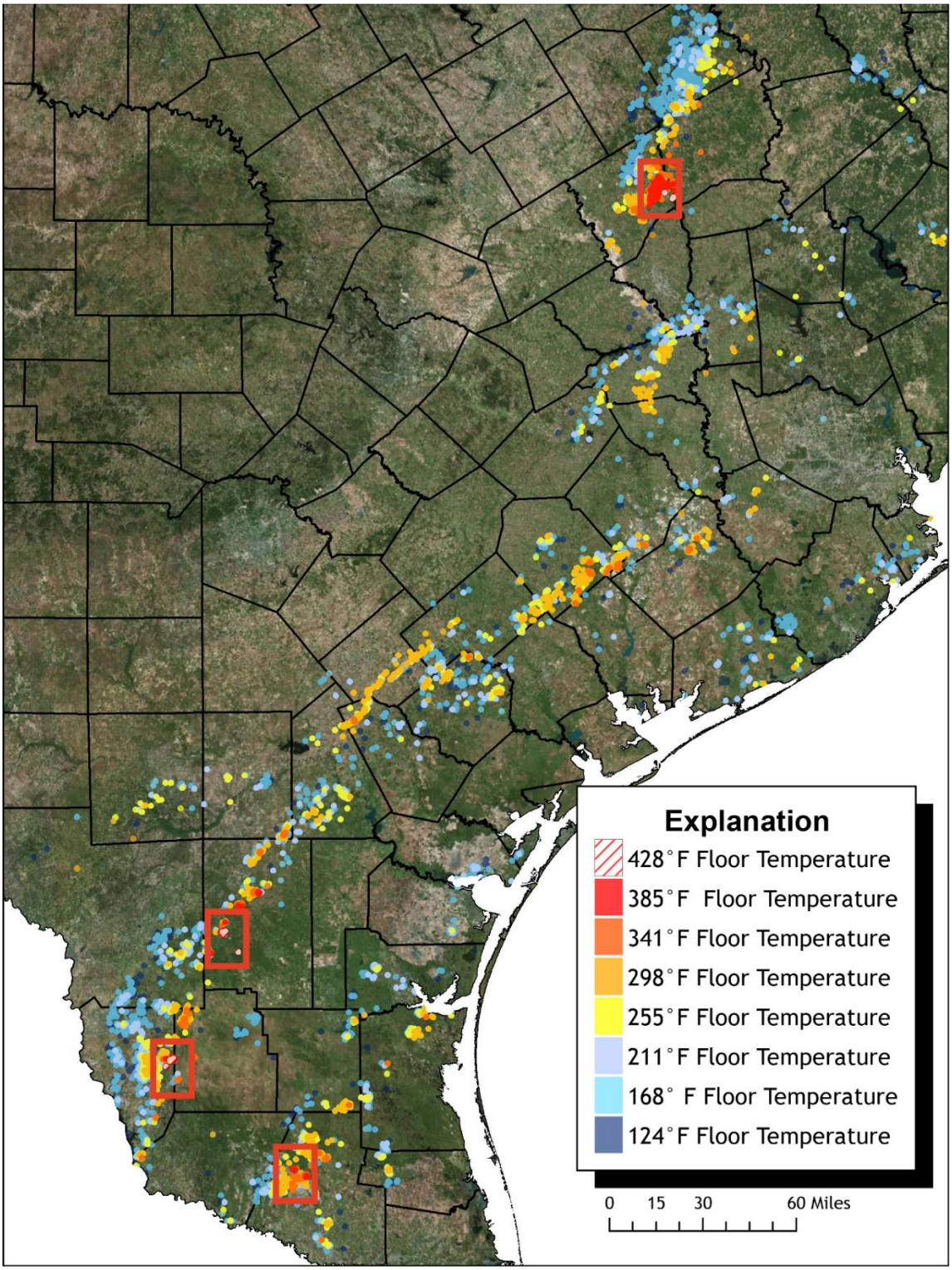

Figure 54. Regional geopressured geothermal composite cluster analysis results.

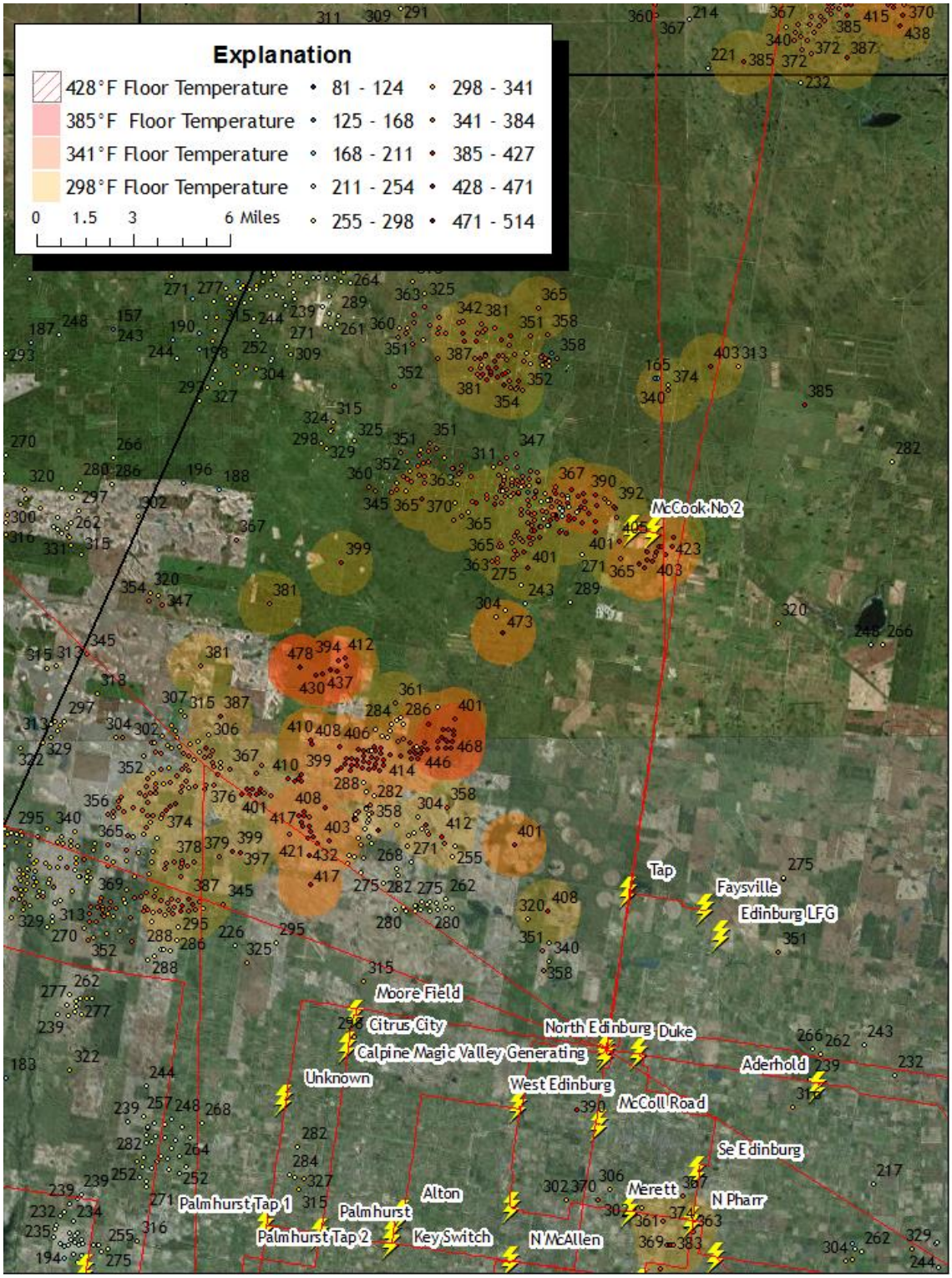

Figure 55. Frio/Vicksburg composite clusters near the cities of McAllen and Edinburg

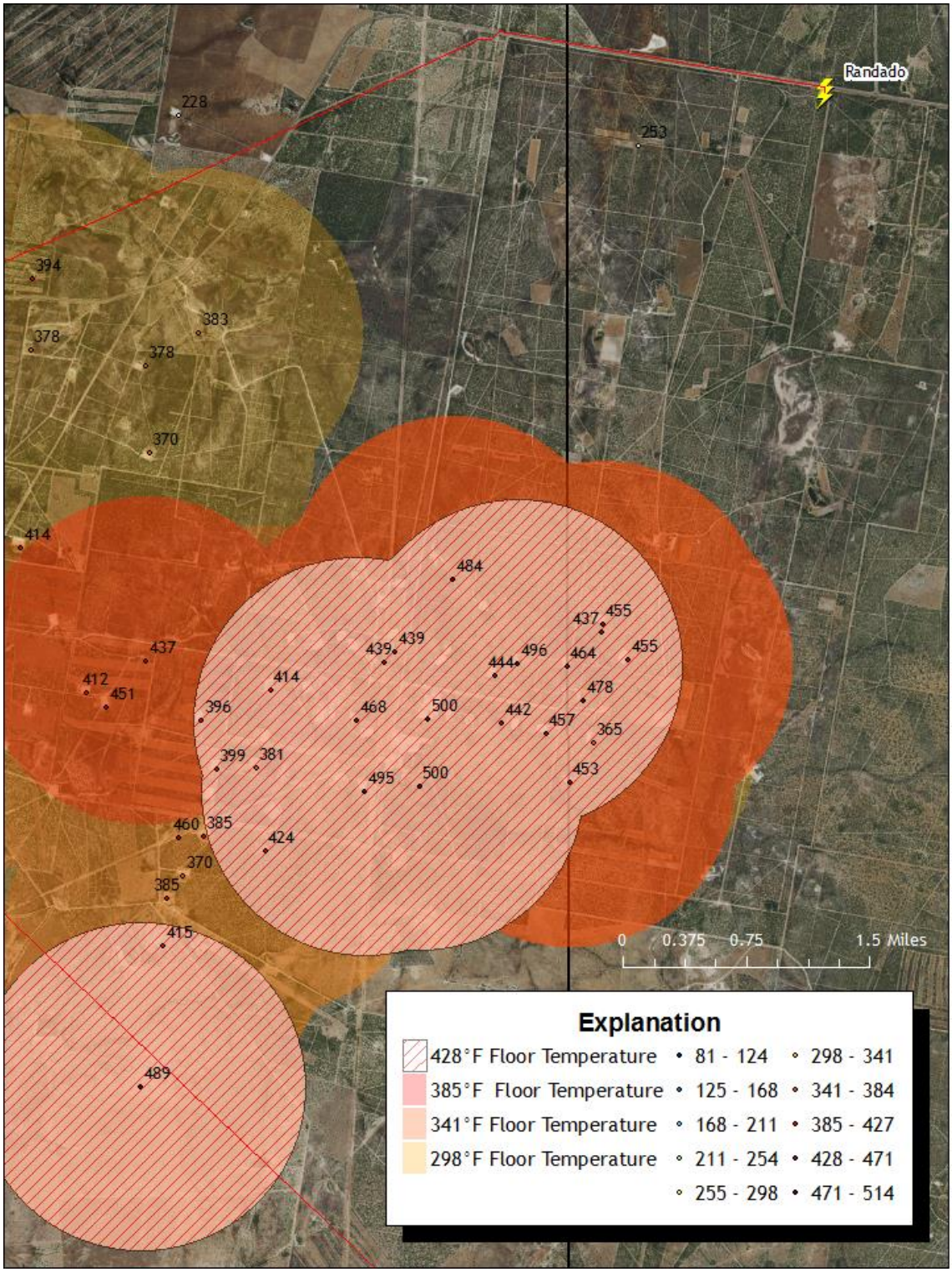

Figure 56. Wilcox composite clusters in Zapata and Jim Hogg Counties

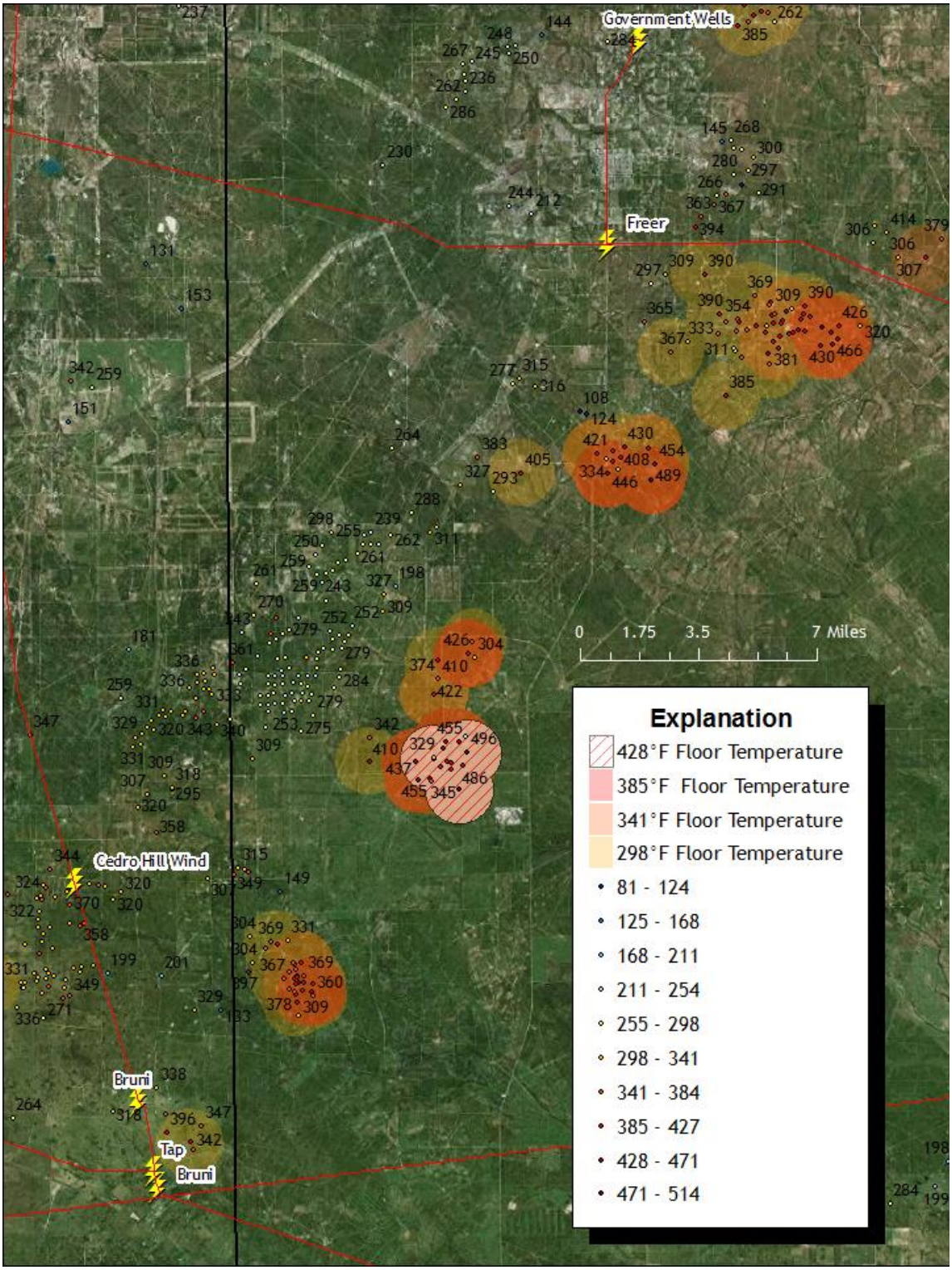

Figure 57. Wilcox composite clusters in Duval and Webb Counties

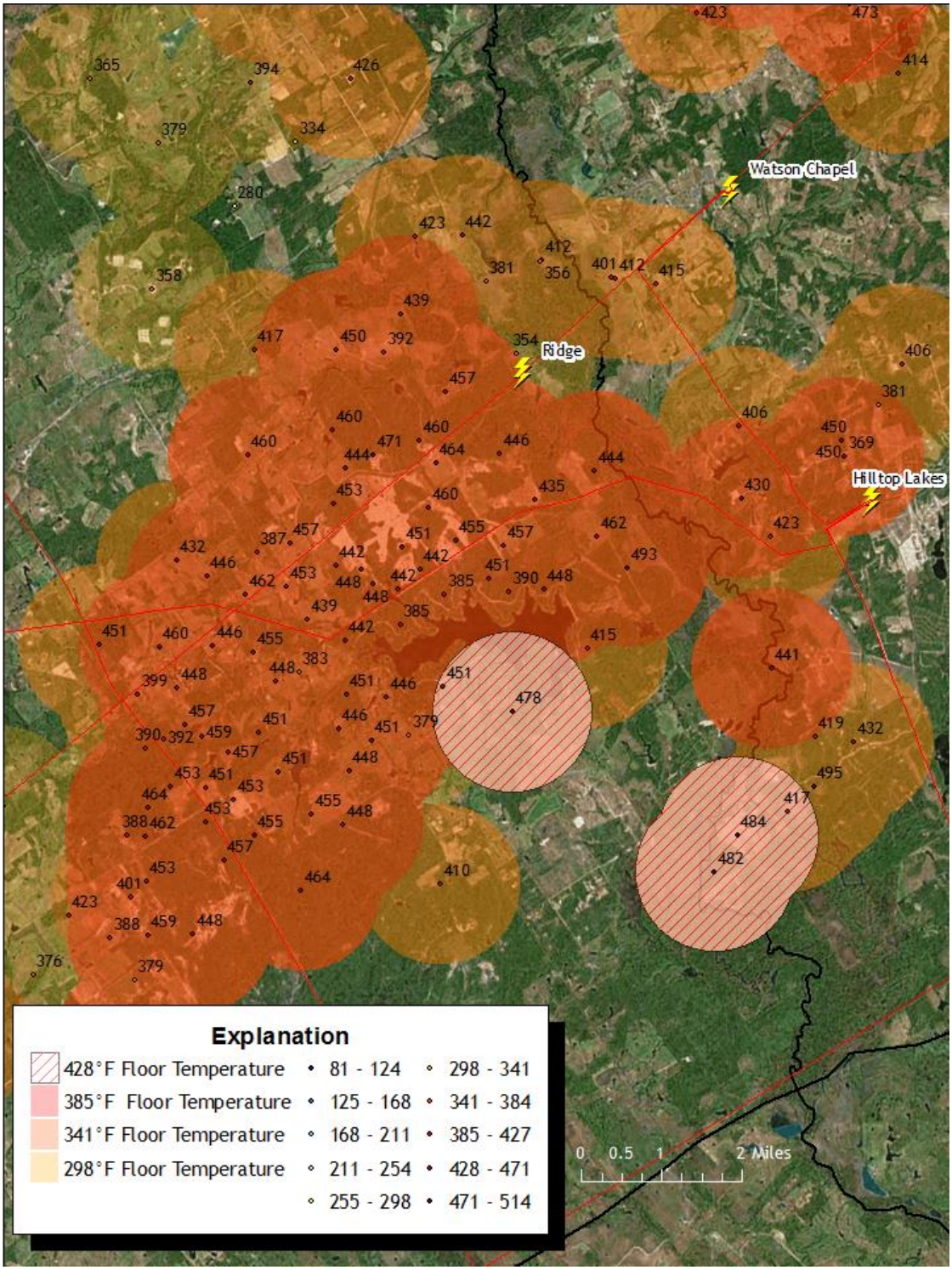

Figure 58. Cotton Valley Bossier Formation composite clusters in Leon & Robertson Counties

5.2 Discussion

Based on the locations of these areas, the southernmost extents of the Frio/Vicksburg and Wilcox trends within the tertiary wedge play, as well as the tight Bossier turbidite sands of the Jurassic Cotton Valley play represent the formations with the highest applicability to clustered WBHX geothermal production. Electricity distribution infrastructure is displayed alongside cluster boundaries in Figures 54 through 58 in order to consider the potential optimum power generation facility layout. When considering the field maturity assessment of the previous chapter, fields producing from Frio/Vicksburg plays have the highest probability of containing existing abandoned wells and are more likely to experience more well abandonment in the near future. Further assessments of the potential application of WBHX systems to abandoned oil and gas wells should therefore be concentrated in the McAllen/Edinburg area.

Other important issues and implications remain to be considered if this novel approach to geothermal energy production is to be considered viable. WBHX generation can only move forward into development if the strengths, such as the immense number of gas wells whose life cycles will be extended, are accentuated and system weaknesses, exemplified by the low generation capacity and high parasitic costs of condenser systems, are improved upon.

6.0 CONCLUSION

This study has outlined the various resource classifications and production methods associated with both conventional and unconventional geothermal energy. Basic thermodynamic principals were then presented in order to properly conceptualize these systems and applications. On this basis, the geopressured geothermal systems of Texas were analyzed in a context that attempts to merge the disciplines of the geothermal and hydrocarbon exploration and production industries. Several geologic groups and formations from two distinct geothermal plays were evaluated in terms of their depositional environment, current oil and gas development, hydrocarbon reservoir properties, and previously studied geothermal fairways. This scope of analysis was performed in an attempt to update and extend the limited existing geothermal systems research in the state by applying the ever-expanding subsurface knowledge base that is constantly being developed in the oil and gas industry. After assessing the geopressured geothermal systems of the state, an unconventional geothermal energy electricity generation method referred to as a well bore heat exchanger (WBHX) was recommended for application. While this WBHX model has only undergone limited direct heating applications and has never been applied to electricity generation, this study summarized several numerical models describing the possibility of applying this novel system to retrofitted abandoned oil and gas wells for the purpose of generating small quantities of electricity. Successful application of this unconventional system would utilize an otherwise burdensome liability in order to generate clean energy from a resource previously considered depleted. Finally, a simple geospatial model was created in order

to define ideal locations for the application of WBHX generation. Data from the National Geothermal Data System (NGDS) were processed via ArcMap into "composite clusters" of primarily gas wells that were associated with high bottom hole temperature values. High value composite clusters were observed in four areas across the state. These areas are associated with gas wells producing from geopressured reservoirs present in the Tertiary Frio/Vicksburg Formations and Wilcox Group, as well as the Jurassic Bossier Formation of the Cotton Valley Group. A final recommendation was made for further assessment regarding the use of WBHX systems on current or future abandoned gas wells in and around the south Texas towns of Edinburg and McAllen. Further assessment would possibly include the development of well re-entry and workover procedures, electrical grid infrastructure implications, and overall system optimization studies including well bore circulating fluid selection.

REFERENCES

Alimonti, C., & Soldo, E. (2016). Study of geothermal power generation from a very deep oil well with a wellbore heat exchanger. *Renewable Energy, 86*, 292-301.

Babadagli, T. (2007). Development of mature oil fields — A review. *Journal of Petroleum Science and Engineering, 57*(3-4), 221-246.

Baker, E. T. (1995). *Stratigraphic nomenclature and geologic sections of the Gulf Coastal Plain of Texas*. Austin, TX: U.S. Geological Survey.

Bebout, D. G., Agagu, O. K., & Dorfman, M. H. (1975.). *Regional sand distribution of the Frio Formation, South Texas - A preliminary step in prospecting for Geothermal Energy*. Austin, TX: Bureau of Economic Geology, University of Texas at Austin.

Bebout, D. G., Loucks, R. G., & Gregory, A. R. (1978). *Frio sandstone reservoirs in the deep subsurface along the Texas gulf coast: Their potential for production of geopressured geothermal energy*. Austin, TX: Bureau of Economic Geology, University of Texas at Austin.

Bebout, D. G., Weise, B. R., Gregory, A. R., & Edwards, M. B. (1982). *Wilcox sandstone reservoirs in the deep subsurface along the Texas Gulf Coast: Their potential for production of geopressured geothermal energy*. Austin, TX: Bureau of Economic Geology, University of Texas at Austin.

Berg, R. R., & Habeck, M. F. (1982). Abnormal pressures in Lower Vicksburg, McAllen Ranch Field, South Texas. *Transactions--Gulf Coast Association of Geological Societies, 32*, 247-253.

Breede, K., Dzebisashvili, K., Liu, X., & Falcone, G. (2013). A systematic review of enhanced (or engineered) geothermal systems: Past, present and future. *Geothermal Energy, 1*(1), 4.

Bu, X., Ma, W., & Li, H. (2012). Geothermal energy production utilizing abandoned oil and gas wells. *Renewable Energy, 41*, 80-85.

Burnett, R. C. (1990). Seismic amplitude anomalies and AVO analyses at Mestena Grande Field, Jim Hogg Co., Texas. *Geophysics, 55*(8), 1015-1025.

Cheng, W., Li, T., Nian, Y., & Wang, C. (2013). Studies on geothermal power generation using abandoned oil wells. *Energy, 59*, 248-254.

Coleman, J., & Galloway, W. (1990). Petroleum geology of the Vicksburg Formation, Texas. *Transactions--Gulf Coast Association of Geological Societies, 40*, 119-130.

Combes, J. M. (1993). The Vicksburg Formation of Texas: Depositional systems distribution, sequence stratigraphy, and petroleum geology. *Bulletin AAPG Bulletin, 77*(11), 1942-1970.

Division of Geothermal Energy. (1980) *Research and development program plans for geopressured-geothermal resources.* Washington, D.C.: U.S. Department of Energy.

D'Agostino, A. (1985). Petrography, reservoir qualities, and depositional setting of the Howell Sand, deep Upper Wilcox, East Seven Sisters Field, Duval County, Texas. *Habitat of Oil and Gas in the Gulf Coast: Proceedings of the Fourth Annual Research Conference Gulf Coast Section Society of Economic Paleontologists and Mineralogists Foundation.* 243-262.

Davis, A. P., & Michaelides, E. E. (2009). Geothermal power production from abandoned oil wells. *Energy, 34*(7), 866-872.

Deming, D. (2002). *Introduction to hydrogeology*. Boston: McGraw-Hill.

Dingus, W. F. (1987). *Morphology, paleogeographic setting, and origin of the Middle Wilcox Yoakum Canyon, Texas Coastal Plain* (Unpublished master's thesis). University of Texas at Austin.

DiPippo, R. (2012). *Geothermal power plants: Principles, applications, case studies and environmental impact* (3rd ed.). Amsterdam: Butterworth-Heinemann.

Doust, H. (2010). The exploration play: What do we mean by it? *AAPG Bulletin, 94*(11), 1657-1672.

Dramis, L. A., Jr. (1981). Structural control of Lower Vicksburg (Oligocene) turbidite channel sandstones, McAllen Ranch Field, Texas. *Transactions--Gulf Coast Association of Geological Societies, 31*, 81-88.

Dyman, T. S., & Condon, S. M. (2006). *Assessment of undiscovered conventional oil and gas resources—Lower Cretaceous Cotton Valley Group, Jurassic Smackover interior salt basins total petroleum system, in the East Texas Basin and Louisiana-Mississippi salt basins provinces*. Reston, VA: U.S. Geological Survey.

Elders, W., Friðleifsson, G., & Albertsson, A. (2014). Drilling into magma and the implications of the Iceland Deep Drilling Project (IDDP) for high-temperature geothermal systems worldwide. *Geothermics, 49*, 111-118.

Elshayeb, T. A. (2004). *Integrated sequence stratigraphy, depositional environments, diagenesis, and reservoir characterization of the Cotton Valley Sandstones (Jurassic), east Texas Basin, USA* (Unpublished doctoral dissertation). University of Texas at Austin.

Energy Policy Modernization Act of 2016, §§ 3007 (2016)

Ewing, T. E. (1986). *Structural styles of the Wilcox and Frio growth-fault trends in Texas: Constraints on geopressured reservoirs*. Austin, TX: Bureau of Economic Geology, University of Texas at Austin.

Fisher, W. L. (1969). Facies characterization of Gulf Coast basin delta systems, with some Holocene analogues. *Transactions--Gulf Coast Association of Geological Societies, 19*, 239-261.

Fisher, W. L., & Kim, E. M. (2000). *Assessing and forecasting, by play, natural gas ultimate recovery growth and quantifying the role of technology advancements in the Texas Gulf Coast Basin and East Texas*. Austin, TX: Bureau of Economic Geology, University of Texas at Austin.

Galloway, W. E. (1989). Genetic stratigraphic sequences in basin analysis I: Architecture and genesis of flooding-surface bounded depositional units. *Bulletin AAPG Bulletin, 73*(2), 125-142.

Galloway, W. E., Dingus, W. F., & Paige, R. E. (1991). Seismic and Depositional Facies of Paleocene-Eocene Wilcox Group Submarine Canyon Fills, Northwest Gulf Coast, U.S.A. *Frontiers in Sedimentary Geology Seismic Facies and Sedimentary Processes of Submarine Fans and Turbidite Systems*, 247-271.

Galloway, W. E., & Williams, T. A. (1991). Sediment accumulation rates in time and space: Paleogene genetic stratigraphic sequences of the northwestern Gulf of Mexico basin. *Geology, 19*(10), 986-989.

Galloway, W. E., Ganey-Curry, P. E., Li, X., & Buffler, R. T. (2000). Cenozoic depositional history of the Gulf of Mexico basin. *Bulletin AAPG Bulletin, 84(11),* 1743-1774.

Glassley, W. E. (2010). *Geothermal energy: Renewable energy and the environment*. Boca Raton: CRC Press.

Gu, Z., & Sato, H. (2002). Performance of supercritical cycles for geothermal binary design. *Energy Conversion and Management, 43*(7), 961-971.

Guevara, E. H., & Garcia, R. (1972). Depositional systems and oil-gas reservoirs in the Queen City Formation (Eocene), Texas. *Transactions--Gulf Coast Association of Geological Societies, 22*.

Hackley, P. C., & Ewing, T. E. (2010). Assessment of undiscovered conventional oil and gas resources, onshore Claiborne Group, United States part of the northern Gulf of Mexico Basin. *Bulletin AAPG Bulletin, 94*(10), 1607-1636.

Hackley, P. C. (2012). *Geologic assessment of undiscovered conventional oil and gas resources—Middle Eocene Claiborne Group, United States Part of Gulf of Mexico Basin*. Reston, VA: U.S. Geological Survey.

Halbouty, M. T. (2003). Giant oil and gas fields of the 1990s: An introduction. *Bulletin AAPG Memoir, 78*, 1-13.

Han, J. H. (1981). *Genetic stratigraphy and associated growth structures of the Vicksburg Formation, south Texas.* (Unpublished doctoral dissertation). University of Texas at Austin.

Hanson, M. C., Oze, C., & Horton, T. W. (2014). Identifying blind geothermal systems with soil CO2 surveys. *Applied Geochemistry, 50*, 106-114.

Hart, B. S., Flemings, P. B., & Deshpande, A. (1995). Porosity and pressure: Role of compaction disequilibrium in the development of geopressures in a Gulf Coast Pleistocene basin. *Geology, 23*(1), 45.

Hill, H. B., & Vogel, F. A., Jr. (1949). *Petroleum-engineering study of Sheridan Field Colorado County, Tex.* (R.I. 4367). Washington, DC: U.S. Department of the Interior, Bureau of Mines.

Höök, M., Xu, T., Xiongqi, P., & Aleklett, K. (2010). Development journey and outlook of Chinese giant oilfields. *Petroleum Exploration and Development, 37*(2), 237-249.

IHS Energy Group, 2005b [includes data current as of December 2005], *PI/Dwights Plus US well data*.

John, C. J., Maciasz, G., & Harder, B. J. (1998). *Gulf Coast geopressured-geothermal program summary study compilation*. Baton Rouge, LA: Basin Research Institute, Louisiana State University.

Kohl, T., Brenni, R., & Eugster, W. (2002). System performance of a deep borehole heat exchanger. *Geothermics, 31*(6), 687-708.

Kujawa, T., Nowak, W., & Stachel, A. A. (2006). Utilization of existing deep geological wells for acquisitions of geothermal energy. *Energy, 31*(5), 650-664.

Langford, R. P., Grigsby, J. D., Collins, R. E., Sippel, M. A., & Wermund, E. G. (1994). *Reservoir heterogeneity and permeability barriers in the Vicksburg S Reservoir, McAllen Ranch Gas Field, Hidalgo County, Texas.* Austin, TX: Bureau of Economic Geology, University of Texas at Austin.

Li, T., Zhu, J., Xin, S., & Zhang, W. (2014). A novel geothermal system combined power generation, gathering heat tracing, heating/domestic hot water and oil recovery in an oilfield. *Geothermics, 51*, 388-396.

Lienau, P. J., Lund, J. W., Rafferty, K. D., & Culver, G. G. (1994). *Reference book on geothermal direct use*. Klamath Falls, OR.: Geo-Heat Center, Oregon Institute of Technology.

Loucks, R. G. (1978). Sandstone distribution and potential for geopressured geothermal energy production in Vicksburg Formation along Texas Gulf Coast. *Transactions--Gulf Coast Association of Geological Societies, 28*, 239-271.

Loucks, R. G., Dodge, M. M., & Galloway, W. E. (1984). Regional controls on diagenesis and reservoir quality in lower tertiary sandstones along the Texas Gulf Coast: Part 1. Concepts and Principles. *AAPG Memoirs*, 15-45.

Loucks, R. G. (2005). Revisiting the importance of secondary dissolution pores in Tertiary sandstones along the Texas Gulf Coast. *Transactions--Gulf Coast Association of Geological Societies, 55*, 447-455.

Lund, J. W. (2003). The use of downhole heat exchangers. *Geothermics, 32*(4-6), 535-543.

Marshall, W. D. (1978). *Depositional environment and reservoir characteristics of the lower Vicksburg sandstones, west McAllen Ranch Field, Hidalgo County, Texas* (Unpublished doctoral dissertation). Texas A&M University.

Matek, B. (2015). *2015 Annual U.S. & Global Geothermal Power Production Study*. Geothermal Energy Association.

McCulloh, R. P., & Eversull, L. G. (1986). Shale-filled channel system in Wilcox Group (Paleocene-Eocene), North-Central South Louisiana. *Transactions--Gulf Coast Association of Geological Societies, 36*, 213-218.

Meehan, D. N., & Pennington, B. F. (1982). Numerical simulation results in the Carthage Cotton Valley Field. *Journal of Petroleum Technology, 34*(01), 189-198.

Michaelides, E. (2012). *Alternative energy sources*. Heidelberg: Springer.

Miller, R. S. (1993). Characteristics of deep-water Yegua sandstones, Texas and Louisiana. *Houston Geological Society Bulletin, 35*(8), 8.

MIT. (2006). *The future of geothermal energy impact of enhanced geothermal systems on the United States in the 21st century*. Cambridge, MA: Massachusetts Institute of Technology.

Moeck, I. S. (2014). Catalog of geothermal play types based on geologic controls. *Renewable and Sustainable Energy Reviews, 37*, 867-882.

Nalla, G., Shook, G., Mines, G., & Bloomfield, K. (2004). *Parametric sensitivity study of operating and design variables in wellbore heat exchangers.* Idaho Falls, ID: Idaho National Engineering and Environmental Laboratory

Newsham, K., & Rushing, J. (2002). Laboratory and field observations of an apparent sub capillary-equilibrium water saturation distribution in a tight gas sand reservoir. *Proceedings of 2002 SPE Gas Technology Symposium*.

NPC Operations and Environment Task Group. (2011) Plugging and abandonment of oil and gas wells. *NPC North American Resource Development Study, 2*(25).

NRG Associates, Inc., 2006 [includes data current as of December 2004], *The significant oil and gas fields of the United States*

Ormenda, P., & Teklemariam, M. (2010). *Overview of geothermal resource utilization in the East African Rift System*. Lecture presented at Short Course V on Exploration for Geothermal Resources, Lake Bogoria and Lake Naivasha, Kenya.

Popov, M. A., Nuccio, V. F., Dyman, T. S., Gognat, T. A., Johnson, R. C., Schmoker, J. W., . . . Bartberger, C. (2001). *Basin-centered gas systems of the U.S.* Denver, CO: U.S. Dept. of the Interior, U.S. Geological Survey.

Robinson, B. M., Holditch, S. A., & Lee, W. J. (1986). A case study of the Wilcox (Lobo) trend in Webb and Zapata Counties, TX. *Journal of Petroleum Technology, 38*(12), 1355-1364.

Ritch, H. J., & Kozik, H. G. (1971). Petrophysical study of overpressured sandstone reservoirs, Vicksburg Formation McAllen Ranch Field Hidalgo County, Texas. *Society of Petrophysicists and Well-Log Analysts 12th Annual Logging Symposium*.

Rybach, L., & Muffler, L. J. (1981). *Geothermal systems: Principles and case histories*. Chichester: Wiley.

Seni, S. J., Walter, T. G., & Raney, J. A. (1992.). *Consolidation of geologic studies of geopressured-geothermal resources in Texas: Colocation of heavy-oil and geothermal resources in South Texas*. Austin, TX: Bureau of Economic Geology, University of Texas at Austin.

Seni, S. J., & Walter, T. G. (1994). *Geothermal and heavy-oil resources in Texas: Topical study*. Austin, TX: Bureau of Economic Geology, University of Texas at Austin.

Society of Petroleum Engineers (2007). *SPE petroleum resources management system guide for non-technical users.* SPE-PRMS

Spetseris, J. J. (1984). Geology of the Upper Wilcox (Eocene), East Seven Sisters Field, Duval County, Texas. *Society of Exploration Geophysicists,* 500-502.

Swanson, S. M., Karlsen, A. W., & Valentine, B. J. (2013). *Geologic assessment of undiscovered oil and gas resources—Oligocene Frio and Anahuac Formations, United States Gulf of Mexico Coastal Plain and state waters*. Reston, VA: U.S. Geological Survey.

Swanson, R. K., Oetking, P., Osoba, J. S., & Hagens, R. C. (1976). *Development of an assessment methodology for geopressured zones of the upper Gulf Coast based on a study of abnormally pressured gas fields in south Texas: Final study*. San Antonio, TX: Southwest Research Institute.

Templeton, J., Ghoreishi-Madiseh, S., Hassani, F., & Al-Khawaja, M. (2014). Abandoned petroleum wells as sustainable sources of geothermal energy. *Energy, 70,* 366-373.

Warwick, P. D., Coleman, J. L., Hackley, P. C., Hayba, D. O., Karlsen, A. W., Rowan, E. L., & Swanson, S. M. (2007). USGS assessment of undiscovered oil and gas resources in Cenozoic strata of the U.S. Gulf of Mexico Coastal Plain and state waters. *The Paleogene of the Gulf of Mexico and Caribbean Basins: Processes, Events, and Petroleum Systems: 27th Annual*, 2-44.

Warwick, P. D. (2008). USGS assessment of undiscovered, technically recoverable oil and natural gas resources of the Lower Paleogene Midway and Wilcox Groups, and Carrizo Sand, Claiborne Group, Onshore Gulf of Mexico Basin, U.S.A. *2008 AAPG Annual Convention; San Antonio, TX*.

Weathers, M., Hass, E., Thomas, H., Ziegenbein, M., Prisjatschew, A., Garchar, L., Emmons, S. (2015). *Geothermal play fairway projects initiated by the U.S. Department of Energy*. Lecture presented at Fortieth Workshop on Geothermal Reservoir Engineering at Stanford University.

Williams, R. A., & Mitchum, R. M. (1997). Sequence stratigraphic controls on Cotton Valley tight gas sandstones, Carthage Field, Panola County, Texas. *Shallow Marine and Nonmarine Reservoirs: Gulf Coast Section, Society of Economic Paleontologists and Mineralogists Foundation 18th Annual Reservoir Conference Proceedings* (pp. 409-425).

Winker, C. D. (1982). Cenozoic shelf margins, Northwestern Gulf of Mexico. *Transactions—Gulf Coast Association of Geological Societies, 32*, 427-448.

U.S. Department of Energy Geothermal Technologies Office (DOE GTO). (n.d.) Play fairway analysis phase II selections. from http://www.energy.gov/eere/geothermal/downloads/play-fairway-analysis-phase-ii-selections

U.S. Department of Energy: Energy Efficiency and Renewable Energy Geothermal Technologies Program (DOE GTP). (2010) Geothermal energy production with co-produced and geopressured resources (Fact Sheet).

U.S., Energy Information Administration, Office of Energy Statistics. (2016). *Monthly Energy Review March 2016*. Washington D.C.: U.S. EIA.

U.S. Geological Survey (2007). *Assessment of undiscovered oil and gas resources in Tertiary strata of the Gulf Coast, 2007*. Reston, VA: U.S. Dept. of the Interior, U.S. Geological Survey.

Xin, S., Liang, H., Hu, B., & Li, K. (2012). A 400 kW geothermal power generator using co-produced fluids from Huabei Oilfield. *GRC Transactions, 36*, 219-226.

Xue, L., & Galloway, W. E. (1995). High-Resolution Depositional Framework of the Paleocene Middle Wilcox Strata, Texas Coastal Plain. *Bulletin AAPG Bulletin, 79*, 205-230.